THE SYNTHESIS AND COORDINATION CHEMISTRY OF FUNCTIONALISED AND MACROCYCLIC PHOSPHINES AND ARSINES

by

Matthieu Limon

Submitted in fulfilment of the requirements of the Degree of

Doctor of Philosophy

School of Chemistry

Cardiff University

Wales, UK

2009

The work described in this thesis was carried out in the Department of Chemistry

at The University of Wales Cardiff under the supervision of Prof. Peter G. Edwards

ProQuest LLC
789 East Eisenhower Parkway
P.O. Box 1346
Ann Arbor, MI 48106-1346

Declaration

This work has not previously been accepted in substance for any degree and is not being concurrently submitted in candidature for any degree.

Signed ..... Dated 29/01/2009

Statement 1

This thesis is being submitted in partial fulfilment of the requirements for the degree of PhD.

Signed ..... Dated 29/01/2009

Statement 2

This thesis is the result of my own investigations, except where otherwise stated. Other sources are acknowledged by footnotes giving explicit references. A bibliography is appended.

Signed ..... Dated 29/01/2009

Statement 3

I hereby give consent for my thesis, if accepted, to be available for photocopying and for inter-library loan, and for the title and summary to be made available to outside organisations.

Signed ..... Dated 29/01/2009

Abstract

The results presented in this thesis are separated into three distinct sections. Chapter 2 describes the reaction of the manganese precursors [Mn(OTf)(CO)$_3${*o*-C$_6$H$_4$(PH$_2$)$_2$}], **2.6**, and [Mn(OTf)(CO)$_3${C$_2$H$_4$(PH$_2$)$_2$}], **2.7**, with a silver carbene transfer agent, 1,3-diallylbenzimidazol-2-ylidiene, **2.10**, to give the new phosphido-phosphine manganese species **2.11** and **2.12**. The resultant species **2.11** and **2.12** exist in two geometric forms, *cis* and *trans*, which have been characterised by X-Ray crystallography for **2.11**.

A new chiral rigid phospholane ligand 3(*R*)-hydroxy-phenylphospholane, **3.7**, has been prepared from the reaction of phenylphosphine with enantiopure (*R*)-2-(oxiran-2-yl)ethyl-4-methylphenylsulfonate, **3.4**. In order to enlarge the family of heterocyclic coordinated complexes, we herein report in Chapter 3 the synthesis of compounds [Mo(k-P$_{R,S}$-**3.7**)$_2$(CO)$_4$], **3.16**, [Re(CO)$_5$(k-P$_{R,S}$-**3.7**)], **3.17**, [Mn(OTf)(CO)$_4$(k-P$_{R,S}$-**3.7**)], **3.18**, [Ru(cymene)Cl(k-P$_{R,S}$-**3.7**)], **3.19**, [FeCp'(CO)$_2$(k-P$_{R,S}$-**3.7**)]PF$_6$, **3.20**, [Rh(cod)Cl(k-P$_{R,S}$-**3.7**)], **3.21**, *cis*-[(k-P$_{R,S}$-**3.7**)$_2$PtCl$_2$], **3.22**, *cis*-[(k-P$_{R,S}$-**3.7**)$_2$PdCl$_2$], **3.23**.

Finally, Chapter 4 presents the synthesis of new tribenzannulated diarsine monophosphine macrocycle complexes prepared by a template method via dehydrofluorinative cyclisation of the di-*ortho*-fluorophenylbisarsinobenzene ligand with PhPH$_2$ at [Mn(CO)$_3$]$^+$ or [Re(CO)$_3$]$^+$ templates. The new macrocycles formed may expand the scientific understanding about phosphorus and arsenic chemistry. In order to enlarge this knowledge, other ways to introduce diarsenic ligands; in our case 1,2-bis(arsino)benzene, **4.a**, on a metal centre were attempted on MnBr(CO)$_5$, **4.2**, Mn(OTf)(CO)$_5$, **4.3**, [Mn(CO)$_3$(NCCH$_3$)$_3$]PF$_6$, **4.4**, [Mn(CO)$_3$(ace)$_3$]PF$_6$, **4.5**, ReBr(CO)$_5$, **4.6**, Mn(OTf)(CO)$_5$, **4.7**, [Cr(CO)$_3$(NCCH$_3$)$_3$], **4.8**, and [Mo(CO)$_3$(NCCH$_3$)$_3$], **4.9**, precursors but no discrete complexes could be isolated and characterised.

Contents

Acknowledgements

Many thanks have to go to my supervisor Professor Peter Edwards for excellent supervision and advice throughout the course of this work and for giving me the opportunity to live and study in a different country from which I have learnt a lot about chemistry, gained a real sense of accomplishment and camaraderie, and probably most important I have learnt a bit more about myself. I am very grateful for the patience and understanding you showed me along all these years.

Thanks also to Dr. Paul Newman for his tremendous help and ideas in more practical aspects of my work, entertaining discussions about other matters and his continual support during all these years.

The backstage technical staff from the Chemistry department should be also credited for their willingness to help in all situations especially Dr Rob Jenkins for his patience running my VT NMR spectra and his help fixing the capricious JEOL and Dr Benson Kariuki for his help in the determination of my crystal structures.

My appreciation goes to my lab mates past and present for keeping me amused: Chris, Thusith, Elisenda, Wenjian, Sultan and others, thanks for your patience. I would also like to acknowledge specially Huw and Craig for making the last few years of my work in the lab totally unforgettable and for perfecting my English vocabulary in a very distinguishing way!

Most importantly to my family, Mum, Dad, and my sister Katell, for all the support, belief, and love they have shown me, not just over the last few years, but throughout. Last, but by no means least, to Krishna for her love and moral support. I could not have done it without you, nothing else I find could ever bring more beauty from a heart so kind, you are my best friend, my soul mate and I will never forget you.

Glossary

ace		acetone
Ar		aryl group
cod		1, 5-cyclooctadiene
Cp		cyclopentadienyl
Cp'		pentamethylcyclopentadienyl
DCM		dichloromethane
dcpe		1,2-bis(dichlorophosphino)ethane
dfpab		1,2-bis(di-2-fluorophenyl)arsinobenzene
dfppb		di-*ortho*-fluorophenylbisphosphinobenzene
dmpe		1,2-bis(dimethylphosphino)ethane
dppe		1,2-bis(diphenylphosphino)ethane
dppm		1,2-bis(diphenylphosphino)methane
dppp		1,2-bis(diphenylphosphino)propane
DMSO		dimethylsulfoxide
ESI		electrospray ionisation
Et_2O		diethyl ether
GC		gas chromatography
i-Pr		*iso*-propyl
IR		infra-red
	(s)	strong

	(m)	medium
	(w)	weak
L		neutral, 2 electron donor ligand
M		metal
Me		methyl
MS		mass spectrum
n-Bu		*n*-Butyl
NHC		N-heterocyclic carbene
NMR		Nuclear Magnetic Resonance
	(s)	singlet
	(d)	doublet
	(t)	triplet
	(q)	quartet
	(m)	multiplet
	(br)	broad
	(v)	virtual
	$^{n}J_{x,y}$	n-bond coupling between atom x and y
Ph		phenyl
pip		piperidine
Pr		propyl
ppm		parts per million
R		generic alkyl

r.t.	room temperature
t-Bu	*t*-Butyl
THF	tetrahydrofuran
UV	ultra violet
VT NMR	variable temperature NMR
X	anionic ligand e.g. halogen

Chapter 1

Introduction

Over the past 50 years, the development of organometallic chemistry has had a major impact on the growth of homogeneous catalysis, much of which has been justified on the basis of the insight it gives into catalytic reactions. Several have proven practical for large-scale industrial synthesis of organic compounds. While our ability to design catalyst systems is still in its infancy, it is clear that phosphorus ligands are often involved and that their steric and electronic character plays extremely important roles.

Homogeneous catalysis is an elegant method of chemical synthesis and can provide new products and processes as well as efficient and clean solutions to many current problems in the petrochemical, pharmaceutical and agrochemical industries. In recent years, olefin metathesis catalysis has received tremendous attention as a powerful technology for the formation of carbon-carbon bonds and has found numerous applications in organic synthesis and polymer chemistry.

Olefin metathesis is a popular and useful reaction, transforming the carbon-carbon double bond in a number of different ways, including cross-metathesis,[1] ring closing metathesis,[2] ring opening metathesis polymerisation[3] and acyclic diene metathesis polymerisation[4] as seen in the Figure 1 below

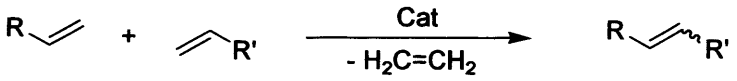

- Cross Metathesis

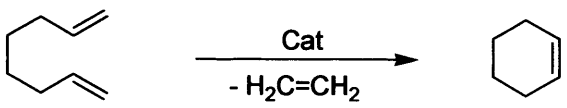

- Ring Closing Metathesis (RCM)

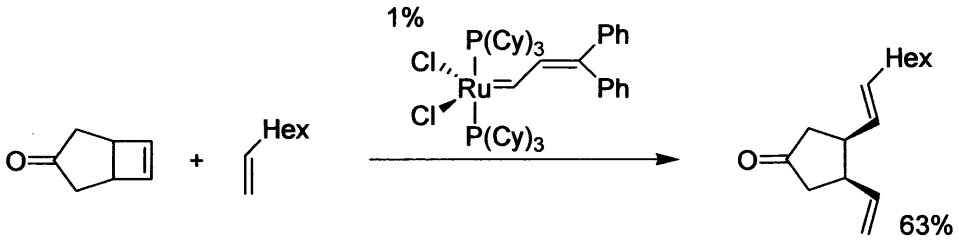

- Ring Opening Metathesis (Polymerization) (ROM(P))

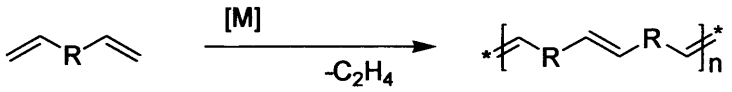

- Acyclic diene metathesis (ADMET)

Figure 1: Examples of metathesis reactions.

A major requirement for homogeneous catalysts is the presence of available reaction sites, ideally mutually *cis*, and this is commonly provided by labile spectator ligands. However, although dissociation is a requirement of the system, it can also lead to problems arising from excessive lability if more ligands dissociate than required, leading to deactivation of the catalyst.

Our strategy is to address the control of lability by use of carefully designed ligands to provide free reaction sites by dissociation but only to a well-defined extent. A very robustly coordinating ligand is required, which occupies several of the coordination sites rigidly, but allows remaining sites to be free for other spectator ligands and reactant species to coordinate reversibly.

Triphosphorus macrocyclic ligands have previously been synthesized and used in order to prevent unwanted dissociation by forming a stable "cap", leaving remaining reaction sites mutually *cis*.

The virtues of phosphine ligands have long been known in these systems, and recently, a second generation of catalysts incorporating nitrogen-heterocyclic

carbene ligands as well as the phosphines have been developed and show increased activity in some reactions.

During the last two decades, there have been tremendous advances in the field of homogenous catalyst design for alkene polymerisation. The success of alkene metathesis stems from the development of several well-defined transition metal complexes, such as the Schrock molybdenum catalyst[5, 6] developed in the mid-80s and the Grubbs ruthenium catalyst[7, 8] developed in 1996 (Figure2).

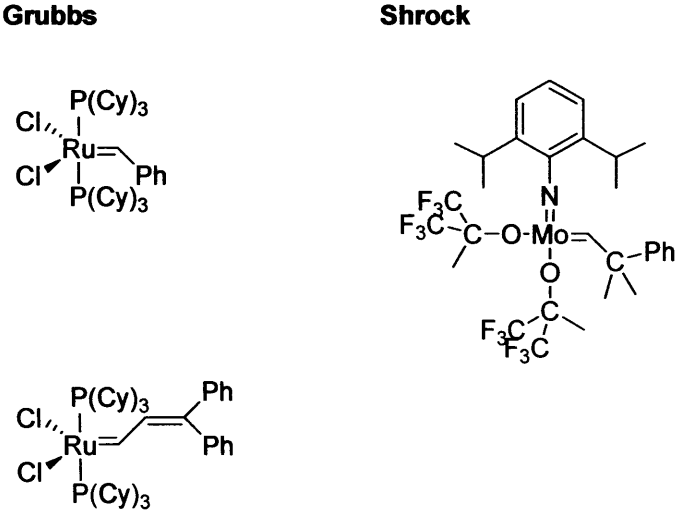

Figure 2: Schrock and Grubb's early catalysts.

Much of the research in this area has focussed on increasing the stability, selectivity, and particularly the activity of ruthenium olefin metathesis catalysts. These efforts have led to the discovery of highly active and fast-initiating complexes that contain saturated nitrogen-heterocyclic carbene ligands.[9] The incorporation of the carbene functionality into ligands systems containing other donor groups such as phosphines offers exciting opportunities for ligand design, which promises the discovery of new efficient catalysts.

This thesis discusses the requirement for new precursors in the area of homogeneous catalysis, as well as explanations of the chemistry involved, and reasons for synthesising this type of ligand. Discussion of related complexes will be given as well as a comprehensive review of the work carried out and the results obtained therein.

1.1 Generals properties of phosphine ligands

The number of known transition metal complexes containing mono-, bi-dentate or polydentate chelating phosphine ligands is vast and the diversity of the phosphorus substituents further increases the range of these ligands and of their complexes.[10]

Figure 3 shows non exhaustive examples of phosphines containing ligands which reveal different steric and electronic properties. PH_3 is the smallest known phosphine while P(*t*-Bu)$_3$ is one of the biggest phosphines as defined by Tolman's cone angle.[11] Due to the electron-withdrawing effects of the fluorine atoms, PF_3 rivals CO as a π-acceptor ligand.[10]

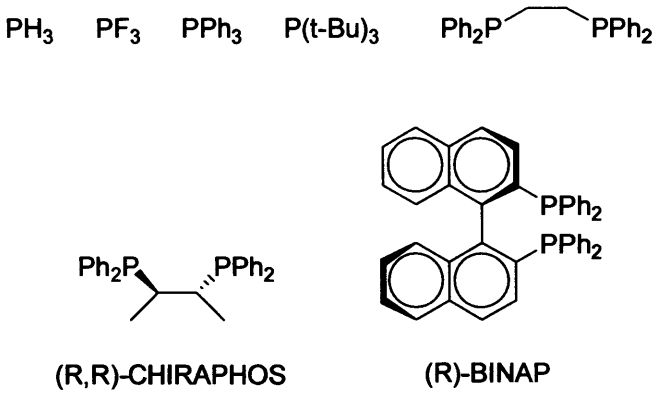

Figure 3: Representative examples of phosphine containing ligands.

Numerous bidentate phosphines are also known, as well as the development for asymmetric catalysis of chiral bidentate ligands like CHIRAPHOS or BINAP. The latter is used in organic synthesis for enantioselective transformations catalyzed by its complexes of ruthenium, rhodium, and palladium (Scheme 1).[12]

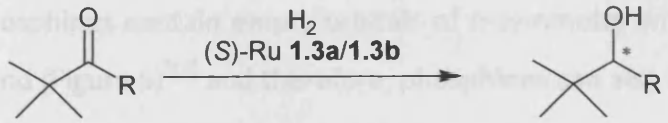

1.1 **1.2**

R = Me, n-C_8H_{17}, (E)-CH=CHC_6H_5, (E)-CH=CH-n-C_6H_{13}, $CH(Me)_2$, C_6H_5, 2-furyl, 2-thienyl

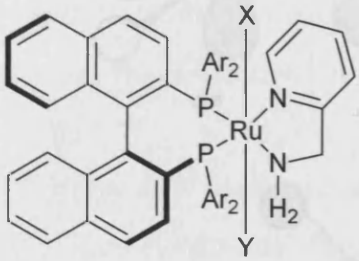

1.3 (*S*)-**a**, X = Y = Cl
(*S*)-**b**, X = H, Y = BH_4
Ar = *p*-MeC_6H_4

Catalyst	Yield (%)	*ee* (%)
(*S*)-**1.3a**	<5 to 100	97 to 98
(*R*)-**1.3a**	99 to 100	97 to 98
(*S*)-**1.3b**	100	97

Scheme 1: Asymmetric hydrogenation of *tert*-butyl ketones **1.1** using BINAP/PICA - Ru complex as catalyst.

Phosphines, like compounds other Group 15 atoms (oxidation state 3), have a lone pair of electrons and a pyramidal structure. Phosphines have 2 electrons in the s subshell and 3 unpaired electrons in the p subshell and therefore can act as an electron pair donor (Lewis base) and coordinate to a metal centre through a σ-bond by the lone pair on the phosphorus atom (Figure 4).

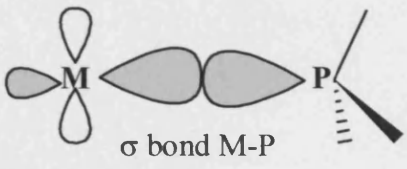

Figure 4

Phosphines contain empty orbitals of π-symmetry with respect to the metal-ligand bond (Figure 5)[13] and therefore, phosphines can also be π-acceptor ligands.

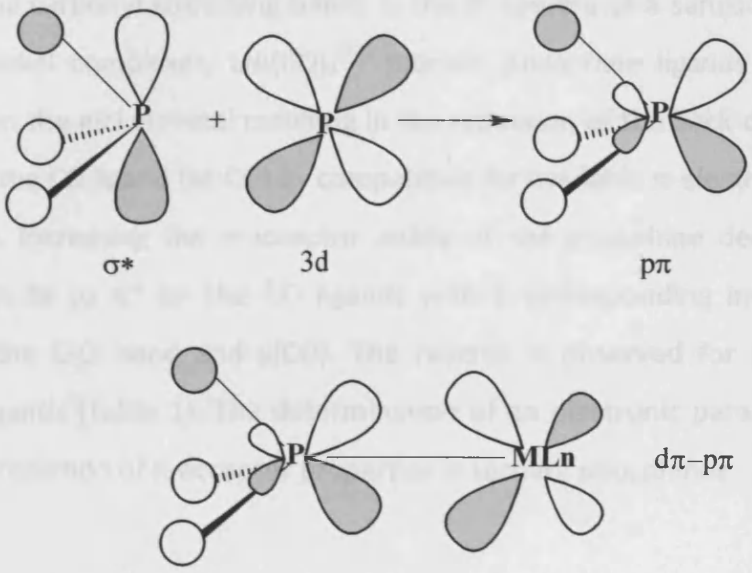

Figure 5

It is now generally established that the M-P bonding acceptor orbital is a combination of a 3d orbital of the phosphorus with a vacant σ^* antibonding orbital of the P-R bond.[14] Thus, the degree of the donor/acceptor ability of the phosphine ligand is predisposed by the nature of the R substituents on the phosphorus atoms. As previously reported, alkyl phosphines are generally less π-acidic than aryl phosphines with more electronegative substituents.[10, 13, 15]

1.1.1 Electronic factors

The electronic properties of phosphine ligands were quantified by Tolman by comparing the carbonyl stretching bands in the IR spectra of a series of tricarbonyl phosphine nickel complexes, $LNi(CO)_3$[11] π-acidic phosphine ligands accept back-donation from the nickel metal resulting in the reduction of the back-donation from the metal to the CO ligand (M-CO) by competition for available π-electron density on the Ni atom. Increasing the π-acceptor ability of the phosphine decreases back-bonding from Ni to π* on the CO ligands with a corresponding increase in the strength of the C-O bond and γ(CO). The reverse is observed for pure σ-donor phosphine ligands (Table 1). The determination of an electronic parameter can be used in the prediction of π-acceptor properties in tertiary phosphines.

PR_3	γ/cm^{-1}	PR_3	γ/cm^{-1}
$P(t\text{-}Bu)_3$	2056	$P(OMe)Ph_2$	2072
PCy_3	2056	$P(OPr^i)_3$	2076
$P(i\text{-}Pr)_3$	2059	$P(OMe)_3$	2080
PBu_3	2060	PH_3	2083
PEt_3	2062	$P(OPh)_3$	2085
PMe_3	2064	PCl_3	2097
PPh_3	2069	PF_3	2111

Table 1: Electronic parameters of phosphine ligands in $Ni(CO)_3(PR_3)$.[13]

1.1.2 Steric factors

If the electronic properties of phosphines can be modified by changing the substituents, the steric effects of the ligand can also be "fine tuned". Tolman defined the cone angle to quantify the steric properties of phosphines and generally tertiary phosphine ligands are commonly classified using this parameter, but the method can be applied to any ligand.[11] The cone angle, θ, is defined as the angle of the virtual cone defined by the van der Waals surface generated by a phosphine ligand bound to a metal (Table 2, Figure 6). The concept of cone angle is most easily visualized with symmetrical ligands, e.g. PR_3. But the approach has been refined to include less symmetrical ligands of the type PRR'R" as well as diphosphines.[16]

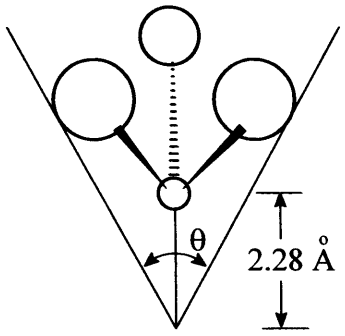

Figure 6: Definition of cone angle θ.

The understanding of the electronic and steric parameters of phosphine ligands has become a useful tool. Both factors affect the reactivity of the complexes formed with the phosphine ligand. The quantification of these parameters has allowed alteration of the phosphine substituents in a systematic and predictable manner for the optimisation of catalytic reactions.

Ligand	angle (deg)	Ligand	angle (deg)
PH_3	87	dppe	125
PF_3	104	dppp	127
$P(OMe)_3$	107	$P(CH_2CH_3)_3$	132
dmpe	107	dcpe	142
depe	115	$P(C_6H_5)_3$	145
$P(Me_3)_3$	118	$P(t\text{-}Bu)_3$	182
dppm	121	$P(C_6F_5)_3$	184

Table 2: Cone angles of common phosphine ligands in degrees.

Finally, phosphine ligands typically have large energetic barriers to pyramidal inversion (120-150 kJ/mol).[17] The resolved chiral phosphines retain their configuration at the phosphorus atom, and as a result the complexes created can show selectivity towards the production of one specific enantiomer in asymmetric catalysis.

1.1.3 Polydentate phosphines

Growing attention has been given to polydentate phosphine ligands since the advantages of polyphosphines over comparable monodentate phosphines became evident.[18, 19, 20] The chelate effect is one of these observed advantages, where a complex formed with a polydentate ligand is kinetically more inert and thermodynamically more stable than the complex formed with analogous monodentate ligands. This effect is entropically favoured. It is more pronounced with five or six membered rings; with very large and flexible chains the effect becomes insignificant.[21]

However, complexes with polydentate ligands are also formed under restricted control of the co-ordination number, stoichiometry and stereochemistry; although they display a variety of metal oxidation states. The metal centres are affected by an increased nucleophilicity, which can be monitored together with other detailed structural and bonding information from $^{31}P\{^{1}H\}$ NMR spectroscopy. All these advantages have promoted the development of polydentate phosphines with several arrangements and donor atoms.

Most of the studies of polydentate phosphines have been concerned with bidentate, tridentate and tetradentate, although hexadentate and pentadentate phosphines are also known.

1.2 Arsines

Upon descending the Group 15 of the periodic table from phosphorus to arsenic there is a general increase in the metallic character of the elements. Arsenic displays some metallic behaviour and the increase in metallic character is a result of the significant decrease in electronegativity upon descending the Group 15.

In general, the lack of a convenient NMR probe, increased toxicity and the fact that compounds containing low co-ordination Group 15 elements become progressively less stable as the Group is descended, has meant that arsenic containing ligands have received far less attention than their phosphorus containing analogous ligands. This statement is also true for the other heavier Group 15 elements antimony and bismuth.

In 1980 Evan P. Kyba and Shang-Shing P. Chou reported the first synthesis and formation of transition metal complexes of three new tertiary-arsine-containing macrocycles.[22] The stereochemistries of the new complexes were deduced on the basis of molybdenum carbonyl complexes. The arsino-macrocycles **1.7.a, 1.7.b** and **1.7.c** were obtained in boiling THF under high-dilution conditions as shown in Scheme 2. The macrocycles were described as viscous oils at room temperature and appeared to be less susceptible to air oxidation than the corresponding phosphorus macrocycles.

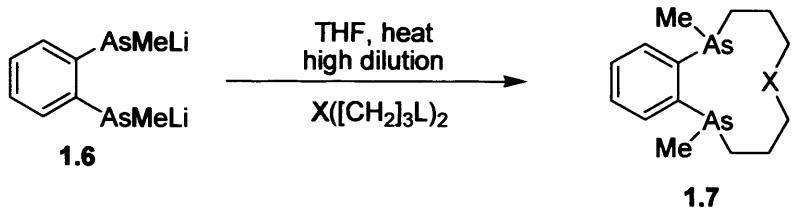

1.6 **1.7**

a, X = AsPh
b, X = PPh
c, X = S

L = Cl, Br or SO_3Me

Scheme2

To our knowledge no other tertiary-arsine-continaing cyclic rings have been reported prior to Kyba's work.

Given this interest, extending our studies to include the synthesis and the coordination chemistry of a tridentate donor macrocycle comprising both phosphine and arsine ligands would be of value, although such ligands remain extremely rare.

1.3 N-Heterocyclic carbenes NHC

A persistent carbene (also known as a stable carbene) is a type of carbene demonstrating particular stability despite also being a reactive intermediate. The instability in these carbenes involves reactivity with substrates, or dimerisation as seen in the Wanzlick equilibrium.[23]

Persistent carbenes can exist in the singlet state or the triplet state, with the singlet state carbenes being more stable.

In 1970, Wanzlick *et al.* prepared but did not isolate the first imidazol-2-ylidene by the deprotonation of imidazolium salt.[24] Wanzlick as well as Hoffmann[25] believed that these imidazole-based carbenes, with a 4n+2 π-electron ring system, should be more stable than the 4,5-dihydro analogues, due to Hückel-type aromaticity. Unfortunately, perhaps believing that these carbenes were still too reactive to be isolated, they resorted to trapping these carbenes with reagents such as mercury and isothiocyanate (Scheme 3).

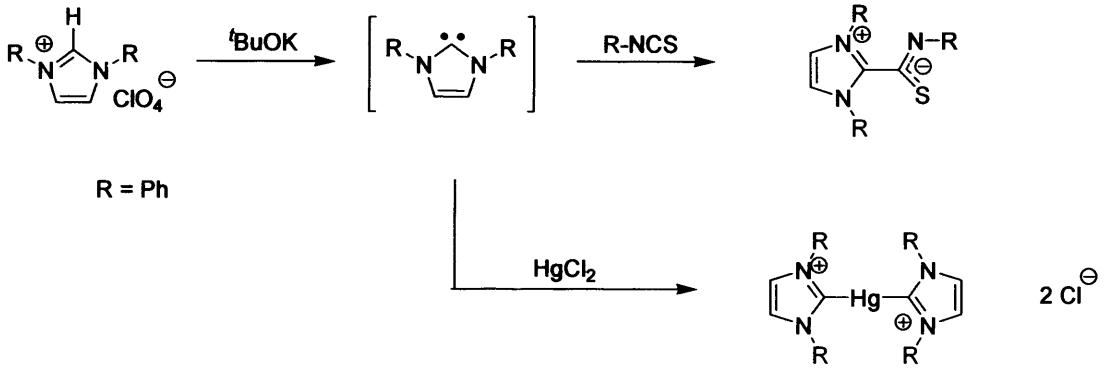

Scheme 3: Preparation and trapping of an imidazol-2-ylidene.

The field of stable carbene research was awakened in 1991 with a landmark discovery by Arduengo *et al.*,[26] who managed to isolate and obtain an X-ray structure of the stable carbene N,N'-diadamantyl-imidazol-2-ylidene, **1.9**, (Scheme 4).

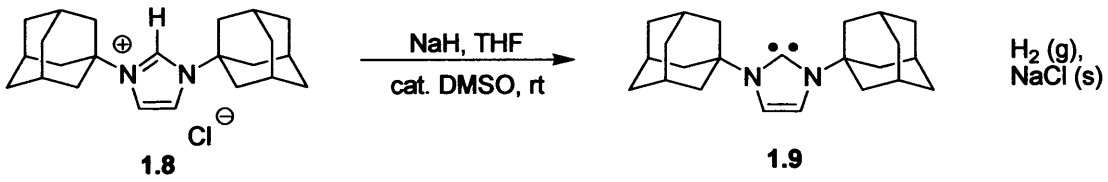

1.8 **1.9**

Scheme 4: Preparation of the stable carbene N,N'-diadamantyl-imidazol-2-ylidene.

However, prior to this isolation, persistent carbenes had been proposed to exist by Breslow in 1957.[27, 28] In 1989 Guy Bertrand's group[29, 30] were the first to make and isolate a stable carbene.

Typically, carbenes are very reactive short lived molecules that cannot be isolated, and are usually studied by observing the reactions they undergo. However, persistent carbenes are much more stable and considerably longer lived. This means that in many cases these carbenes are thermodynamically stable in the absence of moisture and in most cases, oxygen, and can be isolated and indefinitely stored. Some persistent carbenes are not thermodynamically stable and dimerise slowly over days. The less stable triplet state carbenes have half-lives measured in seconds, and cannot be stored but merely observed.

1.3.1 General methods of preparing stable carbenes

Stable carbenes are very reactive molecules and so it is important to consider the reaction conditions carefully when attempting to prepare these molecules. Stable carbenes are strongly basic (the pKa value of the conjugate acid of an imidazol-2-ylidene was measured at ca. 24)[31] and react with oxygen. Clearly these reactions must be performed under a dry, inert atmosphere, avoiding protic solvents or compounds of even moderate acidity. Several approaches have been developed in order to prepare stable carbenes including deprotonation, the use of metal hydride bases, potassium tert-butoxide[32] and alkyllithiums, which are outlined below, but also by other methods like lithium amides,[33, 34] metal hexamethyldisilazides,[35] dechalcogenation[36, 37, 38]and vacuum pyrolysis.[39]

Deprotonation of carbene precursor salts with strong bases has proved a reliable route to almost all stable carbenes (Scheme 5).

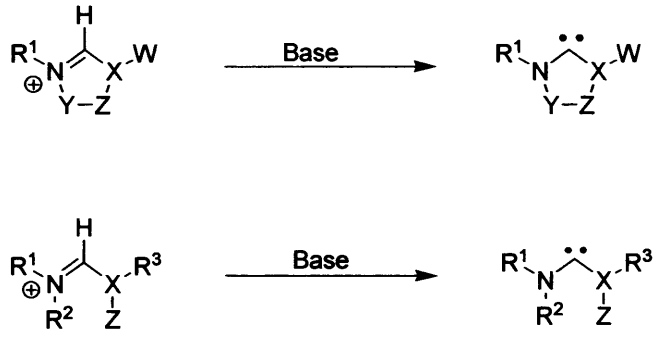

	W	X	Y	Z
a	R^2	N	CR^3	CR^4
b	-	S	CR^2	CR^3
c	R^2	N	N	CR^3
d	R^2	N	CH_2	CH_2
e	R^2	N	CH_2	C_2H_4

a	-	N	-	R^4
b	-	O	-	-
c	-	S	-	-

Scheme 5: Deprotonation of precursor salts to give stable carbenes.

Several bases and reaction conditions have been employed with varying success. The degree of success has been principally dependent on the nature of the precursor being deprotonated. The major drawback with this method of preparation is the problem of isolation of the free carbene from the metals ions used in their preparation.

One might believe that sodium or potassium hydride[40, 41] would be the ideal base for deprotonating these precursor salts. The hydride should react irreversibly with the loss of hydrogen to give the desired carbene, with the inorganic by-products and excess hydride being removed by filtration. In practice this reaction is often too slow in suitable solvents (e.g. THF) due to the relative insolubility of the metal hydride and the salt.

Deprotonation with sodium or potassium hydride in a mixture of liquid ammonia/THF at -40 °C has been reported by Hermann *et al.*[42] to work for imidazole based carbenes. Arduengo and co-workers[41] managed to prepare a dihydroimidazol-2-ylidene using NaH. However, this method has not been applied to the preparation of diaminocarbenes.

The use of alkyllithiums as strong bases[26] has not been extensively studied. They are unreliable for deprotonation of precursor salts. With non-aromatic salts, *n*-BuLi and PhLi can act as nucleophiles whilst *t*-BuLi can on occasion act as a source of hydride, reducing the salt with the generation of isobutene (Scheme 6).

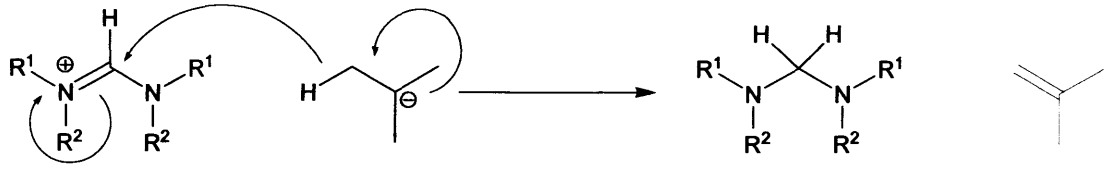

Scheme 6: Reduction of formamidinium salts with tert-butyllithium.

1.3.2 Basicity and nucleophilicity of stable carbenes

The nucleophilicity and basicity of imidazol-2-ylidenes have been studied by Alder *et al.*[43] who revealed that these molecules are strong bases, the conjugate acids having a pKa of ca. 24 in DMSO (Scheme 7).

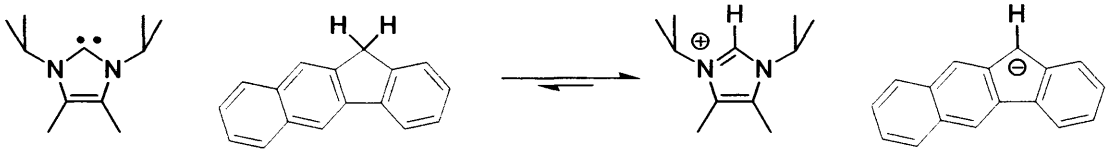

Scheme 7: Measurement of the pKa value for the conjugate acid of an imidazol-2-ylidene.

However, further work by Alder has shown that diaminocarbenes will deprotonate the DMSO solvent, with the resulting anion reacting with the resulting amidinium salt (Scheme 8).

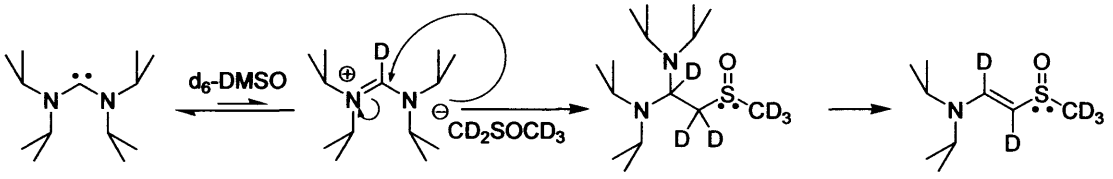

Scheme 8: Using d_6-DMSO as an NMR solvent can have unexpected results.

Reaction of imidazol-2-ylidenes with 1-Bromohexane gave 90 % of the 2-substituted adduct, with only 10 % of the corresponding alkene, indicating that these molecules are also reasonably nucleophilic.

1.3.3 Reactivity of stable carbenes

The chemistry of stable carbenes has not been fully explored. However, Enders *et al.*[39, 44, 45] have performed a range of organic reactions involving a triazol-5-ylidene. Care must be taken to check that a stable carbene is truly stable. The discovery of a stable isothiazole carbene, **1.11**, from an isothiazolium perchlorate, **1.10**, by one research group[46] was questioned by another group[47] who were only able to isolate 2-imino-2H-thiete, **1.13**, (Scheme 9). The intermediate, **1.12**, was proposed in a rearrangement reaction. This carbene is no longer considered stable.[48]

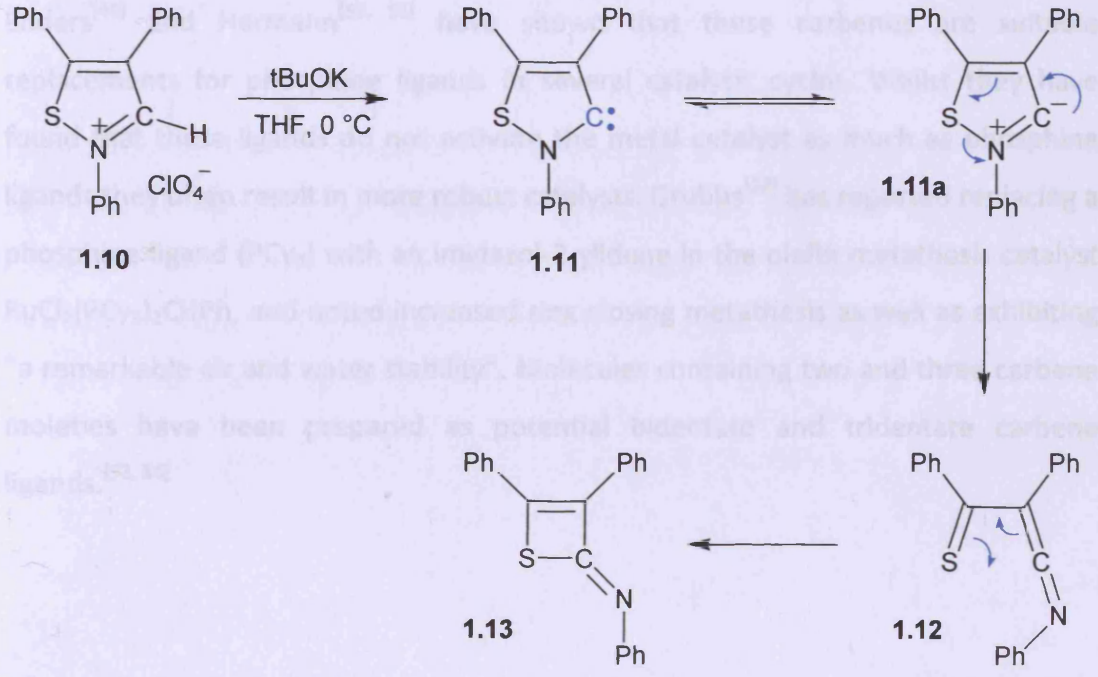

Scheme 9

1.3.4 Carbene complexation

Imidazol-2-ylidenes, triazol-5-ylidenes and less so, diaminocarbenes have been shown to co-ordinate to a plethora of elements, from alkali metals, main group elements, transition metals and even lanthanides and actinides.

Stable carbenes are believed to behave in a similar manner to organophosphines in their co-ordination properties to metals. These ligands are good σ-donors through the carbonic lone pair, but poor π-acceptors due to internal ligand back-donation from the nitrogen atoms adjacent to the carbene centre, and so are able to co-ordinate to even relatively electron deficient metals.

Enders[49] and Hermann[50, 51] have shown that these carbenes are suitable replacements for phosphine ligands in several catalytic cycles. Whilst they have found that these ligands do not activate the metal catalyst as much as phosphine ligands they often result in more robust catalysts. Grubbs[52] has reported replacing a phosphine ligand (PCy_3) with an imidazol-2-ylidene in the olefin metathesis catalyst $RuCl_2(PCy_3)_2CHPh$, and noted increased ring closing metathesis as well as exhibiting "a remarkable air and water stability". Molecules containing two and three carbene moieties have been prepared as potential bidentate and tridentate carbene ligands.[53, 54]

1.4 Macrocycles

Coordination chemists study macrocycles with three or more donor atoms in rings of greater than nine atoms as these compounds often have strong and specific binding with metals.[55] This binding property of coordinating macrocyclic molecules is known as the macrocycle effect. It is in essence a specific case of the chelation effect: *complexes of bidentate and polydentate ligands are more stable than those with unidentate ligands of similar donor atoms.* A macrocycle has donor atoms arranged in more fixed positions and thus there is less of an entropic effect in the binding energy of macrocycles than monodentate or bidentate ligands with an equal number of donor atoms.[56]

However, unlike the chelate effect, the entropic effect is not the only factor contributing to the increased macrocyclic stability; thus changes in enthalpy, ring size and conformation are factors which favour the formation of macrocycle complexes. The sum of these factors has been defined as the macrocyclic coordination effect.[57] There is a favourable thermodynamic change on passing from an open-chain ligand complex to a cyclic ligand complex (Scheme 10).

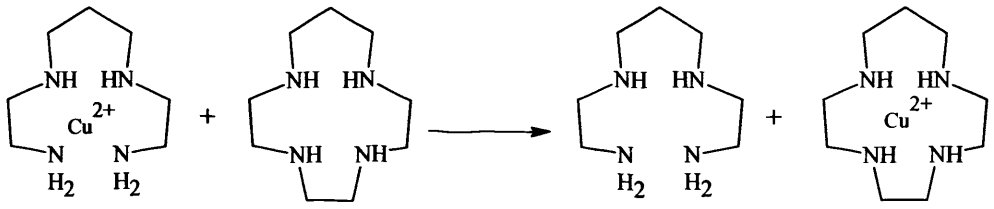

log K (27 °C)= 5.2

Scheme 10

The ring size of macrocycles also strongly influences the stability of the complexes formed.

1.4.1 Synthesis

The synthesis of macrocyclic ligands has been principally limited to N, S or O donor atoms.[57] The deficiency of related phosphorus macrocycles is due to complications in handling the precursors, as primary or secondary phosphines are habitually volatile, toxic and air-sensitive. The improvement of synthetic routes to phosphine macrocycles has represented an important synthetic challenge.

1.4.1.1 Cycloaddition Reactions.

Macrocycles are generally synthesized from smaller, usually linear, molecules. To create a ring, a purely conventional intermolecular organic or an intramolecular reaction normally by nucleophilic substitution of an electrophile occurs.

Because the formation of macrocycles uses the same chemistry that polymerization does, steps need to be taken to prevent polymerization from happening. Conventionally, this involved high dilution chemistry where large amounts of solvent and low concentrations of precursor were used. It is important to mention that at low concentration, the reagents often needed to be added slowly and the generally intermolecular reactions of the molecules are likely to occur. This method is frequently ineffective, using large quantities of solvents and giving low yields.

The groups of Kyba and Ciampolini have been the major earlier contributors to this field. Whilst Kyba prepared various 11- and 14-membered macrocycles containing phosphorus donor atoms,[58, 59] Ciampolini obtained 18-membered sexidentate macrocycles with four phosphorus atoms combined with two other donor atoms such as O, N and S (Figure 7).[60]

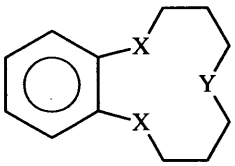

11[ane]X_2Y

X=P, S, As

Y=N, O, S, P, As

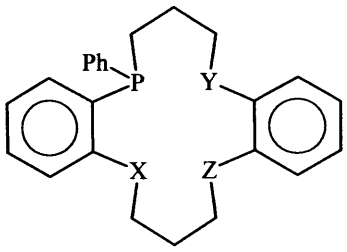

14[ane]PXYZ

X=P, S

Y=N, O, S, P, As

Z=N, O, S, P, As

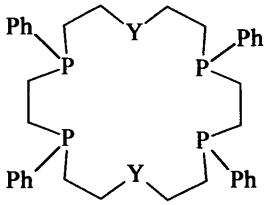

18[ane]P_4Y_2

Y=N, O, S

Figure 7

Moreover, the lack of stereoselectivity using this method produces generally a mixture of stereoisomers which decrease considerably the yield of each macrocycle isomer.

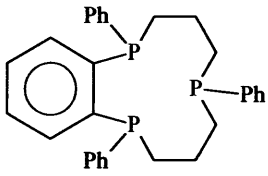

11[ane]P_3

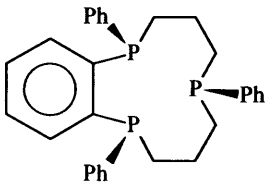

meso-*cis*

(syn, syn)

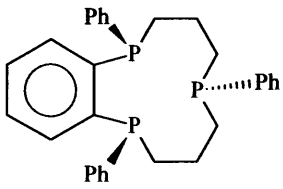

meso-*trans*

(syn, anti)

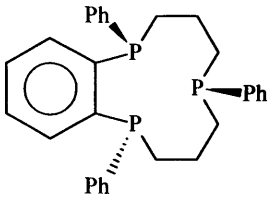

dl

(syn, anti)

Figure 8

As previously reported by Kyba, the 11[ane]P_3 macrocycles synthesis by high dilution method illustrate the lack of stereoselectivity.The 11[ane]P_3 has three different stereoisomers but only the meso-*trans* isomer was isolated by crystallization in 5 % yield (Figure 8),[58, 61] while only the meso-*cis* (syn, syn) isomer is required for tridentate coordination to a single metal centre.

Larger rings with an increased number of phosphorus atoms are even more complex due to the increase in the number of possible stereoisomers.

To achieve high yields of macrocycles at high concentrations, a way to orient the reactive sites such that they readily undergo cyclization was needed. Transition metals, with their ability to gather and dispose ligands in a given predictable geometry, can induce a "template effect." By binding to the acyclic molecule, to influence its geometry, a metal "template" can accelerate the intramolecular reaction. Thus the judicious choice of a metal ion and the relative locations of donor atoms would allow a metal to control the cyclization process.

1.4.1.2 Template methods.

The template effect can be separated into two slightly additional specific effects: The kinetic template effect describes the directive influence of the metal ion in controling the steric course of a sequence of stepwise reactions. In cases where the thermodynamic template effect operates, the metal ion perturbs an existing equilibrium in an organic system and the required product is produced often in high yield as a metal complex. In most cases, the kinetic template effect is operative; however an assignment cannot be made in all cases.[62]

In a metal template assisted reaction, a metal centre directs and controls the synthesis of a macrocycle by pre-organizing the acyclic intermediates prior to the cyclisation reaction.

Thus, the problems associated with the conformation of the acyclic intermediates are eliminated, and formation of polymers is inhibited by the proximity of pre-organised reagents. However, the role of the metal is not only conformational (in placing the reactants in the correct spatial arrangement for cyclisation) but may also function as a stabilising agent of otherwise unstable intermediates.[56]

The use of metal directed reactions can also induce more selectivity in the cyclisation due the reduction of reactivity of the functional groups involved in the cyclisation process. Electrophilic functional groups have their electrophilic abilities reduced by the back-bonding effect of the metal, whereas nucleophilic functional groups have their electron density reduced by the electrophilicity of a cationic centre.[62]

Previously known phosphorus macrocyclic complexes have been prepared by using a square-planar metal like Ni(II)[63, 64, 65] or Pd(II)[66, 67, 68] and therefore are tetradentate. However, these reactions have not shown the required stereoselectivity, and mixtures of stereoisomers have been obtained which reduce the yield and availability of specific compounds in those mixtures which are commonly difficult to separate efficiently.

In 1982, Norman and co-workers prepared a novel tridentate secondary phosphorus macrocycle complex by intramolecular hydrophosphination of tris(allyl)phosphine on a molybdenum centre[69] as well as the analogous 15-membered triphosphorus macrocyclic molybdenum complex using CH_2=$CHCH_2CH_2PH_2$.[70] The addition was regio- and stereoselective and only one stereoisomer was obtained in very good yield (85 %).

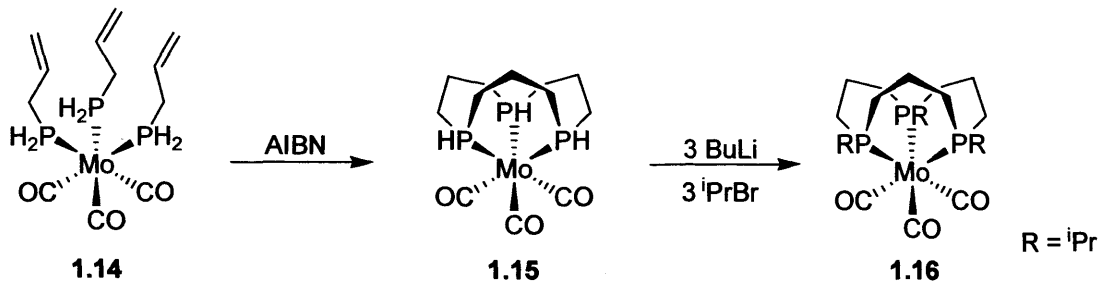

1.14 **1.15** **1.16**

Scheme 11

Norman was unable to liberate the macrocycle ligands from the metal centre however, the preparation of the tertiary triphosphorus macrocycle , **1.16**, was performed later by Edwards and co-workers[71, 72] (Scheme 11), who also achieved its liberation in 1996 by treatment of the molybdenum complex with bromine followed by strong base (NaOH) in ethanol.[73] Edwards' group has also prepared various 9- and 10-membered triphosphorus macrocycles using different metals as a template.[74, 75]

1.5 References

[1] For recent reviews, see: G. P. Marsh, P. J. Parsons, C. McCarthy, X. G. Corniquet, *Org. Lett.*, **2007**, *9*, 2613; T. W. Baughman, J. C. Sworen, K. B. Wagener, *Tetrahedron*, **2004**, *60*, 10943.

[2] For recent reviews, see: R. Castarlenas, C. Vovard, C. Fischmeister, P. H. Dixneuf, *J. Am. Chem. Soc.*, **2006**, *128*, 4079; H. A. Dondas, B. Clique, B. Cetinkaya, R. Grigg, C. Kilner, J. Morris, V. Sridharan, *Tetrahedron*, **2005**, *61*, 10652.

[3] For recent reviews, see: E. Arstad, A. G. M. Barrett, B. T. Hopkins, J. Koebberling, *Org. Lett.*, **2002**, 1975.

[4] For recent reviews, see: H. Hou, K. C. F. Leung, D. Lanari, A. Nelson, J. Fraser Stoddart, R. H. Grubbs, *J. Am. Chem. Soc.*, **2006**, *128(48)*, 15358.

[5] R. R. Schrock, J. S. Murdzek, G. C. Bazan, J. Robbins, M. DiMare, M. O'Regan, *J. Am. Chem. Soc.* **1990**, *112(10)*, 3875.

[6] G. C. Bazan, J. H. Oskam, H. N. Cho, L. Y. Park, R. R. Schrock, *J. Am. Chem. Soc.*, **1991**, *113(18)*, 6899.

[7] R. H. Grubbs (Ed) *Handbook of Metathesis*, Wiley-VCH, Germany, **2003**.

[8] R. H. Grubbs, T. M. Trnka, *Ruthenium-Catalyzed Olefin Metathesis* (S.-I. Murahashi, Ed.), Wiley-VCH, Germany, **2004**.

[9] A. J. Arduengo, R. L. Harlow M. Kline, *J. Am. Chem. Soc.*, **1991**, *113 (1)*, 361.

[10] J. P. Collman, L. S. Hegedus, J. R. Norton, R. G. Finke, *Principles and applications of organotransition metal chemistry,* 2nd. ed., University Science Books, Mill Valley, California, **1987**.

[11] C. A. Tolman, *Chem. Rev.*, **1977**, *77*, 313.

[12] T. Ohkuma, C.A. Sandoval, R. Srinivasan, Q. Lin, Y. Wei, K. Muniz, R. Noyori, *J. Am. Chem. Soc.*, **2005**, *127*, 8288.

[13] A. F. Hill, *Organotransition Metal Chemistry*, The Royal Society of Chemistry, Cambridge, **2002**.

[14] A. G. Orpen, N. G. Connelly, J. Chem. Soc., *Chem. Commun.*, **1985**, 1310.

[15] R. H. Crabtree, *The Organometallic Chemistry of the Transition Metals*, 3rd ed., John Wiley & Son, New York, **2001**.

[16] N.Fey, A. C. Tsipis, S. E. Harris, J. N. Harvey, A. G. Orpen, R. A. Mansson, *Chem. Eur. J.*, **2005**, *12(1)*, 291-302.

[17] R. D. Baechler, K. D. Mislow, *J. Am. Chem. Soc.*, **1970**, *92*, 3090.

[18] F. A. Cotton, B. Hong, *Prog. Inorg. Chem.*, **1992**, *40*, 179.

[19] C. Bianchini, A. Meli, M. Peruzzini, F. Vizza, F. Zanobini, *Coord. Chem. Rev.*, **1992**, *120*, 193.

[20] D. W. Meek, *Homogeneous Catalysis with metal phosphine Complexes* (Ed., L. H. Pignolet), Plenum, New York, **1983**, 257.

[21] F. A. Cotton, G. Wilkinson, C. A. Murillo, M. Bochmann, *Advanced Inorganic Chemistry,* 6th ed., John Wiley & Sons, Inc., New York, **1999**.

[22] E. P. Kyba, S. P. Chou, *J. Am. Chem. Soc.*, **1980**, *102*, 7012.

[23] H. W. Wanzlick, *Angew. Chem., Int. Ed. Engl.*, **1962**, *1*, 75.

[24] H. W. Wanzlick, H. J. Schonherr, *Liebigs Ann. Chem.*, **1970**, *731*, 176.

[25] R. Gleiter, R. Hoffmann, *J. Am. Chem. Soc.*, **1968**, *90*, 5457.

[26] A. J. Arduengo, R. L. Harlow, M. Kline, *J. Am. Chem. Soc.*, **1991**, *113 (1)*, 361.

[27] R. Breslow, *Chem. And Ind.*, **1957**, 893.

[28] R. Breslow, *J. Am. Chem. Soc.*, **1957**, *79 (7)*, 1762.

[29] A. Igau, H. Grutzmacher, A. Baceiredo, G. Bertrand, *J. Am. Chem. Soc.*, **1988**, *110*, 6463.

[30] G. Bertrand, R. Reed, *Coordination Chemistry Reviews*, **1994**, *137*, 323.

[31] R. W. Alder, P. R. Allen, S. J. Williams, *J. Chem. Soc., Chem. Commun.*, **1995**, 1267.

[32] A. J. Arduengo, H. V. R. Dias, R. L. Harlow, M. Kline, *J. Am. Chem. Soc.*, **1992**, *114*, 5530.

[33] R. W. Alder, P. R. Allen, M. Murray, A. G. Orpen, *Angew. Chem. Int. Ed. Engl.*, **1996**, *35*, 1121.

[34] R. W. Alder, M. E. Blake, *Chem. Commun.*, **1997**, 1513.

[35] R. W. Alder, M. E. Blake, C. Bortolotti, S. Buffali, C. P. Butts, E. Lineham, J. M. Oliva, A. G. Orpen, M. J. Quayle, *Chem. Commun.*, **1999**, 241.

[36] M. K. Denk, A. Thadani, K. Hatano, A. J. Lough, *Angew. Chem. Int. Ed. Engl.*, **1997**, *36*, 2607.

[37] N. Kuhn, T. Kratz, *Synthesis*, **1993**, 561.

[38] D. Kovacs, M. S. Lee, D. Olson, J. E. Jackson, *J. Am. Chem. Soc.*, **1996**, *118*, 8144.

[39] D. Enders, K. Breuer, G. Raabe, J. Runsink, J. H. Teles, J. P. Melder, K. Ebel, S. Brode, *Angew. Chem. Int. Ed. Engl.*, **1995**, *34*, 1021.

[40] A. J. Arduengo, J. R. Goerlich, W. J. Marshall, *J. Am. Chem. Soc.*, **1995**, *117*, 11027.

[41] A. J. Arduengo, J. R. Goerlich, W. J. Marshall, *Liebigs Annalen*, **1997**, *2*, 365.

[42] W. A. Herrmann, C. Kocher, L. J. Goossen, G. R. J. Artus, *Chem. Eur. J.*, **1996**, *2*, 1627.

[43] R. W. Alder, P. R. Allen, S. J. Williams, *J. Chem. Soc., Chem. Commun.*, **1995**, 1267.

[44] D. Enders, K. Breuer, J. Runsink, J. H. Teles, *Liebigs Ann. Chem.*, **1996**, 2019.

[45] D. Enders, K. Breuer, J. H. Teles, K. Ebel, *Journal Fur Praktische Chemie-Chemiker-Zeitung*, **1997**, *339*, 397.

[46] J. Wolf, W. Bohlmann, M. Findeisen, T. Gelbrich, H. Hofmann, B. Schulze, *Angew. Chem. Int. Ed.*, **2007**, *46*, 3118.

[47] A. DeHope, V. Lavallo, B. Donnadieu, W. W. Schoeller, G. Bertrand, *Angew. Chem. Int. Ed.*, ***2007***, *46*, 6922.

[48] J. Wolf, W. Bhlmann, M. Findeisen, T.s Gelbrich, H. Hofmann, B. Schulze, *Angew. Chem. Int. Ed.*, **2007**, *46*, 6926.

[49] D. Enders, H. Gielen, G. Raabe, J. Runsink, J. H. Teles, *Chem. Ber.*, **1996**, *129*, 1483.

[50] W. A. Herrmann, M. Elison, J. Fischer, C. Köcher, G. R. J. Artus, *Angew. Chem. Int. Ed. Engl.*, **1995**, *34 (21)*, 2371.

[51] W. A. Herrmann, L. J. Goossen, C. Köcher, G. R. J. Artus, *Angew. Chem. Int. Ed. Engl.*, **1996**, *35 (23-24)*, 2805.

[52] M. Scholl, T. M. Trnka, J. P. Morgan, R. H. Grubbs, *Tetrahedron Lett.*, **1999**, *40*, 2247.

[53] W. A. Herrmann, M. Elison, J. Fischer, C. Kocher, G. R. J. Artus, *Chem. Eur. J.*, **1996**, *2*, 772.

[54] H. V. R. Dias and W. C. J, *Tetrahedron Lett.*, **1994**, *35*, 1365.

[55] L.R. Milgrom, *The Colours of Life: An Introduction to the Chemistry of Porphyrins and Related Compounds.*, Oxford University Press, New York, **1997**.

[56] E. C. Constable, *Metals and Ligand Reactivity*, Ellis Horwood Limited, Chichiester, **1990**.

[57] C. A. McAulife, *Comprehensive Coordination Chemistry*, Vol. 2 (Eds.: G. Wilkinson, R. D. Gillard, J. A. McCleverty), Pergamon, Oxford, **1987**.

[58] E. P. Kyba, A. M. John, S. B. Brown, C. W. Hudson, M. J. McPhaul, A. Harding, K. Larsen, S. Niedzwiecki, R. E. Davis, *J. Am. Chem. Soc.*, **1980**, *102*, 139.

[59] E. P. Kyba, R. E. Davis, C. W. Hudson, A. M. John, S. B. Brown, M. J. McPhaul, L.-K. Liu, A. C. Glover, *J. Am. Chem. Soc.*, **1981**, *103*, 3868.

[60] M. Ciampolini, N. Nardi, F. Zanobini, *Inorg. Chim. Acta.*, **1983**, *76*, L17.

[61] E. P. Kyba, C. W. Hudson, M. J. McPhaul, A. M. John, *J. Am. Chem. Soc.*, **1977**, *99*, 8053.

[62] E. C. Constable, *Coordination chemistry of macrocyclic compounds*, Oxford University press, Oxford, New York, **1999**.

[63] T. A. DelDonno, W. Rosen, *J. Am. Chem. Soc.*, **1977**, *99*, 8051.

[64] D. J. Brauer, T. Lebbe, O. Stelzer, *Angew. Chem. Int. Ed.*, **1988**, *27*, 438.

[65] J. Riker-Nappier, D. W. Meek, *J. Chem. Soc., Chem. Commun.*, **1974**, 442.

[66] C. Toulhoat, M. Vidal, M. Vincens, *Phosphorus, Sulfur, Silicon Rel. Elem.*, **1992**, *71*, 127.

[67] R. Bartsch, S. Hietkamp, S. Morton, H. Peters, O. Stelzer, *Inorg. Chem.*, **1983**, *22*, 3624.

[68] L. G. Scalon, Y. Y. Tsao, S. C. Cummings, K. Toman, D. W. Meek, *J. Am. Chem. Soc.*, **1980**, *102*, 6851.

[69] B. N. Diel, R. C. Haltiwanger, A. D. Norman, *J. Am. Chem. Soc.*, **1982**, *104*, 4700.

[70] B. N. Diel, P. Brandt, F., R. C. Haltiwanger, M. L. J. Hackeny, A. D. Norman, *Inorg. Chem.*, **1989**, *28*, 2811.

[71] S. J. Coles, P. G. Edwards, J. S. Fleming, M. B. Hursthouse, *J. Chem. Soc., Dalton Trans.*, **1995**, 4091.

[72] S. J. Coles, P. G. Edwards, J. S. Fleming, M. B. Hursthouse, *J. Chem. Soc., Dalton Trans.*, **1995**, 1139.

[73] S. J. Coles, P. G. Edwards, J. S. Fleming, M. B. Hursthouse, S. Liyanage, *J. Chem. Soc., Chem. Commun.*, **1996**, 293.

[74] P. D. Newman, P. G. Edwards, K. M. Abdul Malik, *Angew. Chem. Int. Ed.*, **2000**, *39*, 2922.

[75] P. G. Edwards, M. L. Whatton, *J. Chem. Soc., Dalton Trans.*, **2006**, 442.

Chapter 2

Bridging phosphido-phosphino ligands in bimetallic complexes

2.1 Introduction

A major requirement for homogeneous catalysts is the presence of available reactions sites commonly provided by labile spectator ligands. The virtues of phosphine ligands have been known in these systems, and recently, a second generation of catalysts incorporating heterocyclic carbene ligands as well as phosphines has been developed and show increased activity in some applications.

Our synthetic strategy is based upon our successful synthesis of 12- and 9-membered P_3 macrocycles (Figure 1), the latter on Mn(I),[1] but using the benzannulated carbene ligands developed by Hahn *et. al.*[2]

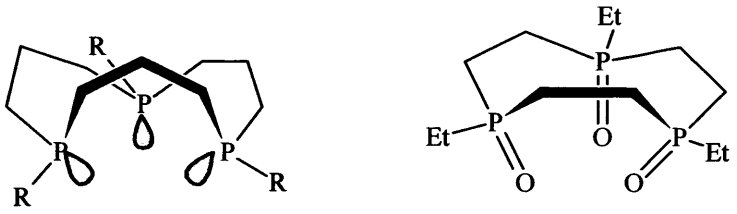

12-[ane]P_3R_3 9-[ane]P_3Et_3

Figure 1: Liberated 12- and 9- membered triphosphorus macrocycles.

The fragment Mn(I)$(CO)_3$ was used as template to synthesise a 9-membered triphosphorus macrocycle.[3] In contrast to Group 6 metal carbonyls $M(CO)_3$, the formation of the macrocycle **2.1.4** (Scheme 1) was possible using the Mn(I)$(CO)_3^+$ template due to the intrinsically smaller radius of the cationic Mn(I) centre compared to that of the neutral metal in the Group 6 metal carbonyls (covalent radii: 1.34 Å for Mn, 1.37 Å for Cr, 1.51 Å for Mo).[4]

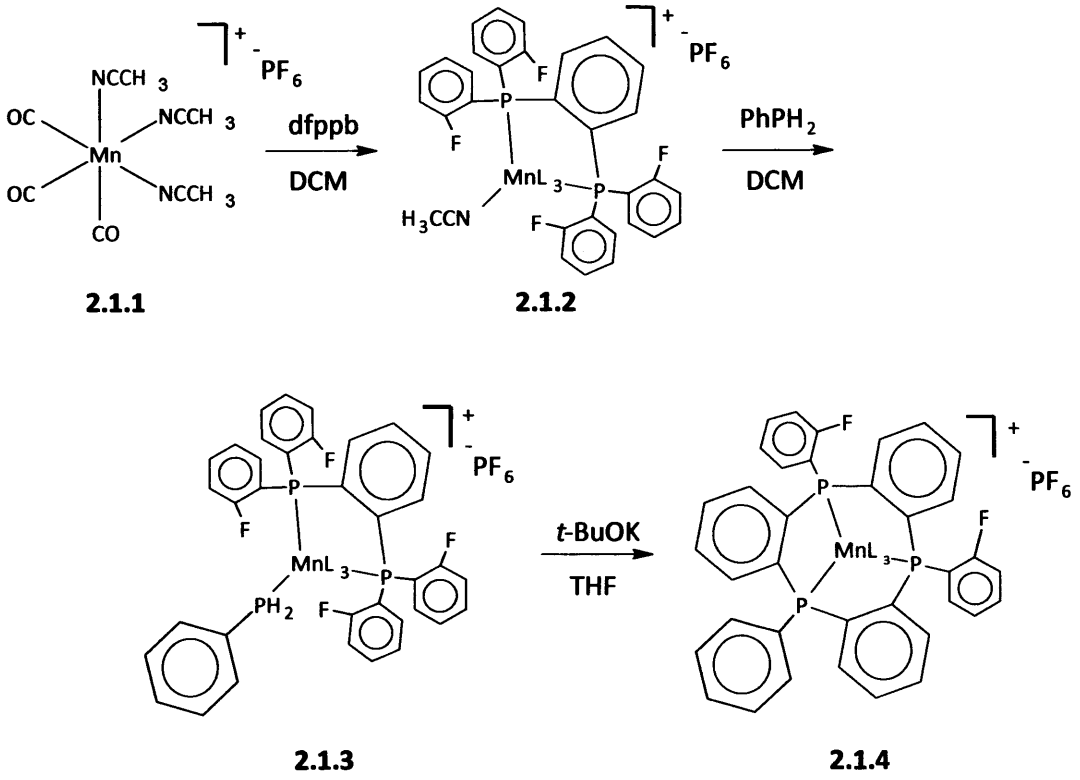

dfppb= 1,2-bis(di-2-fluorophenyl)phosphinobenzene
L= CO

Scheme 1: Synthetic route to, **2.1.4**.

Liberation studies with the Mn(I) macrocycle complex **2.1.4** indicate the possibility of demetallation of the 9-membered triphosphorus macrocycles from the manganese(I) centre.[3]

As mentioned in Chapter 1, both phosphines and nucleophilic heterocyclic carbenes have particular functionalities which make them desirable as ligands in catalysis. Tertiary phosphines are recognised as strong *trans*-effects ligands and are able to activate the coordinated groups in *trans*- position, while carbenes are strong *trans*-influence ligands and are able to labialise the coordinated groups in *trans*- position. Hence, combining both properties with the stability of the macrocycles is of interest and should be effective in promoting migratory reactions of substrate molecules coordinated in *trans*- position. The macrocyclic effect helps prevent unwanted

dissociation (which can lead to the deactivation of the catalyst) by forming a stable 'dust-cap'. They also have the benefit of leaving remaining reaction sites mutually *cis* but *trans* to the good *trans* labilising phosphines/carbenes, both of which are of value in catalysis. Given this recent interest, synthesis of a tridentate donor macrocycle comprising both phosphine and heterocyclic carbene ligands would be of value, although such ligands remain rare.[5] Synthesis of the macrocycle will allow further inverstigation into these properties and potential applications which, given the background research, possibly lie in the field of homogeneous catalysis.

The synthetic strategy (Scheme 2) involved substitution of two carbonyl substituents in **2.2** by a bisphosphino compound, 1,2-bis(phosphino)benzene, **2.a**, 1,2-bis(phosphino)ethane, **2.b**, or 1,3-bis(phosphino)propane, **2.c**, to form fac-tricarbonyl-bis-(1,2-phosphino)bromobenzene manganese(I), **2.3**, and fac-tricarbonyl-bis-(1,2-phosphino)bromoethane manganese(I), **2.4**, respectively. However, the coordination of the 1,3-bis(phosphino)propane to the metal centre, **2.5**, could not be confirmed, which forced us to focus on the *–benzene* and *–ethane* derivatives.

The bromide was then substituted by the weakly coordinating triflate group leading to the disphosphine-triflate derivatives, fac-tricarbonyl-bis-(1,2-phosphino)triflatobenzene manganese(I), **2.6**, and fac-tricarbonyl-bis-(1,2-phosphino)triflatoethane manganese(I), **2.7**, respectively.

Contrary to expectation the introduction of the carbene leads to the deprotonation of one of the phosphorus atoms, **2.11**, **2.12**, rather than coordination to the Mn metal centre, **2.13.a, 2.13.b**.

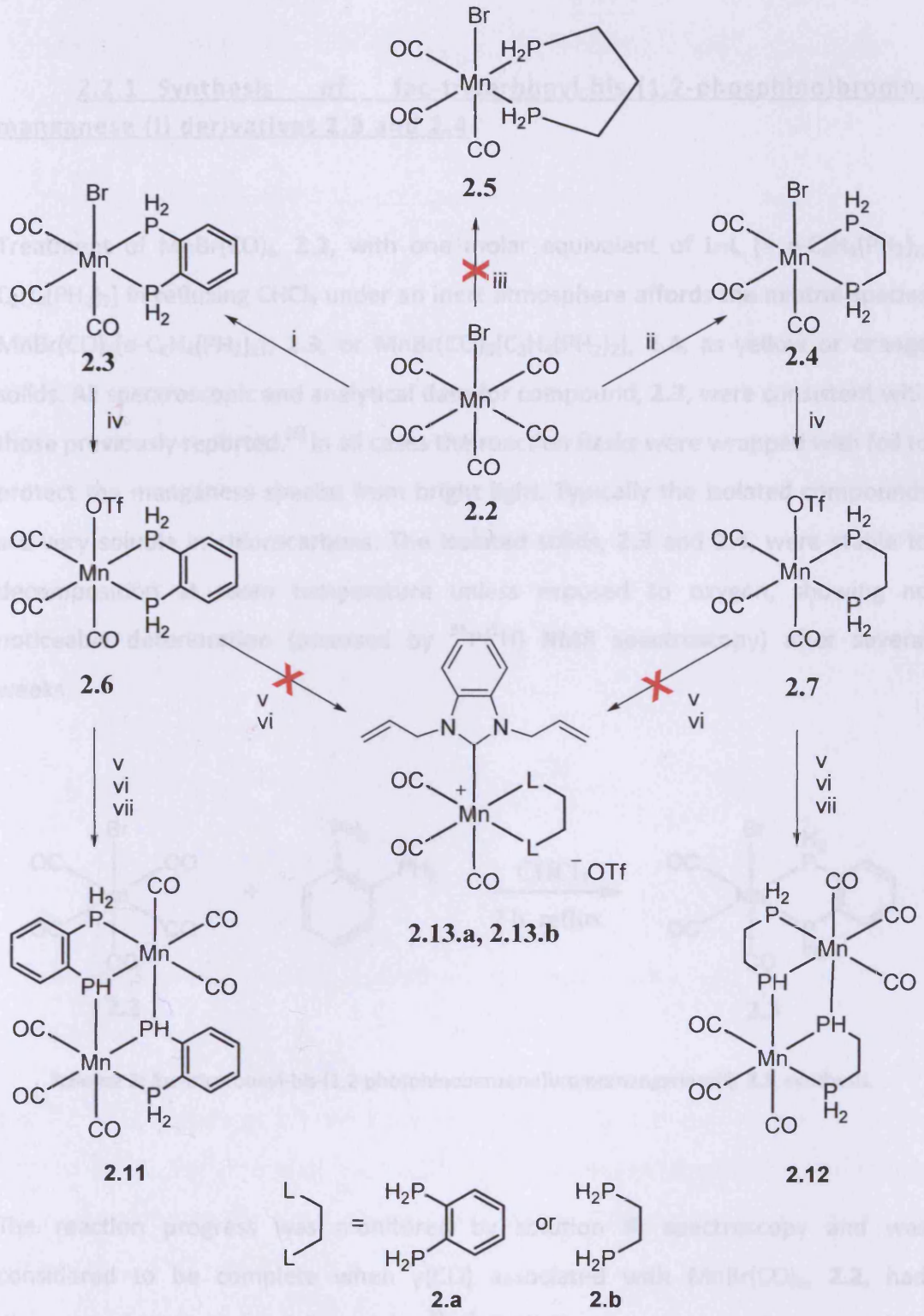

Scheme 2: Synthetic route to **2.11** and **2.12**. Conditions: (i) 1,2-bis(phosphino)benzene, **2.a**, $CHCl_3$; (ii) 1,2-bis(phosphino)ethane, **2.b**, $CHCl_3$; (iii) 1,3-bis(phosphino)propane, **2.c**, $CHCl_3$; (iv) AgOTf, dichloromethane; (v) free carbene, **2.9**, dichloromethane; (vi) Ag(Carbene), **2.10**, dichloromethane; (vii) $KN(SiMe_3)_2$, dichloromethane.

2.2 Results and discussion

2.2.1 Synthesis of fac-tricarbonyl-bis-(1,2-phosphino)bromo-manganese (I) derivatives 2.3 and 2.4

Treatment of $MnBr(CO)_5$, **2.2**, with one molar equivalent of L–L [= *o*-$C_6H_4(PH_2)_2$, $C_2H_4(PH_2)_2$] in refluxing $CHCl_3$ under an inert atmosphere affords the neutral species $MnBr(CO)_3\{o\text{-}C_6H_4(PH_2)_2\}$, **2.3**, or $MnBr(CO)_3\{C_2H_4(PH_2)_2\}$, **2.4**, as yellow or orange solids. All spectroscopic and analytical data for compound, **2.3**, were consistent with those previously reported.[6] In all cases the reaction flasks were wrapped with foil to protect the manganese species from bright light. Typically the isolated compounds are very soluble in chlorocarbons. The isolated solids, **2.3** and **2.4**, were stable to decomposition at room temperature unless exposed to oxygen, showing no noticeable deterioration (assessed by $^{31}P\{^1H\}$ NMR spectroscopy) after several weeks.

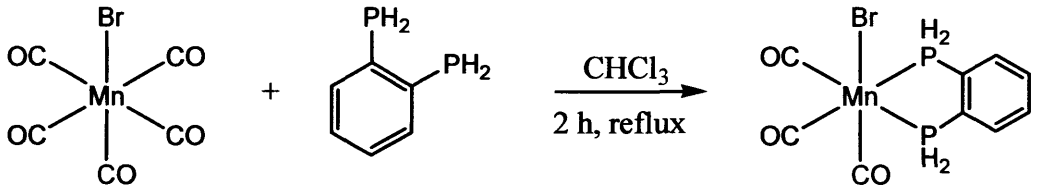

2.2 **2.3**

Scheme 3: *fac*-tricarbonyl-bis-(1,2-phosphinobenzene)bromomanganese(I), **2.3**, synthesis.

The reaction progress was monitored by solution IR spectroscopy and was considered to be complete when ν(CO) associated with $MnBr(CO)_5$, **2.2**, had disappeared. It was also followed by $^{31}P\{^1H\}$ NMR spectroscopy, where complete consumption of starting material 1,2-bis(phosphino)benzene, **2.a**, or 1,2-bis(phosphino)ethane, **2.b**, was observed after 2 hours of reaction.

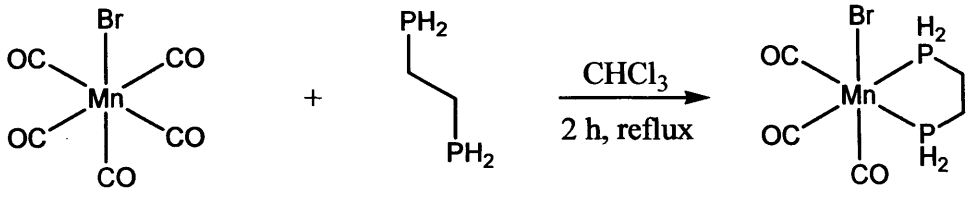

Scheme 4: *fac*-tricarbonyl-bis-(1,2-phosphinoethane)bromomanganese(I), **2.4**, synthesis.

Unfortunately, compound **2.5** could not be fully characterised due to broadening in the NMR spectrum. The reaction produces an unexpected dark-brown "polymer-like" residue and after work up, it appears that most of the free ligand, **2.c**, remained in solution. Different approaches were attempted to try to chelate the bisphosphinopropane ligand, **2.c**, to the Mn metal centre but no discrete metal complex of the ligand could be isolated.

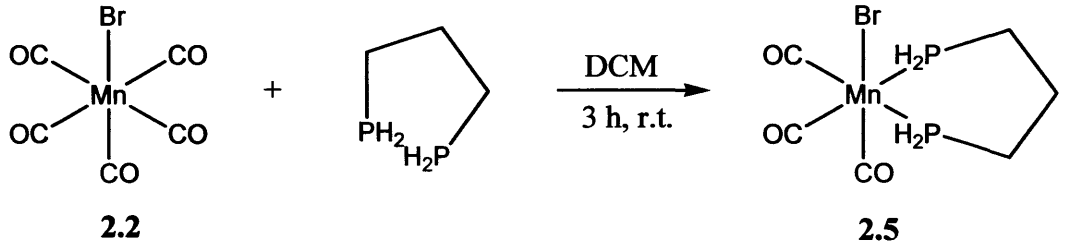

Scheme 5: *fac*-tricarbonyl-bis-(1,3-phosphinopropane)bromomanganese(I), **2.5**, synthesis.

The ^{31}P NMR spectra of **2.3** and **2.4** show signals at δ_P -0.8 ppm (triplet, $^1J_{P\text{-}H}$= 354 Hz) and δ_P -11.2 ppm (triplet, $^1J_{P\text{-}H}$= 353 Hz) respectively confirming that the ligands are facially capping the metal centre as a meridional isomer would present an AB pattern.

The *fac* isomers of $MnBr(CO)_3\{o\text{-}C_6H_4(PH_2)_2\}$, **2.3**, and $MnBr(CO)_3\{C_2H_4(PH_2)_2\}$, **2.4**, have approximate C_s symmetry. Group theory predicts three ν(CO) absorptions for each. Owing to the limited solubility of most of the compounds in non-polar

solvents, and to provide a directly comparable set of data, the IR spectra were recorded in dichloromethane (Table 1). The solution IR spectroscopic studies show three strong CO stretching vibrations at γ(CO) = 2039s, 1976s and 1931s cm^{-1} for **2.3** and γ(CO) = 2037s, 1971s and 1926s cm^{-1} for **2.4** (Table 1) confirming again the facial arrangement of the three carbonyl ligands.

The CO resonances are broad (spanning a few ppm) in the ^{13}C NMR spectrum of **2.4** due to the effect of the directly bonded ^{55}Mn quadrupole.[7] Typically however, two resonances in a 1:2 ratio at δ_C 220.5 ppm and δ_C 216.7 ppm are observed, the one to high frequency being attributed to the CO *trans* to Br and the lower frequency resonance due to the two CO ligands *trans* to L–L. The signal of the two aliphatic carbons is observed at δ_C 15.2 ppm.

As the ligand **2.b** coordinates to the manganese centre, the CH_2 protons in the backbone become diastereotopic, (Figure 2) therefore the ^1H NMR spectrum of **2.4** shows broad resonances at δ_H 5.5 ppm and δ_H 4.6 ppm assigned to the two sets of protons of the primary phosphines and two broad singlets at δ_H 2.3 ppm and δ_H 2.1 ppm for the aliphatic proton of the C_2 backbone. The large P-H observed coupling is also characteristic of coordination.

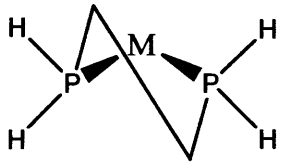

Figure 2: view of the diastereotopic nature of the hydrogens upon coordination.

The ^1H NMR spectrum of **2.3** shows broad resonances at δ_H 5.6 ppm and δ_H 6.5 ppm assigned to the protons of the primary phosphine, identifying clearly two distinct environments for the P-bonded protons and two broad singlets at δ_H 7.6 ppm and δ_H 7.9 ppm assigned to the aromatic protons.

Identification of **2.3** and **2.4** was supported by mass spectrometric measurements which afforded the molecular ions at (m/z: 281.1 amu) for **2.3** and (m/z: 232.9 amu) for **2.4**.

Table 1 : $^{31}P\{^{1}H\}$ NMR[a] and IR spectroscopic data[b] (CO region only)

Complexes	$\delta(^{31}P\{^{1}H\})$	$\gamma(CO)/cm^{-1}$
1,2-bis(phosphino)benzene, 2.a.	-123 ppm	-
1,2-bis(phosphino)ethane, 2.b.	-132 ppm	-
1,3-bis(phosphino)propane, 2.c.	-139 ppm	-
$MnBr(CO)_3\{o\text{-}C_6H_4(PH_2)_2\}$, 2.3.	-0.8 ppm	2039, 1976, 1931
$MnBr(CO)_3\{C_2H_4(PH_2)_2\}$, 2.4.	-11.2 ppm	2037, 1971, 1926
$MnOTf(CO)_3\{o\text{-}C_6H_4(PH_2)_2\}$, 2.6.	-3.5 ppm	2056, 1994, 1944
$MnOTf(CO)_3\{C_2H_4(PH_2)_2\}$, 2.7.	-14.5 ppm	2054, 1989, 1938
Complex, 2.11.	-2.6, -61 ppm	2016, 1993, 1916
Complex, 2.12.	-9.8, -75 ppm	2000 (broad), 1926

[a] Spectra recorded in dichloromethane–$CDCl_3$ solution at 300 K. [b] Solutions in dichloromethane.

2.2.2 Synthesis of fac-tricarbonyl-bis-(1,2-phosphino)triflato-manganese(I) derivatives **2.6** and **2.7**

2.6 and **2.7** were prepared respectively from **2.3** and **2.4**, following a previously reported procedure of Pereira *et al.*[8] The treatment of **2.3** with an equimolar amount of silver triflate in dichloromethane, handled carefully in the dark at room temperature, afforded the metal-triflate complex, **2.6**.

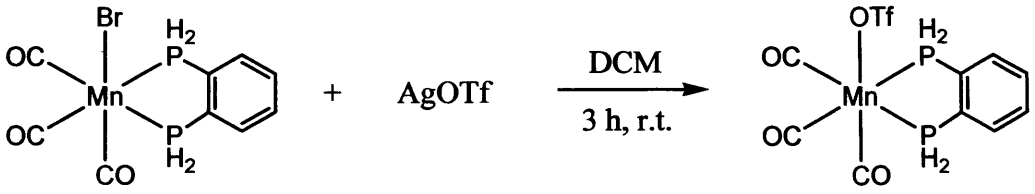

2.3 2.6

Scheme 6: *fac*-tricarbonyl-bis-(1,2-phosphinobenzene)triflatomanganese(I), **2.6**, synthesis.

The same general procedure was applied for the synthesis of compound **2.7** from **2.4**.

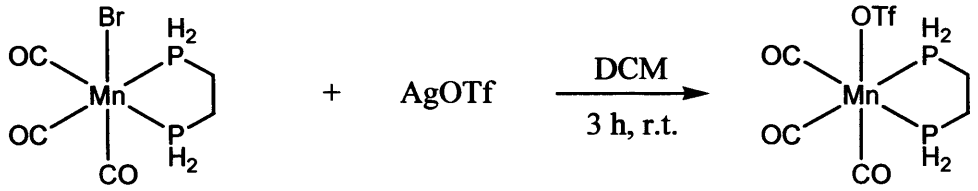

2.4 2.7

Scheme 7: *fac*-tricarbonyl-bis-(1,2-phosphinoethane)triflatomanganese(I), **2.7**, synthesis.

The reaction was followed in solution by IR spectroscopy. The IR spectrum of **2.7** in the terminal carbonyl region shows three strong bands at ν(CO) = 2054s, 1989s and 1938s cm^{-1}. This is consistent with the facial arrangement of the three CO ligands in the coordination sphere. Two bands arise from the symmetric and asymmetric stretching vibrations of the two equivalent *cis*-carbonyls. The remaining band at lowest frequency might be assigned to the ligand *trans* to bromide or triflate since the greatest degree of Mn-CO π bonding is expected for **2.4**, where Br^- is a good π-donor. The increase of the lowest energy CO frequency on going from Br^- to the triflate ligand is consistent with the trans-influence of the axial ligands. The increased electron withdrawing ability of the triflate group results in a weaker π-

bonding in the metal-carbonyl bond. The three initial carbonyls bands of the facial compound **2.3** (γ(CO) = 2039s, 1976s and 1931s cm^{-1}) were shifted to higher frequency during formation of **2.6** (γ(CO) = 2054s, 1989s and 1938s cm^{-1}) for the same reasons as previously described.

The compounds **2.6** and **2.7** show a single resonance in their ^{31}P NMR spectra at δ_P -3.5 ppm (triplet, $^1J_{P-H}$ = 369 Hz) and δ_P -14.5 ppm (triplet, $^1J_{P-H}$ = 356 Hz), respectively, consistent with a facial configuration. The small ^{31}P NMR high field shift (about ~ 3 ppm) when compared to the neutral bromo precursor complex **2.3** δ_P -0.8 ppm (triplet, $^1J_{P-H}$ = 354 Hz) or **2.4** δ_P -11.2 ppm (triplet, $^1J_{P-H}$ = 353 Hz) might be attributed to the electonegativity of the triflate ligand.

The ^1H NMR spectrum of **2.6** shows two broad singlets at δ_H 7.6 and δ_H 8.0 ppm assigned to the aromatic protons, and a broad doublet of multiplets at δ_H 6.0 ppm (dm, $^1J_{H-P}$= 350 Hz) assigned to the protons of the primary phosphines. The ^{13}C NMR spectrum also confirms the synthesis of **2.6**, with a quartet with a large coupling at δ_C 118.8 ppm (d, $^1J_{C-F}$= 320 Hz) is assigned to the quaternary carbon of the triflate group, whilst the virtual triplet at δ_C 130.1 (vt, $^{1,2}J_{C-P}$= 44.6 Hz) is assigned to the quaternary aromatic carbon. The signal of the two other aromatic carbons are observed as a singlet at δ_C 132.1 and a triplet at δ_C 135.3 ppm (t, $^2J_{C-P}$= 6.2 Hz). The two different carbonyl carbons are observed at δ_C 213.6 and 217.9 ppm as broad singlets in a 2:1 ratio, assigned to the equatorial and axial carbonyls respectively.

The ^1H NMR spectrum of **2.7** shows a broad doublet at δ_H 5.0 ppm (d, $^1J_{H-P}$= 356 Hz) assigned to the protons of the primary phosphine, and a very broad doublet at δ_H 2.2 ppm assigned to the aliphatic protons. The ^{13}C NMR spectrum also confirms the synthesis of **2.7** as previously described a typical large doublet at δ_C 123.0 ppm (d, $^1J_{C-F}$= 318 Hz) is assigned to the quaternary carbon for the triflate group, whilst the triplet at δ_C 14.8 ppm (t, $^1J_{C-H}$= 23 Hz) is assigned to the aliphatic carbons. The two different carbonyl carbons are observed at δ_C 213.8 and 219.0 ppm as broad singlets in a 2:1 ratio, assigned to the equatorial and axial carbonyls respectively.

Identification of **2.6** and **2.7** was unequivocally confirmed by mass spectrometric measurement which afforded the molecular ion at (m/z: 281.2 amu) for **2.6** and (m/z: 233 amu) for **2.7**.

As previously stated, the directly bonded ^{55}Mn quadrupolar nucleus results in the different spectrum resonances being broadened. The data are in accord with other phosphine complexes, exhibiting the same trends in co-ordination shift and chelate ring-size effects.[6] $Mn(OTf)(CO)_3\{o\text{-}C_6H_4(PH_2)_2\}$, **2.6**, and $Mn(OTf)(CO)_3\{C_2H_4(PH_2)_2\}$, **2.7**, show a large, high frequency coordination shift consistent with the presence of a five-membered chelate ring.

The isolated solids **2.6** and **2.7** were stable to decomposition at room temperature unless exposed to oxygen, showing no noticeable deterioration (assessed by $^{31}P\{^1H\}$ NMR spectroscopy) after several weeks. These complexes were normally generated *in situ* as their isolation is not necessary for the next step.

2.2.3 Synthesis of free carbene **2.9** and silver-carbene transfer agent **2.10**

The preparation of the free carbene was conducted as previously reported,[9] and was generated *in situ* at low temperature within 20 min to 30 min (Scheme 8) to avoid any pericyclic reactions.

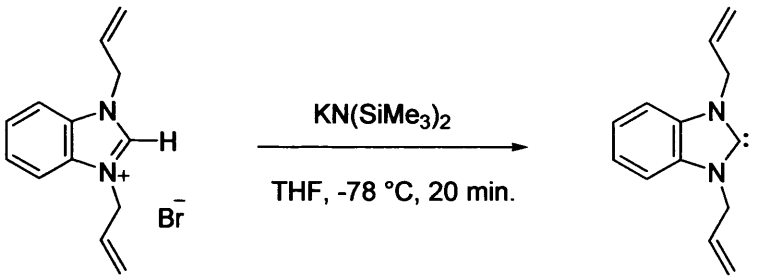

2.8 **2.9**

Scheme 8: Synthesis of free carbene, **2.9**.

As previously reported[10] free benzimidazol-2-ylidenes dimerize unless protected with sterically demanding N-substituents. In the case of N-allyl substituted derivatives the C=C double bond of the resulting dibenzotetraazafulvalene reacts with the double bond of the allyl group in a series of pericyclic reactions (Scheme 9).

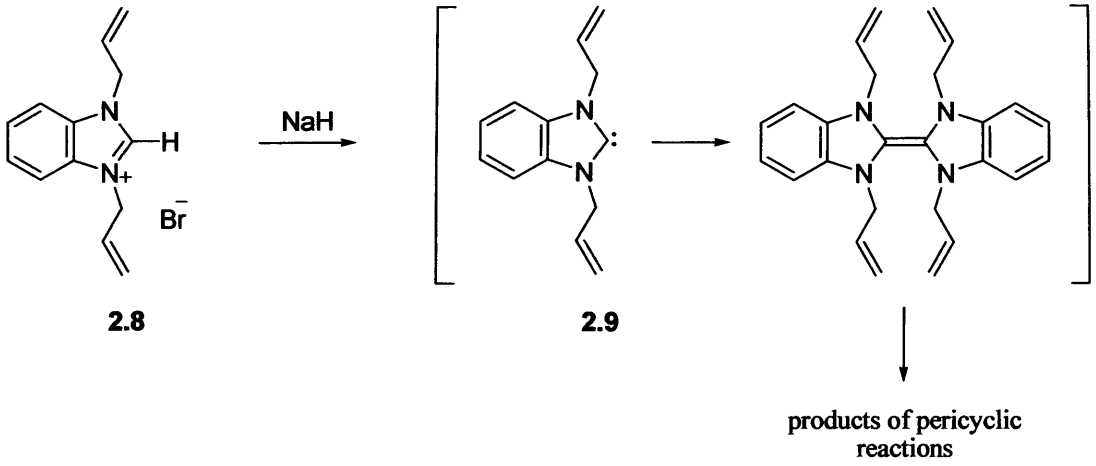

2.8 2.9

Scheme 9: Preparation of free carbene and possible pericyclic reactions.

The preparation of a carbene transfer agent was also required since attempts at coordinating the carbene from the free carbene were unsuccessful.

Silver has recently been shown to form excellent carbene transfer agents,[11] which are prepared by simply stirring **2.8** with silver(I) oxide (Ag_2O) in the absence of light to produce the 1,3-diallylbenzimidazol-2-ylidene complex **2.10** which may be isolated as white crystals (Scheme 10).

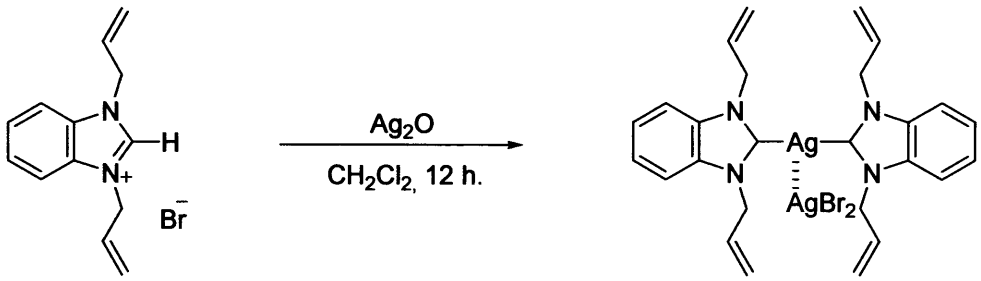

2.8 **2.10**

Scheme 10: Silver-carbene transfer agent, **2.10**, synthesis.

Compound **2.10** Consists of a linear $[Ag(1,3\text{-di}(2\text{-propenyl})benzimidazol\text{-}2\text{-ylidene})_2]^+$ cation and a linear $[AgBr_2]^-$ anion.[11] These two ions associate through an Ag^I-Ag^I interaction. The ^1H NMR spectrum of **2.10** clearly indicates the desired reaction has gone to completion. In the ^1H NMR spectrum of **2.8**, the imidazoliuim proton is seen at δ_H 11.5 ppm, this is not present in complex **2.10** indicating coordination and hence loss of the proton, it can also be seen that a general downfield shift of about 2 ppm of the protons signals has occurred in complex **2.10** compared with **2.8**, which also indicates coordination.

The Ag_2O method offers a number of advantages. The silver NHC complexes can be prepared in air and purified solvents or an additional base are not necessary. The preparation of the silver-carbene complexes and the transfer of the carbene ligand to other transition metals has become a standard procedure in spite of a few reported cases where the method failed.[12]

2.2.4 Coordination chemistry of NHC ligand **2.9** or **2.10** to fac-tricarbonyl-bis-(1,2-phosphino)(L)manganese(I) (L= Br, OTf) derivatives **2.6** or **2.7**

Treatment of **2.6** with free-carbene, **2.9**, or Ag-carbene, **2.10**, in dichloromethane carefully handled in the absence of light at -78 °C, after 2 hours stirring, give rise to an orange-yellow precipitate, **2.11**.

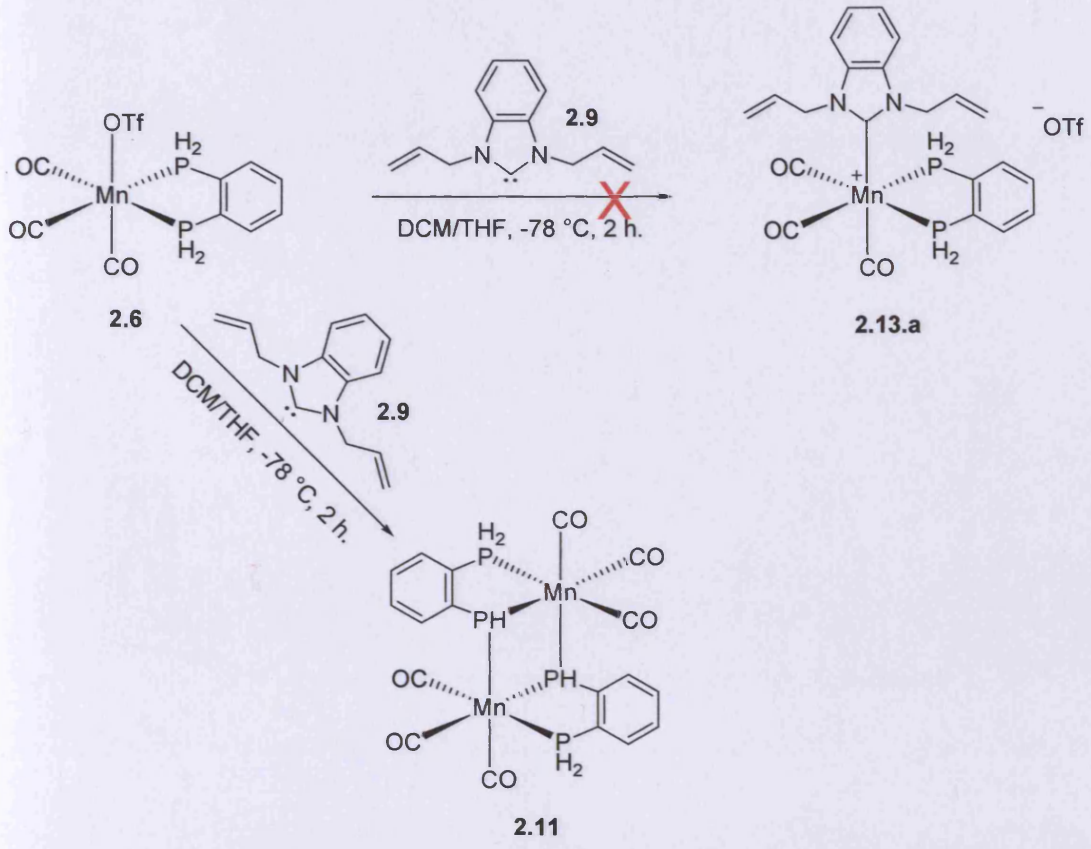

Scheme 11: Bridging bisphosphido-phosphinobenzene di-manganese complex, **2.11**.

The same general procedure was applied to synthesise compound **2.12** from **2.7**. The resultant solid formed was isolated and characterised to identify a new class of bridging phosphido-phosphino di-manganese compounds.

Compounds **2.11** and **2.12** were characterised by analytical and spectroscopic methods and by an X-ray crystal structure determination for **2.11**.

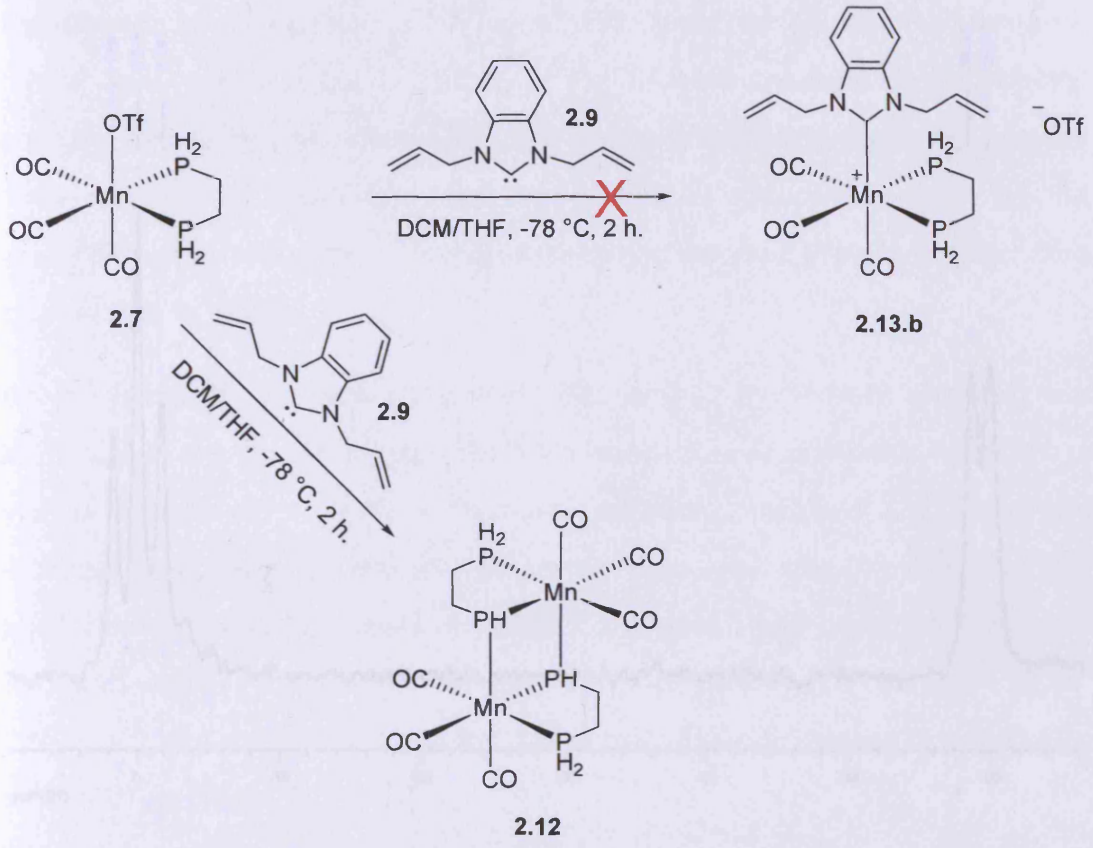

Scheme 12: Bridging bisphosphido-phosphinoethane di-manganese complex, **2.12**.

At room temperature the ^{31}P NMR spectra of the new complexes, **2.11** and **2.12**, were not well resolved and low temperature acquisition method was required.

The ^{31}P NMR spectra of **2.11** (Spectrum 1) or **2.12** (Spectrum 2) at -70 °C shows the presence of two new resonances, a triplet at δ_P 0.1 ppm (triplet, $^1J_{P\text{-}H}$ = 349 Hz, **P**H_2) and a doublet at δ_P -59.2 ppm (d, $^1J_{P\text{-}H}$ = 285 Hz, **P**H) or a triplet at δ_P -3.1 ppm (triplet, $^1J_{P\text{-}H}$ = 335 Hz, **P**H_2) and a doublet at δ_P -62.3 ppm (doublet, $^1J_{P\text{-}H}$ = 273 Hz, **P**H) respectively. The resonances of the precursor complexes seen at δ_P -3.5 ppm (triplet, $^1J_{P\text{-}H}$ = 369 Hz) for **2.6**, and δ_P -14.5 ppm (triplet, $^1J_{P\text{-}H}$ = 356 Hz) for **2.7** are no longer evident. This unexpected pattern suggests the presence of both primary and secondary phosphines in the new compound.

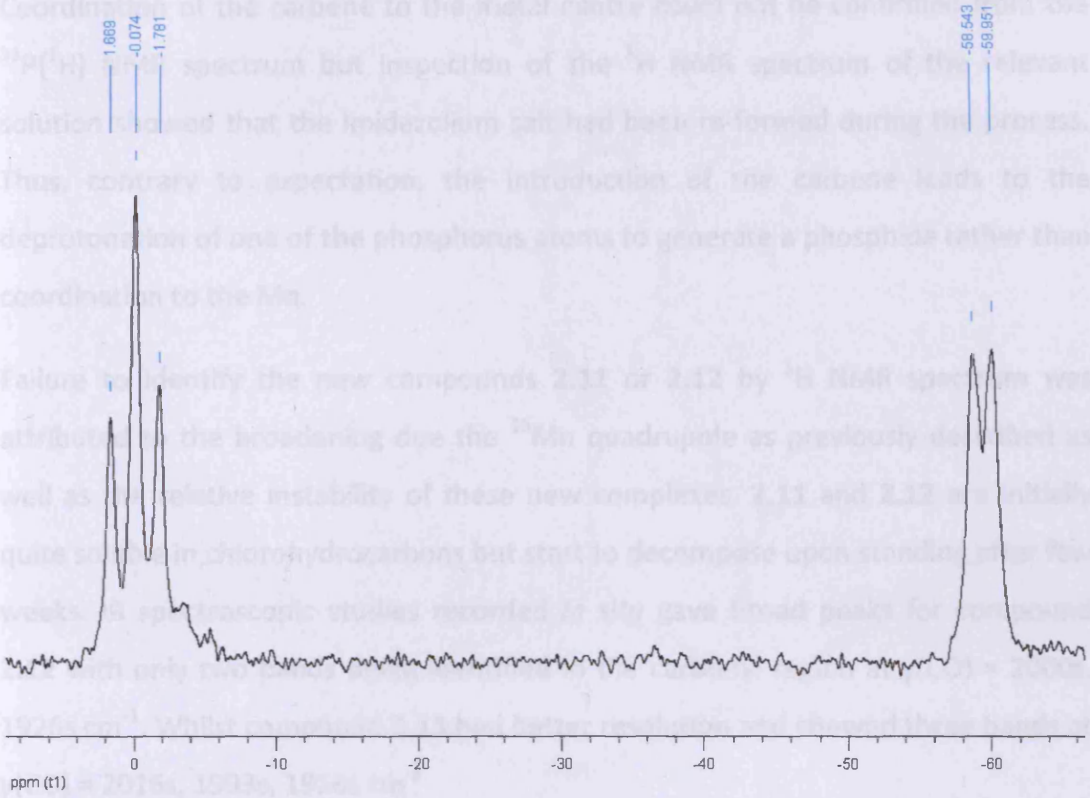

Spectrum 1: ^{31}P NMR spectrum at -70 °C of **2.11**.

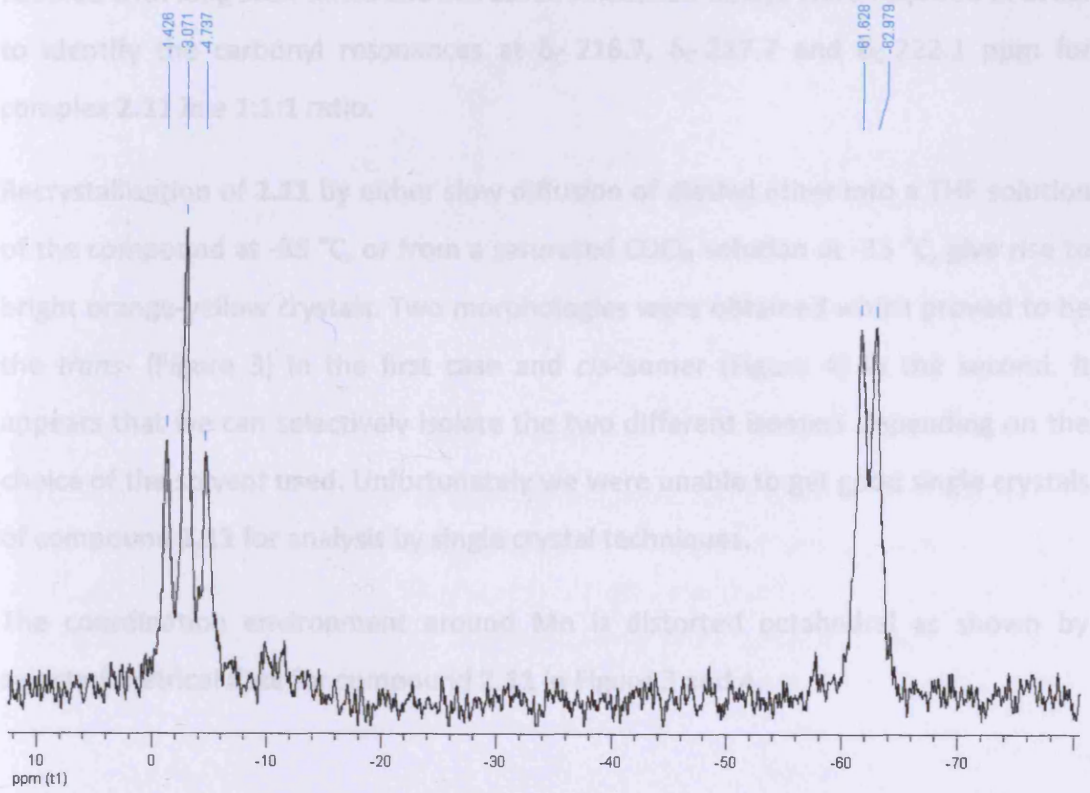

Spectrum 2: ^{31}P NMR spectrum at -70 °C of **2.12**.

Coordination of the carbene to the metal centre could not be confirmed from the $^{31}P\{^{1}H\}$ NMR spectrum but inspection of the ^{1}H NMR spectrum of the relevant solution showed that the imidazolium salt had been re-formed during the process. Thus, contrary to expectation, the introduction of the carbene leads to the deprotonation of one of the phosphorus atoms to generate a phosphide rather than coordination to the Mn.

Failure to identify the new compounds **2.11** or **2.12** by ^{1}H NMR spectrum was attributed to the broadening due the ^{55}Mn quadrupole as previously described as well as the relative instability of these new complexes. **2.11** and **2.12** are initially quite soluble in chlorohydrocarbons but start to decompose upon standing after few weeks. IR spectroscopic studies recorded *in situ* gave broad peaks for compound **2.12** with only two bands being identified in the carbonyl region at $\gamma(CO)$ = 2000s, 1926s cm^{-1}. Whilst compound **2.11** had better resolution and showed three bands at $\gamma(CO)$ = 2016s, 1993s, 1916s cm^{-1}

The $^{13}C\{^{1}H\}$ NMR spectra were also very broad such that a low temperature (-70 °C) coupled with long scan tunes and increased relaxation delays were required in order to identify the carbonyl resonances at δ_C 216.7, δ_C 217.7 and δ_C 222.1 ppm for complex **2.11** in a 1:1:1 ratio.

Recrystallisation of **2.11** by either slow diffusion of diethyl ether into a THF solution of the compound at -35 °C, or from a saturated $CDCl_3$ solution at -35 °C, give rise to bright orange-yellow crystals. Two morphologies were obtained which proved to be the *trans*- (Figure 3) in the first case and *cis*-isomer (Figure 4) in the second. It appears that we can selectively isolate the two different isomers depending on the choice of the solvent used. Unfortunately we were unable to get good single crystals of compound **2.12** for analysis by single crystal techniques.

The coordination environment around Mn is distorted octahedral as shown by selected metrical data for compound **2.11** in Figure 3 and 4.

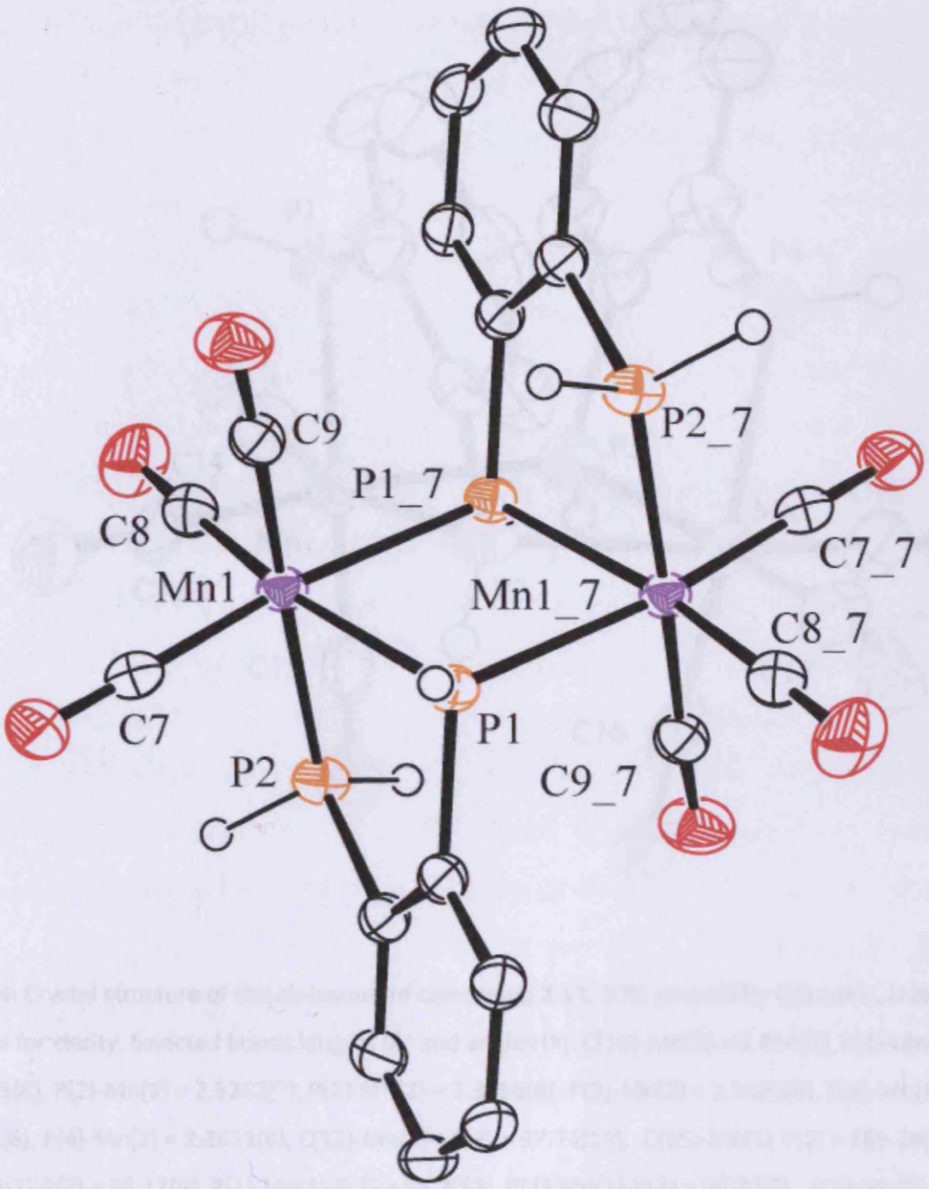

Figure 3: Crystal structure of the *trans*-isomer of compound **2.11**, 50% probability Ellipsoids, H atoms and THF solvent omitted for clarity. Selected bonds lengths (Å) and angles (º): Mn(1)-C(7) = 1.808(2), Mn(1)-C(9) = 1.812(2), Mn(1)-C(8) = 1.812(2), Mn(1)-P(2) = 2.271(1), Mn(1)-P(1) = 2.336(1), Mn(1)-P(1)' = 2.352(1), C(7)-Mn(1)-C(8) =96.35(8), C(9)-Mn(1)-P(2) =173.18(6), C(8)-Mn(1)-P(2) =94.12(6), C(7)-Mn(1)-P(1) =95.50(6), C(8)-Mn(1)-P(1) =167.23(6), P(2)-Mn(1)-P(1) =81.55(3).

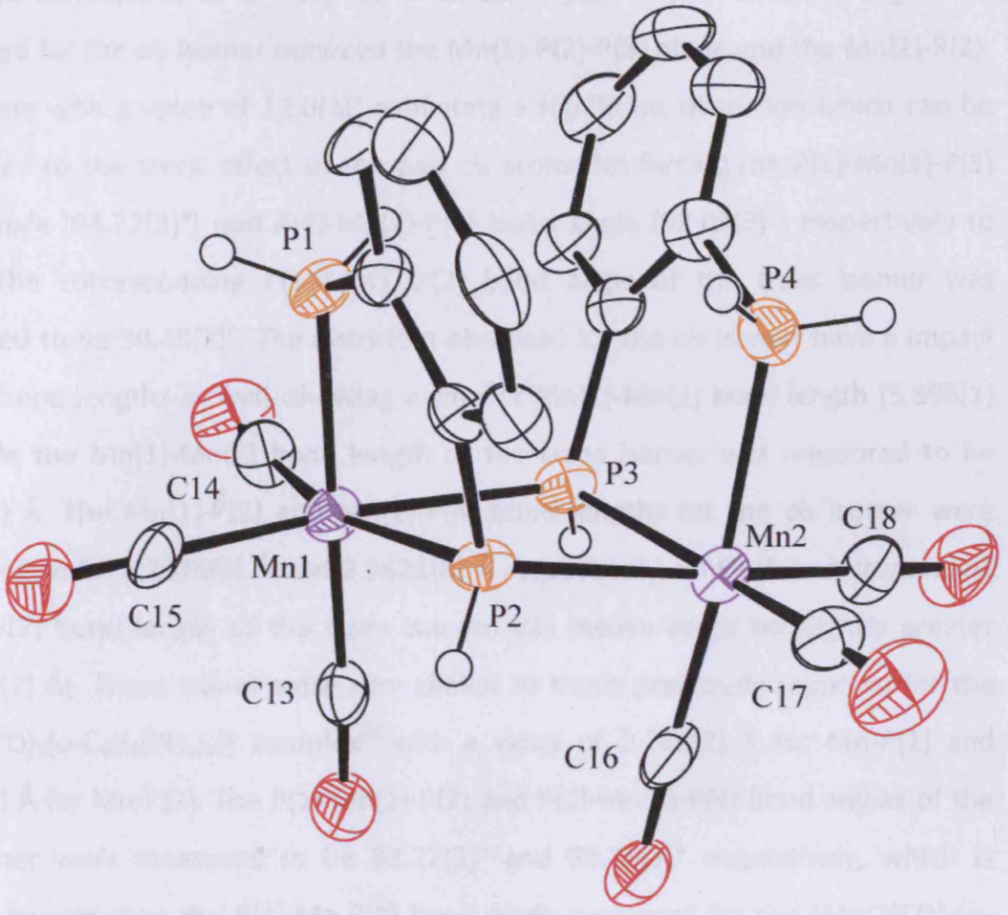

Figure 4: Crystal structure of the *cis*-isomer of compound **2.11**, 50% probability Ellipsoids, H atoms omitted for clarity. Selected bonds lengths (Å) and angles (º): C(18)-Mn(2) = 1.814(3), P(1)-Mn(1) = 2.2625(8), P(2)-Mn(1) = 2.3262(7), P(2)-Mn(2) = 2.3556(8), P(3)-Mn(2) = 2.3188(8), P(3)-Mn(1) = 2.3452(8), P(4)-Mn(2) = 2.2621(8), C(15)-Mn(1)-C(13) = 97.71(13), C(15)-Mn(1)-P(2) = 165.24(10), C(13)-Mn(1)-P(2) = 96.17(9), P(1)-Mn(1)-P(2) = 83.22(3), P(1)-Mn(1)-P(3) = 94.22(3), P(2)-Mn(1)-P(3) = 74.59(3), C(16)-Mn(2)-C(17) = 97.10(14), C(16)-Mn(2)-P(4) = 86.73(10), C(17)-Mn(2)-P(3) = 168.70(10), P(4)-Mn(2)-P(3) = 83.18(3), C(16)-Mn(2)-P(2) = 168.09(10), C(17)-Mn(2)-P(2) = 94.79(10), P(3)-Mn(2)-P(2) = 74.53(3), C(2)-P(2)-Mn(1) = 108.03(8), C(2)-P(2)-Mn(2) = 114.96(9), Mn(1)-P(2)-Mn(2) = 104.33(3), C(7)-P(3)-Mn(2) = 108.08(10), C(7)-P(3)-Mn(1) = 114.67(9), Mn(2)-P(3)-Mn(1) = 104.90(3), C(8)-P(4)-Mn(2) = 111.24(10).

The coordination environment around Mn for the *cis* and the *trans* isomers was found to correspond to a distorted octahedral geometry. A dihedral angle was measured for the *cis* isomer between the Mn(1)-P(2)-P(3) plane and the Mn(2)-P(2)-P(3) plane with a value of 12.0(3)° exhibiting a significant distortion which can be attributed to the steric effect of the two *cis* aromatics forcing the P(1)-Mn(1)-P(3) bond angle [94.22(3)°] and P(4)-Mn(2)-P(2) bond angle [93.06(3)°] respectively to open. The corresponding P(1)-Mn(1)-P(2) bond angle of the *trans* isomer was measured to be 90.49(2)°. The distortion observed for the *cis* isomer have a impact on the bond lengths as well, showing a smaller Mn(1)-Mn(2) bond length [3.698(1) Å], while the Mn(1)-Mn(2) bond length of the trans isomer was measured to be 3.715(1) Å. The Mn(1)-P(1) and Mn(2)-P(4) bond lengths for the *cis* isomer were measured to be 2.2625(8) Å and 2.2621(8) Å respectively, while the corresponding Mn(1)-P(2) bond length of the trans isomer was measured to be slightly greater [2.2710(7) Å]. These values were very similar to those previously reported for the $[MnCl(CO)_3\{o\text{-}C_6H_4(PH_2)_2\}]$ complex[6] with a value of 2.280(2) Å for Mn-P(1) and 2.281(2) Å for Mn-P(2). The P(1)-Mn(1)-P(2) and P(3)-Mn(2)-P(4) bond angles of the *cis* isomer were measured to be 83.22(3)° and 83.28(3)° respectively, which is slightly greater than the P(1)-Mn-P(2) bond angle measured for the $[MnCl(CO)_3\{o\text{-}C_6H_4(PH_2)_2\}]$ complex.[6] The P(1)-Mn(1)-P(2) of the analogous bond angle of the *trans* isomer was smaller [81.55(3)°].

Despite the fact that the NMR spectroscopic data for **2.11** and **2.12** were not well resolved, the discovery of two isomers in the solid state helps shed some light on the broad nature of the ^1H and $^{13}C\{^1H\}$ NMR resonances. At room temperature the ^1H NMR spectrum shows very broad resonances. This broadening can be attributed not only to the quadrupolar Mn nucleus but may be due to a dynamic equilibrium between the two isomers interconverting rapidly in solution at room temperature. Low temperature ^1H NMR spectroscopy of **2.11** did not slow this process sufficiently to allow acquisition of a better resolved spectrum.

At room temperature the $^{13}C\{^1H\}$ NMR spectrum consist of two resonances attributable to the carbonyl carbons at δ_C 215.2 ppm and δ_C 219.0 ppm in an approximate ration of 2:1 respectively. These two resonances are consistent with either static structure (*cis* or *trans*) of compound **2.11** since the structures consist of two sets of carbonyls including two equivalent equatorial and one axial carbonyl. A time average spectrum at room temperature would display the same features. At low temperature (-70 °C), however, three resonances are observed in the $^{13}C\{^1H\}$ NMR spectrum (δ_C 222.1 ppm, δ_C 216.7 ppm and δ_C 217.7 ppm) indicating that any dynamic process inerconverting the isomer is slow (on the NMR time scale) at this temperature. The three resonances may be explained by the spectra of the two individual static structures (which would give rise to two resonances each) overlapping such that one resonance is accidentally coincident. This is reasonable in view of the small differences in environment between each isomer and the broadening of the quadrupolar Mn centre.

Identification of **2.11** was also confirmed by mass spectrometric measurement which afforded the molecular ion at (m/z: 560 amu) as well as satisfactory elemental analysis (see Experimental). Compound **2.12** did not provide satisfactory mass spectrometric measurement but afforded a satisfactory elemental analysis (see Experimental).

2.3 Conclusion

A practical synthesis of novel bridging bimanganese phosphido-phosphino ligands has been achieved. The new complexes have been successfully isolated and characterised by spectroscopic methods, including their precursors. The results show that the carbene acted as a base which was able to deprotonate a proton on one of the phosphorus atoms rather than coordination to the Mn metal centre, leading in the formation of complexes **2.11** and **2.12**. Single crystals were successfully obtained by slow diffusion of diethylether into a tetrahydrofuran solution of **2.11** at -35 °C to produce the *trans*-isomer and from a saturated $CDCl_3$ solution of **2.11** at -35 °C to produce the *cis*-isomer.

Unfortunately the 1,3-bisphosphinopropane analogous derivative could not be prepared, but rather adopts a polymeric nature whilst coordinate to the $MnBr(CO)_5$ in a 1:1 ratio.

2.4 Experimental

2.4.1 Methods and materials

Unless otherwise stated all manipulations were carried out using standard Schlenk techniques under an atmosphere of dry nitrogen. All solvents were dried and degassed by refluxing over standard drying agents under a nitrogen atmosphere. The compounds 1,2-bis(phosphino)ethane, **2.b**, 1,2-bis(phosphino)benzene, **2.a**, 1,3-bis(phosphino)propane, **2.c**, and 1,3-di-(2-propenyl)-bemzimidazolium bromide, **2.8**, were prepared according to literature methods.[2, 13, 14] $KN[Si(Me)_3]_2$, $MnBr(CO)_5$ and $AgSO_3CF_3$ were obtained from Aldrich Chemical Company and used without further purification. Deuterated solvents were dried over 3 or 4 Å molecular sieves and degassed by freeze-pump-thaw methods. The NMR spectra were recorded on a Bruker DPX-500 instrument operating at 500 MHz (^1H), 125.75 MHz (^{13}C) and 202.75 MHz (^{31}P), a Bruker DPX-400 instrument operating at 400 MHz (^1H) and 100 MHz (^{13}C), and a Jeol Lamda Eclipse 300 operating at 121.65 MHz (^{31}P) and 75.57 MHz (^{13}C). ^1H and ^{13}C chemical shifts are quoted in ppm relative to residual solvent resonances, and ^{31}P chemical shifts are quoted in ppm relative to external 85 % H_3PO_4. Infra-red spectra were recorded on a JASCO FT/IR-660 plus Spectrometer and the samples were prepared under N_2 as KBr disks or in solution. Mass spectra of all the samples have been collected by direct injection into a Waters LCT Premier XE mass spectrometer fitted with an ESCI source.

Elemental analyses were performed by MEDAC LTD, UK,[15] Analytical and Chemical Consultancy Services.

2.4.2 Syntheses

2.4.2.1 Synthesis of $MnBr(CO)_3\{o\text{-}C_6H_4(PH_2)_2\}$, **2.3**.

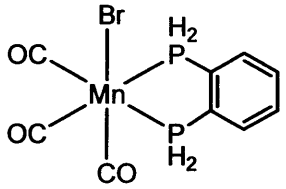

In the absence of light, a solution of 1,2-bis(phosphino)benzene, **2.a**, in chloroform was added to a solution of $MnBr(CO)_5$, **2.2**, in chloroform. The reaction mixture was refluxed for 2 hours, the yellow solution filtered, and the solvent removed *in vacuo* leaving a yellow solid. The solid was washed with cold diethyl ether leading to **2.3** as a pale yellow solid. Yield: 87 %. ^{1}H NMR δ ppm ($CDCl_3$) = 5.57 (d, 2 H, $^1J_{H\text{-}P}$ = 380 Hz, $PH_aH_{a'}$), 6.5 (d, 2 H, $^1J_{H\text{-}P}$ = 334 Hz, $PH_aH_{a'}$), 7.6 (br s, 2 H, Ph), 7.9 (s, 2 H, Ph). ^{13}C NMR δ ppm ($CDCl_3$) = 131.4 (s, Ph), 132.1 (t, $^1J_{C\text{-}P}$ = 44.2 Hz, $^2J_{C\text{-}P}$ = 44.2 Hz, **C**), 135.1 (d, $^2J_{C\text{-}P}$ = 6.9 Hz, Ph), 214.9 (br s, **C**O eq.), 217.9 (br s, **C**O, ax.). ^{31}P NMR δ ppm ($CDCl_3$) = -0.8 (t, $^1J_{P\text{-}H}$ = 354 Hz, PH_2). IR (CH_2Cl_2) = ν(CO) = 2039s, 1976s and 1931s cm^{-1}. Anal. Calc. for $C_9H_8O_3BrMnP_2$ (360.95) = C, 29.95; H, 2.23. Found = C, 30.05; H, 2.28%. (TOF-MS, ES^+): m/z (%): 281.1 (34) $[M - Br]^+$.

2.4.2.2 Synthesis of $MnBr(CO)_3\{C_2H_4(PH_2)_2\}$, **2.4**.

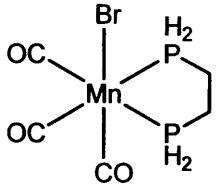

In the absence of light, a solution of 1,2-bis(phosphino)ethane, **2.b**, in chloroform was added to a solution of $Mn(CO)_5Br$, **2.2**, in chloroform. The reaction mixture was refluxed for 3 hours. The yellow solution was filtered, and the solvent removed *in vacuo* leaving a yellow solid. The solid was washed with cold diethyl ether leading to **2.4** as a pale yellow solid. Yield: 86 %. ^{1}H NMR δ ppm ($CDCl_3$) = 2.1 (br s, 2 H, C_bH_2), 2.3 (br s, 2 H, C_aH_2), 4.6 (br d, 2 H, $^1J_{H\text{-}P}$ = 370 Hz, $PH_aH_{a'}$), 5.5 (br d, 2 H, $^1J_{H\text{-}P}$ = 329 Hz, $PH_aH_{a'}$). ^{13}C NMR δ ppm ($CDCl_3$) = 15.2 (m, CH_2), 216.6 (br s, **C**O eq.), 220.5 (br s, **C**O,

ax.). ^{31}P NMR δ ppm ($CDCl_3$) = -11.2 (t, $^1J_{P-H}$ = 353 Hz, PH_2). IR (CH_2Cl_2) = γ(PH) = 2356s cm^{-1}, γ(CO) = 2037s, 1971s and 1926s cm^{-1}. Anal. Calc. for $C_5H_8O_3BrMnP_2$ (312.90) = C,19.19; H,2.58. Found = C,19.47; H,2.67%. (TOF-MS, ES^+): m/z (%): 232.93 (58) $[M - Br]^+$.

2.4.2.3 Synthesis of $Mn(OTf)(CO)_3\{o\text{-}C_6H_4(PH_2)_2\}$, **2.6**.

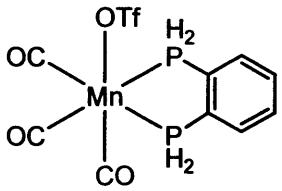

In the absence of light, a solution of AgOTf in dichloromethane was added to a solution of **2.3** in dichloromethane. The reaction mixture was stirred for 3 hours at room temperature during which time a white precipitate formed. The solution was then filtered through celite. All volatiles were removed *in vacuo* to leave a yellow solid. Single crystals were obtained by slow diffusion of diethyl ether into a dichloromethane solution of **2.6** at -35 °C. Yield: 96 %. ^1H NMR δ ppm ($CDCl_3$) = 5.9 (br dm, 4 H, $^1J_{H-P}$ = 350 Hz, PH_2), 7.6 (br s, 2 H, Ph), 8.0 (br s, 2 H, Ph). ^{13}C NMR δ ppm ($CDCl_3$) = 118.8 (d, $^1J_{C-F}$ = 320 Hz, CF_3), 130.1 (t, $^1J_{C-P}$ = 44.6 Hz, PhC), 132.1 (s, Ph), 135.3 (t, $^1J_{C-H}$ = 6.2 Hz, Ph), 213.6 (br s, CO eq.), 217.9 (br s, CO, ax.). ^{31}P NMR δ ppm ($CDCl_3$) = -3.5 (t, $^1J_{P-H}$ = 369 Hz, PH_2). IR (CH_2Cl_2) = γ(PH) = 2256s cm^{-1}, γ(CO) = 2056s, 1994s and 1944s cm^{-1}. Anal. Calc. for $C_{10}H_8O_6F_3MnP_2S$ (431.11) = C, 27.93; H, 1.87. Found = C, 27.88; H, 1.84%. (TOF-MS, ES^+): m/z (%): 281.2 (34) $[M - OTf]^+$.

2.4.2.4 Synthesis of $Mn(OTf)(CO)_3\{C_2H_4(PH_2)_2\}$, **2.7**.

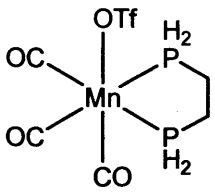

In absence of light, a solution of AgOTf in dichloromethane was added to a solution of **2.4** in dichloromethane. The reaction mixture was stirred for 3 hours at room temperature during which time a white precipitate formed. The solution was then

filtered through celite. All volatiles were removed *in vacuo* to leave a yellow solid. Single crystals were obtained by slow diffusion of ether into a dichloromethane solution of **2.7** at -35 °C. Yield: 94 %. ^{1}H NMR δ ppm ($CDCl_3$) = 2.2 (br dm, 4 H, CH_2), 4.9 (d, 4 H, $^{1}J_{H-P}$ = 356 Hz, PH_2). ^{13}C NMR δ ppm ($CDCl_3$) = 14.8 (t, $^{1}J_{C-H}$ = 23 Hz, CH_2), 123.0 (d, $^{1}J_{C-F}$ = 318 Hz, CF_3), 213.8 (br s, CO eq.), 219.0 (br s, CO, ax.). ^{31}P NMR δ ppm ($CDCl_3$) = -15.0 (t, $^{1}J_{P-H}$ = 356 Hz, PH_2). IR (CH_2Cl_2) = γ(PH) = 2365s cm^{-1} γ(CO) = 2054s, 1989s and 1938s cm^{-1}. Anal. Calc. for $C_6H_8O_6F_3MnP_2S$ (383.06) = C, 18.86; H, 2.11. Found = C, 18.81; H, 2.01%. (TOF-MS, ES^+): m/z (%): 233 (100) $[M - OTf]^+$.

2.4.2.5 Synthesis of **2.11**.

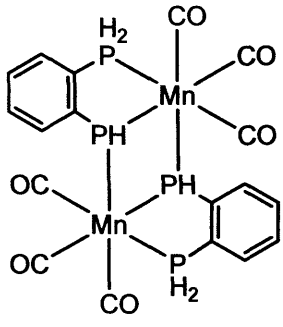

A solution of free carbene was generated by the addition of the 1,3-diallylbenzimidzolium salt and $KN[Si(Me)_3]_2$ in THF at -78 °C. A solution of **2.6** in dichloromethane was then added dropwise while the temperature was carefully maintained at -78 °C. The reaction mixture was stirred overnight leading to a yellow-orange compound. Single crystals were obtained by slow diffusion of diethylether into a tetrahydrofuran solution of **2.11** at -35 °C to produce the *trans*-isomer and from a saturated $CDCl_3$ solution of **2.11** at -35 °C to produce the *cis*-isomer. Yield: 69 %. ^{1}H NMR δ ppm ($CDCl_3$) = 5.2 (br s, PH_2), 6.0 (br s, PH), 7-7.7 (br m, Ph). ^{13}C NMR δ ppm ($CDCl_3$) = 215.0 (br s, CO eq.), 219.0 (br s, CO, ax.). ^{31}P NMR δ ppm ($CDCl_3$) = 0.1 (t, $^{1}J_{P-H}$ = 349 Hz, PH_2), -59.2 (d, $^{1}J_{P-H}$ = 285 Hz, PH). IR (CH_2Cl_2) = γ(CO) = 2016s, 1993, 1916s cm^{-1}. Anal. Calc. for $C_{18}H_{14}O_6Mn_2P_4$ (560.07) = C, 38.60; H, 2.52. Found = C, 38.41; H, 2.81 %. (TOF-MS, ES^+): m/z (%): 560 (7) $[M]^+$.

2.4.2.6 Synthesis of **2.12**.

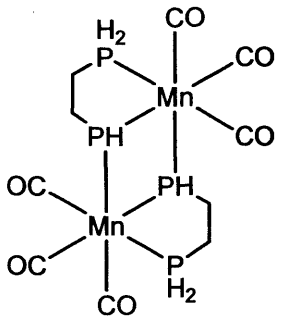

A solution of free carbene was generated by the addition of the 1,3-diallylbenzimidzolium salt and $KN[Si(Me)_3]_2$ in THF at -78 °C. A solution of **2.7** in dichloromethane was then added dropwise while the temperature was carefully maintained at -78 °C. The reaction mixture was stirred overnight leading to a yellow-orange compound. Yield: 63 %. ^{1}H NMR ($CDCl_3$) = 2.52 (br, 8H, **CH2**), 5.40 (br, 4H, **PH2**), 6.08 (br, 2H, **PH**). ^{13}C NMR δ ppm ($CDCl_3$) = 15.2 (br m, **CH_2**) ^{31}P NMR δ ppm ($CDCl_3$) = -3.1 (t, $^1J_{P-H}$ = 335 Hz, **PH_2**), -62.3 (d, $^1J_{P-H}$ = 273 Hz, **PH**). IR (CH_2Cl_2) = γ(PH_2) = 2360s cm^{-1}, γ(PH) = 2308s cm^{-1}, γ(CO) = 2000s, 1926s cm^{-1}. Anal. Calc. for $C_{10}H_{14}O_6Mn_2P_4$ (463.99) = C, 25.89; H, 3.04 Found = C, 26.01; H, 3.18 %.

2.4.3 Crystallography

A summary of crystal data, data collection parameters and model refinement parameters is given in Appendix 2. All single crystal X-ray data was collected at 150K on a Bruker/Nonius Kappa CCD diffractometer using graphite monochromated Mo-Kα radiation (λ = 0.71073 Å), equipped with an Oxford Cryostream cooling apparatus. The data was corrected for Lorentz and polarization effects and for absorption using SORTAV.[16] Structure solution was achieved by direct methods and refined by full-matrix least-squares on F^2 (SHELX-97)[17] with all non hydrogen atoms assigned anisotropic displacement parameters. Hydrogen atoms attached to carbon atoms were placed in idealised positions and allowed to ride on the relevant carbon atom. Molecular structures in the Figures were drawn with Ortep 3.0 for Windows (version 1.08).[18]

2.5 References

[1] R. J. Baker, P. G. Edwards, J. Gracia-Mora, F. Ingold, K. M. A. Malik, *J. Chem. Soc., Dalton Trans.*, **2002**, *21*, 3985.

[2] F. E. Hahn, C. Holtgrewe, T. Pape, M. Martin, E. Sola, L. A. Oro, *Organometallics*, **2005**, *24*, 2203.

[3] W. Zhang, Thesis, Cardiff University (Cardiff), **2005**.

[4] T. K. Ghanty, S. K. Ghosh, *J. Phys. Chem* **1994**, *98*, 9197.

[5] O. Kaufhold, A. Stasch, P. G. Edwards, F. E. Hahn, *chem. Commun.* **2007**, 1822.

[6] S. J. A. Pope, G. Reid, *J. Chem. Soc., Dalton Trans.* **1999**, 1615.

[7] H. Friebolin, *Basic One- and Two-Dimensional NMR Spectroscopy*, 2on ed., VCH Publishers, New York, Weinheim, **1993**.

[8] C. Pereira, H. G. Ferreira, M. S. Schultz, J. Milanez, M. Izidoro, P. C. Leme, R. H. A. Santos, M. T. P. Gambardella, E. E. Castellano, B. S. Lima-Neto, R. M. Carlos, *Inorg. Chim. Acta* **2005**, *358*, 3735.

[9] F. E. Hahn, M. C. Jahnke, T. Pape, *Organometallics* **2006**, *25*, 5927.

[10] L. Jafarpour, S. P. Nolan, *J. Organomet. Chem* **2001**, *17*, 617-618.

[11] H. M. J. Wang, I. J. B. Lin, *Organometallics* **1998**, *17*, 972.

[12] M. Paas, B. Wibbeling, R. Fröhlich, F. E. Hahn, *Eur. J. Inorg. Chem.* **2006**, 158.

[13] L. Maier, *Helv. Chim. Acta.*, **1966**, *49*, 842.

[13] E. P. Kyba, S. T. Liu, R. L. Harris, *Organometallics*, **1983**, *2*, 1877.

[15] Medac LTD, Brunel Science Cntr, Coopers Hill Lane, Englefield Green, Egham, Surrey, TW20 0JZ.

[16] R. H. Blessing, *Acta Crystallogr.*, Sect A **1995**, *51*, 33.

[17] G. M. Sheldrick, SHELX-97, Program for Crystal Structures Analysis, University of Göttingen, Germany **1998**.

[18] L.J. Farrugia, *J. Appl. Cryst.*, **1997**, *30*, 565.

Chapter 3

Synthesis of a new chiral rigid hydroxyphospholane ligand and its coordination chemistry

3.1 Introduction

Chiral heterocyclic phosphines derived from phosphetanes, phospholanes, phosphiranes or phosphepanes play a central role as ligands for catalysis and particularly hydroformylation catalysis and homogeneous metal catalyzed reactions. In most cases, bidentate ligands bearing these heterocycles have been used, but monodentate ligands have also been shown to induce high enantioselectivities.[1] Catalytic enantioselective hydrogenation is of great importance both for science and industry. Prominent examples are commercially available bis(phospholanes) such as DuPHOS,[2] RoPHOS,[3] and ligands of the catASium M series.[4] While selectivity in catalysis often refers to control of absolute stereochemistry, other types of selectivity such as diastereoselectivity, chemoselectivity, and regioselectivity also can play a crucial role in the development of a viable synthetic method based upon chiral transition metal catalysts.

The correlation of stereoelectronic effects in tertiary phosphines ligands with the reactivity of their coordination complexes is key to understanding their efficacy in homogeneous catalysis. Tolman's parameters remain the most widely used guide to the gross feature of stereoelectronic effects for monodentate phosphorus(III) ligands[5] but more modern approaches, developed by Harvey *et al.*,[6] are beginning to supercede Tolman's seminal review. Ligand electronic properties can dramatically influence the reactivity and selectivity of transition metals catalysts and recently more attention have been focussed on monodentate phosphorus based ligands due to their significant potential in various catalytic processes.[7] A number of chiral phosphines have been reported in asymmetric hydrogenation catalysed by rhodium and ruthenium complexes.[8] Phospholane ligands have been used for many transition metal catylized processes such as hydrogenation[9] or hydrovinylation.[10] In 1997 Nozaki and co-workers used a phospholane ligand[11] in the methoxycarbonylation of vinylarenes. The success of phospholanes ligands has been attributed to the rigid chiral environment at the 2,5- positions of the five-membered ring.[12] In general, transition metal complexes containing these ligands show a high

level of enantioselective control and asymmetric induction, the later being increased by the close proximity of the chirality to the metal centre of the complex, in the catalyzed hydrogenation of unsaturated substrates. Another attribute of phospholanes was associated with the modularity of these systems allowing the steric environment imposed by the ligand to be tuned to ideally accommodate the steric demands of the reactants, and therefore facilitate optimization of catalyst efficacity. Hemilability is often a unique feature for promoting catalysis and water solubility is now very desirable. This prompted us to search for a new chiral phospholane motif that included a hemilabile donor with the potential for increased water solubility. Thus, we sought to prepare a hydroxy functionalised phospholane from inexpensive enantiomerically pure (*S*)-aspartic acid, **3.1**.

In this Chapter, complexes of the new ligand 3(*R*)-hydroxy-phenylphospholane, **3.7**, with Pt(II), Pd(II), Fe(II), Rh(I), Ru(II) and Mn(I) are reported and their spectroscopic and crystallographic properties described. Attempts to coordinate **3.7** to $ReBr(CO)_5$ to give **3.17**, and $[Mo(pip)_2(CO)_4]$ to produce **3.16**, (pip=piperidine) were unsuccessful.

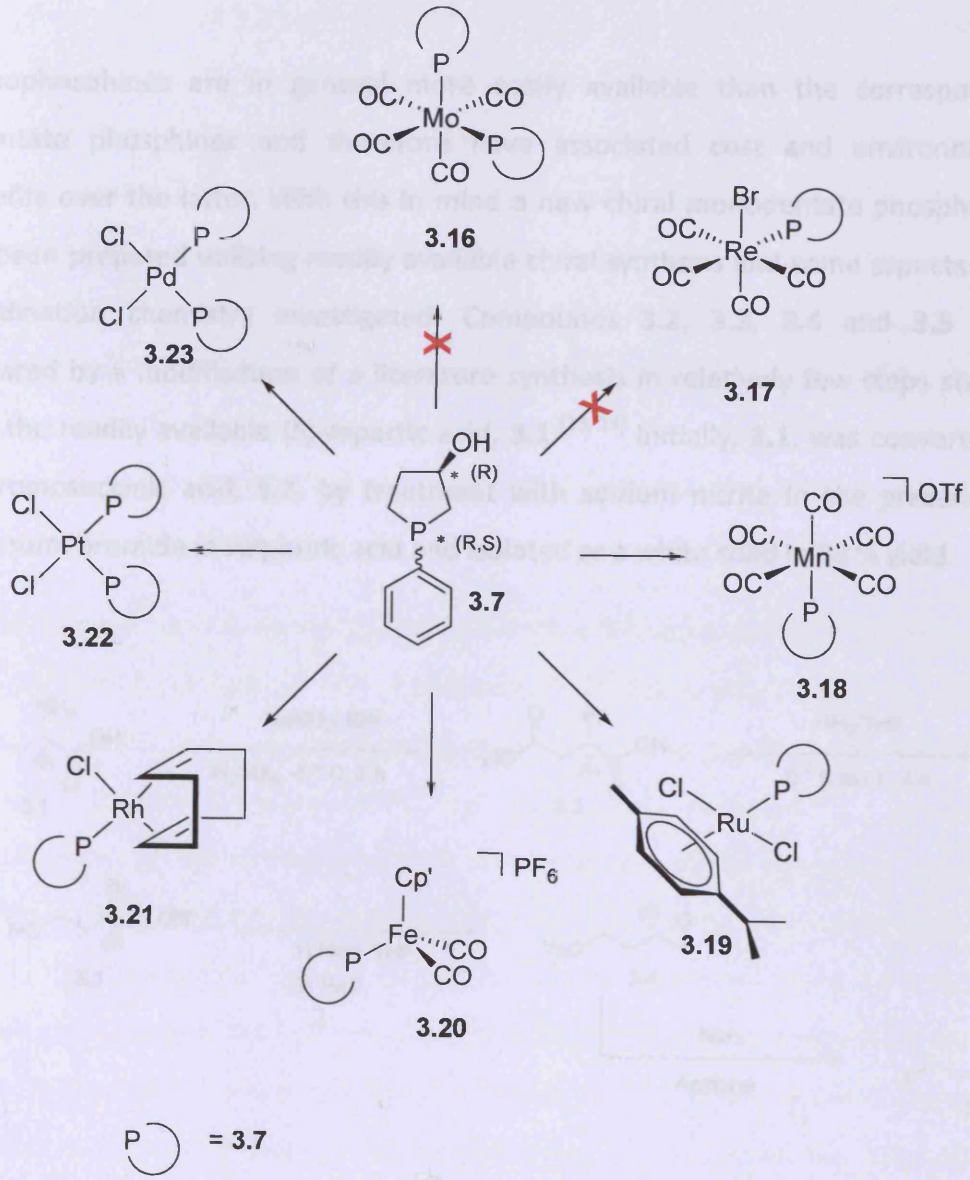

Scheme 1: General scheme for the synthesis or attempted synthesis of metal complexes of **3.7**.

3.2 Results and discussion

3.2.1 Ligand synthesis

Monophosphines are in general more easily available than the corresponding bidentate phosphines and therefore have associated cost and environmental benefits over the latter. With this in mind a new chiral monodentate phospholane has been prepared utilising readily available chiral synthons and some aspects of its coordination chemistry investigated. Compounds **3.2**, **3.3**, **3.4** and **3.5** were prepared by a modification of a literature synthesis in relatively few steps starting with the readily available (*S*)-aspartic acid, **3.1**.[13, 14] Initially, **3.1**, was converted to (*S*)-Bromosuccinic acid, **3.2**, by treatment with sodium nitrite in the presence of potassium bromide in sulphuric acid and isolated as a white solid in 88 % yield.

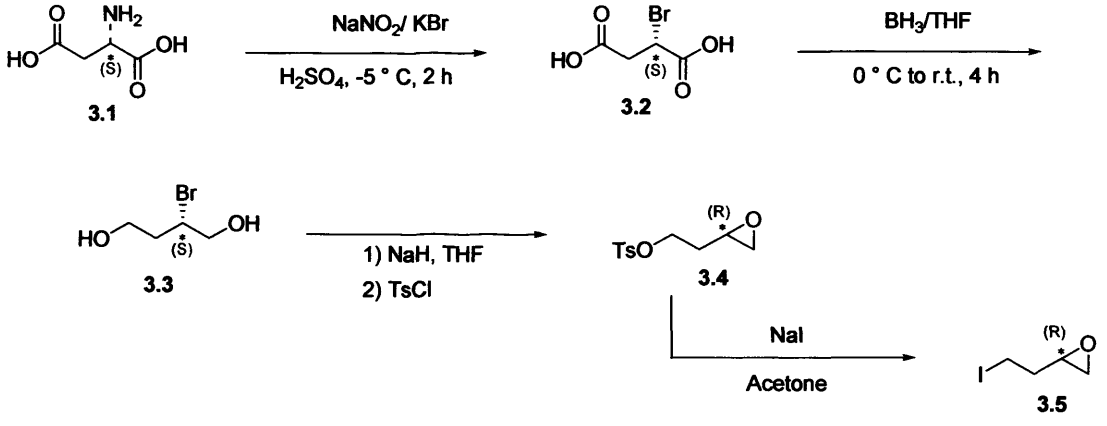

3.1 **3.2** **3.3** **3.4** **3.5**

Scheme 2: Synthesis of (*S*)-bromosuccinic acid, **3.2**, (*S*)-2-bromo-1,4-butanediol, **3.3**, (*R*)-2-(oxiran-2-yl) ethyl-4-methylphenylsulfonate, **3.4**, and (*R*)-2-(2-iodoethyl) oxirane, **3.5**.

The diazotisation reaction started with optically pure (*S*)-aspartic acid, **3.1**, to give **3.2** with the same absolute configuration as the starting material through anchimeric assistance. The diacid, **3.2**, was then reduced to the corresponding diol,

3.3, with retention of stereochemistry, with borane-tetrahydrofuran complex and isolated as a bright orange-yellow viscous oil in 92 % yield. All spectroscopic and analytical data for compounds **3.2** and **3.3** were as previously reported.[15]

The diol, **3.3**, was subsequently cyclised in a one-pot two-component reaction through treatment of **3.3** with an excess of NaH in THF followed by in situ tosylation to afford the optically pure (*R*)-2-(oxiran-2-yl)ethyl-4-methylphenylsulfonate, **3.4**, in 91 % yield. The compound **3.4** was then purified by flash column chromatography followed by a careful evaporation of the solvent to avoid volatization of the product. In an effort to increase the reactivity of the epoxide, **3.4**, the tosylate group was replaced by iodide under standard Finkelstein conditions, providing (*R*)-2-(2-iodoethyl)oxirane in 96 % yield as a dark orange viscous oil. Thus we have prepared (*R*)-2-(oxiran-2-yl)ethyl-4-methylphenylsulfonate, **3.4**, and (*R*)-2-(2-iodoethyl)-oxirane, **3.5**, in 3 and 4 steps respectively from (*S*)-aspartic acid in an overall yield of 74 % for **3.4** and 71 % for **3.5**.

The final stage of the ligand synthesis was the introduction of the phosphorus function and formation of the five-membered heterocyclic ring. The primary phenylphosphine, **3.6**, was freshly prepared in one step starting with the readily available dichlorophenylphosphine as previously reported.[16] Subsequent deprotonation of the phenylphosphine, **3.6**, with two molar equivalents of nBuLi solution in THF generated the diphosphide leading to a nucleophilic attack at -78 °C on **3.4** or **3.5** to give the desired ligand, **3.7**. Some test reactions using **3.4** or **3.5** and various polar solvents like THF provided similar results and in that regard we decided to use the tosylate oxirane derivative, **3.4**, instead of the iodo oxirane derivative, **3.5**, thus reducing the number of steps needed to synthesise the phospholane precursor **3.7**.

Moreover, we decided to use two equivalents of nBuLi to activate the primary phosphine to encourage direct formation of the ligand, **3.7**.

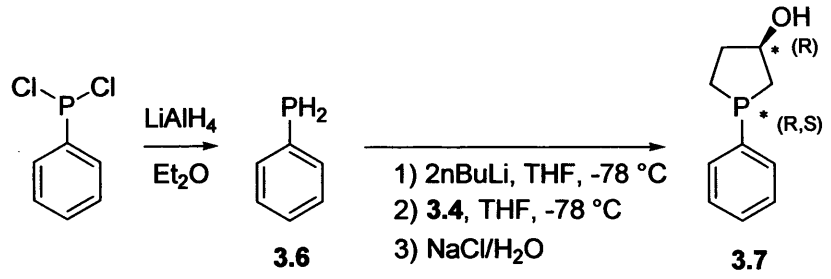

Scheme 3: Synthesis of 3(*R*)-hydroxy-phenylphospholane, **3.7**.

After the appropriate reaction time, *in situ* protonation of residual basic species by treatment with a saturated degassed aqueous solution of NaCl followed by repeated extraction in dichloromethane solvent gave, after removal of volatiles, the phospholane ligand, **3.7**, in quantitative yield as a bright yellow, highly viscous oil. The reaction was followed *in situ* by $^{31}P\{^{1}H\}$ NMR spectroscopy for the duration of the reaction which showed the presence of the desired product. The reaction was considered to be complete after 12 hours when the starting material, **3.6**, was totally consumed.

During the reaction, the growth of a dominant resonance at δ_P -18.2 ppm and a second resonance at δ_P -20.2 ppm was observed in a final ratio of approximately 80:20. The presence of these two resonances suggests that two diastereomers are formed in the reaction. Attempts to separate the diastereomeric product mixture by column chromatography or by recrystallization of their salt derivatives, inducing a possible mechanical separation of the crystals of one isomer from the other were unsuccessful and **3.7** was characterised by spectroscopic and analytical methods as a mixture of diastereomers and used as such for the coordination chemistry.

Given the fact that the chirality at the *C atom of the optically pure oxirane precursor, **3.4**, is fixed and, since the centre is not involved directly in the nucleophilic substitution by the phosphorus, the diastereomeric mixture must result from both *R* and *S* configurations being present for the phosphorus atom. The reaction was carried out at -78 °C to encourage kinetic control in the ring closure

formation. The reaction process will be described in two main steps starting by deprotonation of phenyphosphine, **3.6**, by nBuLi, allowing a nucleophilic attack on either the tosylate carbon (route a) or the oxirane ring (route b) of **3.4** as shown in Scheme 4.

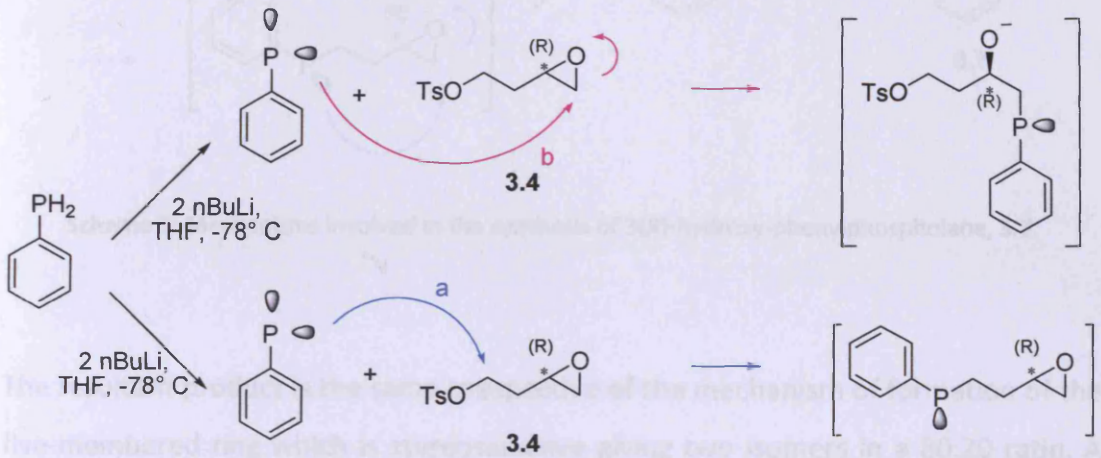

Scheme 4: Mechanisms involved in the synthesis of 3(*R*)-hydroxy-phenylphospholane, **3.7**.

No attempt was made to isolate or characterise the proposed intermediates *in situ* as the reaction cannot be easily controlled once n-BuLi is introduced and control of temperature (-78 °C) is important to avoid formation of a thick yellow precipitate of the dilithiophenylphosphide which appears if the temperature was allowed to increase. Therefore, *in situ* $^{31}P\{^{1}H\}$ NMR could not be performed and the indermediates showed in Scheme 4 and 5 are speculative. The initial nucleophilic attack would be followed by a second nucleophilic attack on the remaining electropositively charged carbon atom of either intermediate leading to the five-membered ring closure formation as stated in Scheme 5 below:

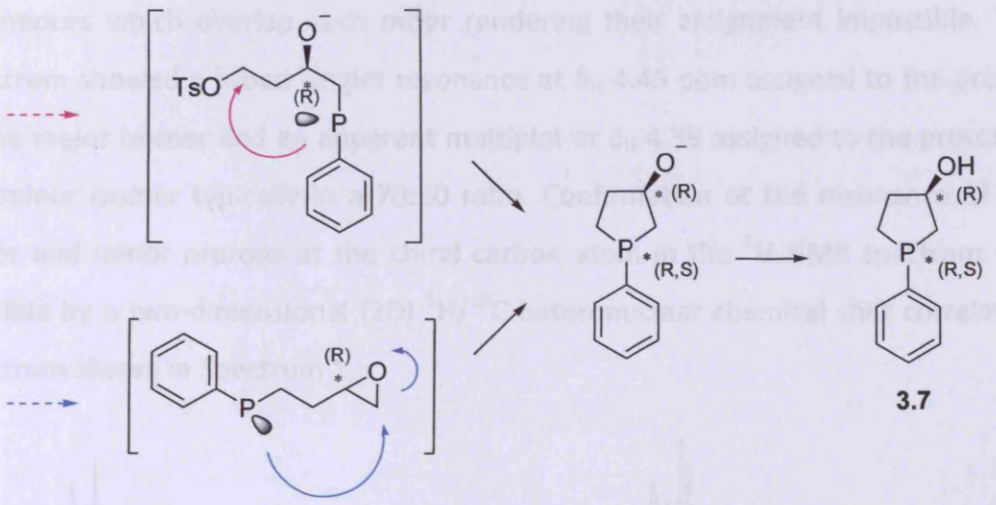

Scheme 5: Mechanisms involved in the synthesis of 3(*R*)-hydroxy-phenylphospholane, **3.7**.

The resultant product is the same irrespective of the mechanism of formation of the five-membered ring which is stereoselective giving two isomers in a 80:20 ratio. A preferential orientation of the phenyl group relative to the position of the hydroxy group on the chiral carbon atom of the heterocycle might have been expected, but efforts to encourage formation of the thermodynamically favoured product by heating the isomeric mixture under N_2 to 200 °C for a period of time between 12 hours and 24 hours were unsuccessful with no change being observed by $^{31}P\{^1H\}$ NMR spectroscopy. This was expected due to the fact that the C-P-C angle of the phospholane is constricted increasing the inversion energy barrier and consequently inhibiting this type of conversion. However, no sign of decomposition was noticed during the heating process highlighting the fact that the ligand, **3.7**, is thermally very robust. The failure to interconvert the two forms suggests that the stereoselectivity is kinetic in origin.

Identification of **3.7** was supported by mass spectrometric measurement which afforded the molecular ion at (m/z = 181.08 amu).

The ^1H NMR spectrum was used for the determination of the diastereomeric ratio. At 500 MHz, the most reliable resonance for this purpose was the one assigned to the proton located on the chiral carbon atom $*C_3$ of the heterocycle. The other hydrogen atoms of the five-membered ring and of the phenyl group provided many

resonances which overlap each other rendering their assignment impossible. The spectrum showed a broad singlet resonance at δ_H 4.45 ppm assigned to the proton of the major isomer and an apparent multiplet at δ_H 4.39 assigned to the proton of the minor isomer typically in a 70:30 ratio. Confirmation of the resonance of the major and minor protons at the chiral carbon atom in the ^1H NMR spectrum was possible by a two-dimensional (2D) $^1H/^{13}C$ heteronuclear chemical shift correlation spectrum shown in Spectrum 1.

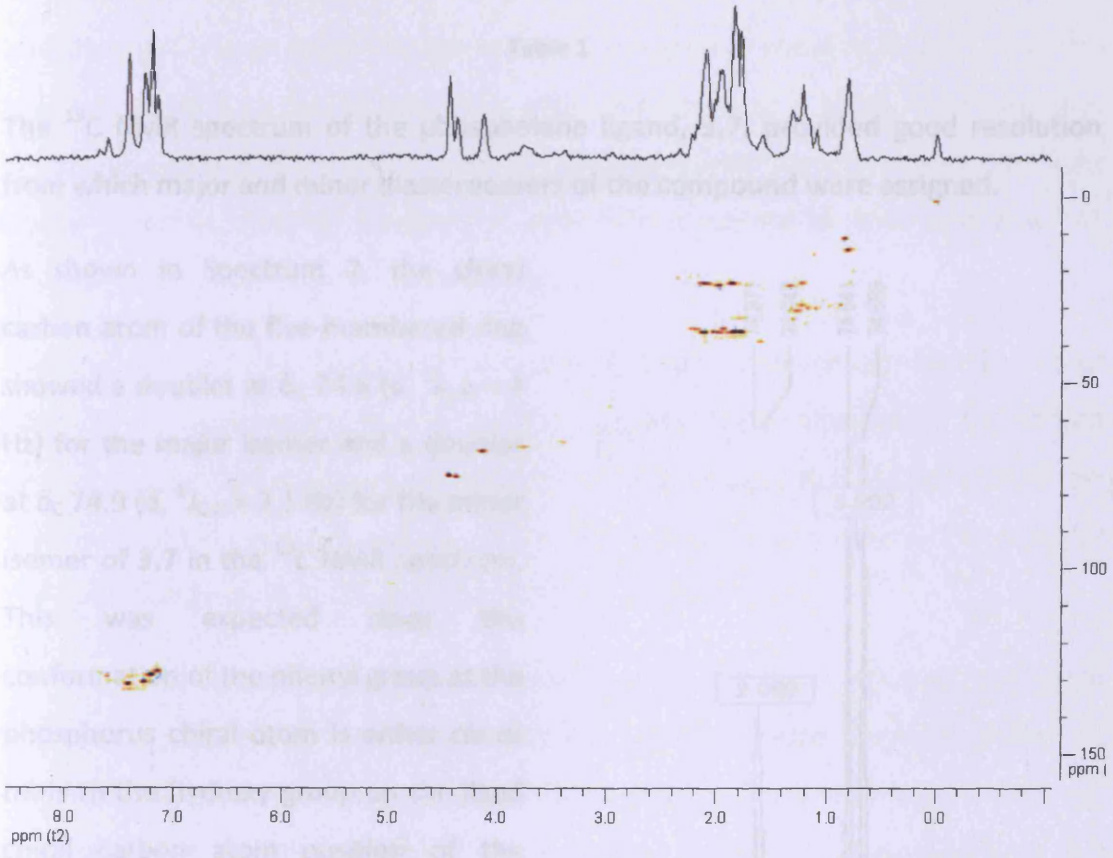

Spectrum 1: Two-dimensional (2D) $^1H/^{13}C$ heteronuclear chemical shift correlation spectrum of **3.7**.

The associated resolved chemical shifts for the different species are listed in Table 1. Although a resonance from the hydroxy is visible in the ^1H spectrum, it is not correlated to any ^{13}C resonance which was expected.

Correlated Atoms	δ ^{1}H	δ ^{13}C{^{1}H}
C_1H_2, C_2H_2,	1 ppm to	22 ppm to
$C_4H_2^{a+b}$	2.4 ppm	37 ppm
$*C_3H^{a}$	4.45 ppm	74.6 ppm
$*C_3H^{b}$	4.39 ppm	74.9 ppm
C_6H, C_7H, C_8H,	7 ppm to	127 ppm to
C_9H, $C_{10}H^{a+b}$	7.8 ppm	135 ppm

[a] related data of the major isomer. [b] related data of the minor isomer.

Table 1

The ^{13}C NMR spectrum of the phospholane ligand, **3.7**, provided good resolution from which major and minor diastereomers of the compound were assigned.

As shown in Spectrum 2, the chiral carbon atom of the five-membered ring showed a doublet at δ_C 74.6 (d, $^{1}J_{C\text{-}H}$ = 4 Hz) for the major isomer and a doublet at δ_C 74.9 (d, $^{1}J_{C\text{-}H}$ = 2.1 Hz) for the minor isomer of **3.7** in the ^{13}C NMR spectrum. This was expected since the conformation of the phenyl group at the phosphorus chiral atom is either *cis* or *trans* to the hydroxy group on the fixed chiral carbon atom position of the heterocycle as reported in Figure 1.

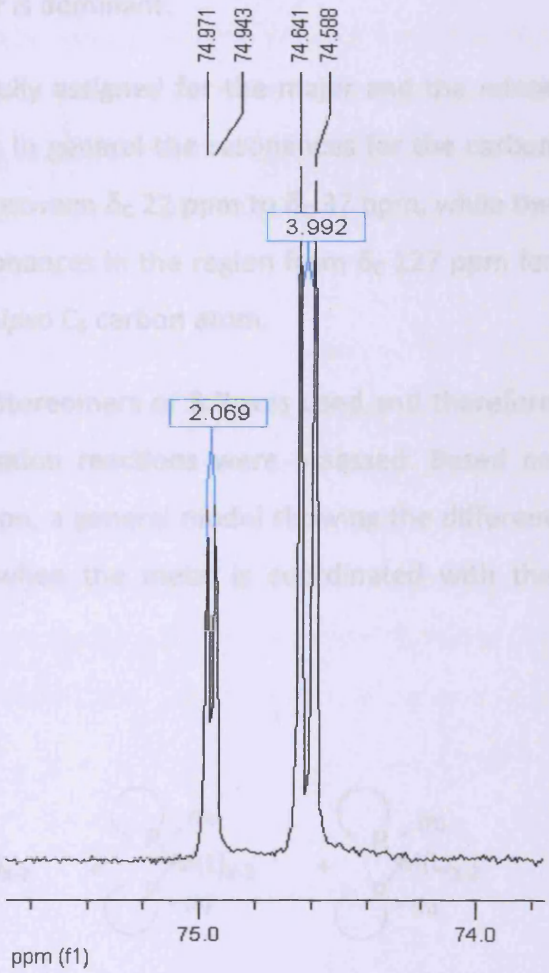

Spectrum 2: ^{13}C NMR spectrum of **3.7** highlighting the $*C_3$ resonances.

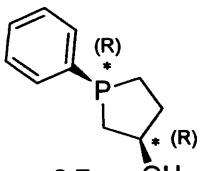

3.7a

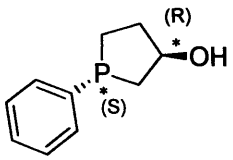

3.7b

Figure 1

The value of $^{2}J_{P\text{-}C}$ is known to show a dependence on the orientation of the phosphorus lone pair relative to the carbon.[17] In general, coupling is large when the lone pair is close to the carbon atom, while the coupling is small, even negative, when the lone pair is remote. The small coupling in both the major and the minor isomer suggests that the phosphorus lone pair is remote in both and it is not possible to determine which diastereomer is dominant.

The rest of the ^{13}C NMR spectrum was fully assigned for the major and the minor isomers (see Experimental for full detail). In general the resonances for the carbon on the phospholane ring were observed between δ_C 22 ppm to δ_C 37 ppm, while the carbons of the aromatic ring showed resonances in the region from δ_C 127 ppm for the C_8 carbon atom to δ_C 142 ppm for the *ipso* C_5 carbon atom.

As mentioned before, the mixture of diastereomers of **3.7** was used and therefore speculative predictions for the complexation reactions were assessed. Based on either a 2:1 or a 1:1 stoichiometric reaction, a general model showing the different possibilities of diastereomers products when the metal is coordinated with the ligand as shown in Figure 2.

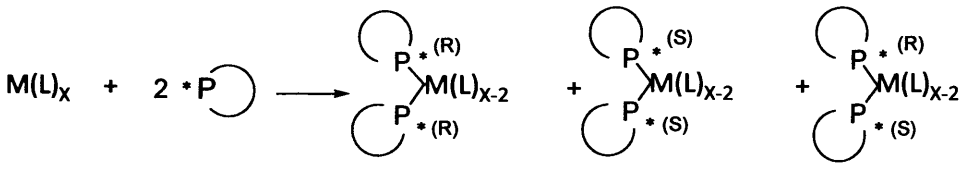

- 2:1 ligands:metal precursor stoichiometry reaction scheme

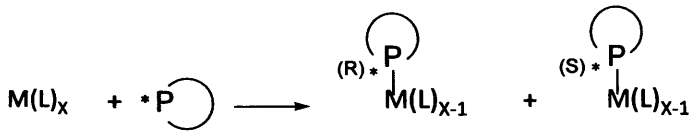

- 1:1 ligand:metal precursor stoichiometry reaction scheme

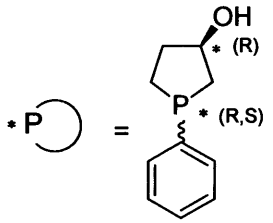

3.7

Figure 2

Starting with the mixture of **3.7a** and **3.7b** was not ideal since it increases the number of possible metal-complex products particularly for the 2:1 (ligand:metal) complexes as shown in Figure 2, but it was hoped that purification/separation of the mixture might be achievable once the ligand was coordinated to the metal centre affording a more robust and air-stable compound.

All the new complexes formed were characterised by a combination of ^{1}H, $^{13}C\{^{1}H\}$ and $^{31}P\{^{1}H\}$ NMR spectroscopy, mass spectrometry, elemental analysis, and in some cases X-ray crystallography. Unless otherwise stated, all reactions were carried out in dichloromethane at room temperature under inert atmosphere and left stirring overnight to go to completion. As air-stable compounds, most of the new complexes were subjected to flash column chromatography for purification followed by recrystallisation by slow vapor diffusion techniques, leading in some cases to the separation of the diastereomers.

3.2.2 Coordination chemistry

3.2.2.1 Attempts to coordinate 3(*R*)-hydroxy-phenylphospholane, **3.7**, to $[Mo(pip)_2(CO)_4]$, **3.8**.

Addition of two molar equivalents of **3.7** to a solution of $[Mo(pip)_2(CO)_4]$, **3.8**, in dichloromethane was expected to lead to substitution of the piperidine ligands to give the compound $[Mo(k\text{-}P_{R,S}\text{-}\mathbf{3.7})_2(CO)_4]$, **3.16** as shown in Scheme 6 below:

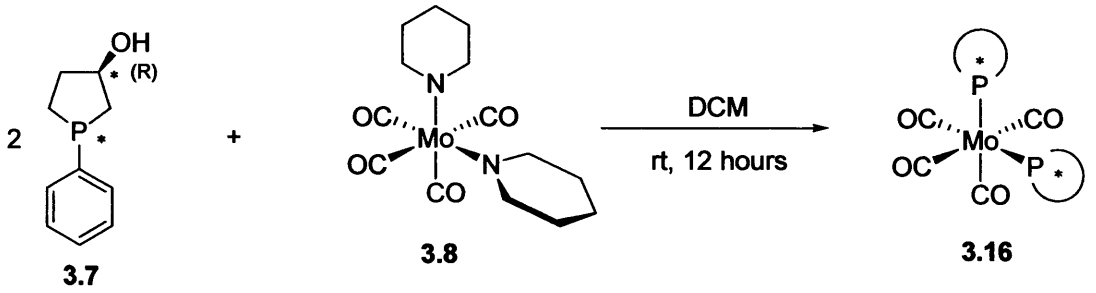

Scheme 6: Synthesis of $[Mo(k\text{-}P_{R,S}\text{-}\mathbf{3.7})_2(CO)_4]$, **3.16**.

The reaction was monitored by $^{31}P\{^1H\}$ NMR spectroscopy.The reaction appeared to work initially as two new signals appeared at δ_P 27.1 ppm (major) and δ_P 27.8 ppm (minor) in the $^{31}P\{^1H\}$ NMR spectrum shortly after mixing, the downfield shift being consistant with coordination of the free ligand.[18] After a few hours several other resonances started to appear indicating a mixture of products. Unfortunately, we were unable to isolate any pure compounds from the reaction mixture. Attempts to clean the crude product by flash column chromatography were unsuccesful and a rapid color change of the molybdenum complex was noticed in air indicating instability if not handled under an inert atmosphere. The green color of the compound may indicate that some oxidation had occurred at the metal centre. When the reaction was also conducted in a 1:1 ratio the preliminary results were very similar to those obtained for the 2:1 stoichiometric reaction. The decay of the resonance of the free phospholane ligand, **3.7**, and the rise of two new resonances

in the $^{31}P\{^{1}H\}$ NMR spectrum was noticed before decomposition of the product occured leading to the presence of many secondary resonances (Spectrum 3).

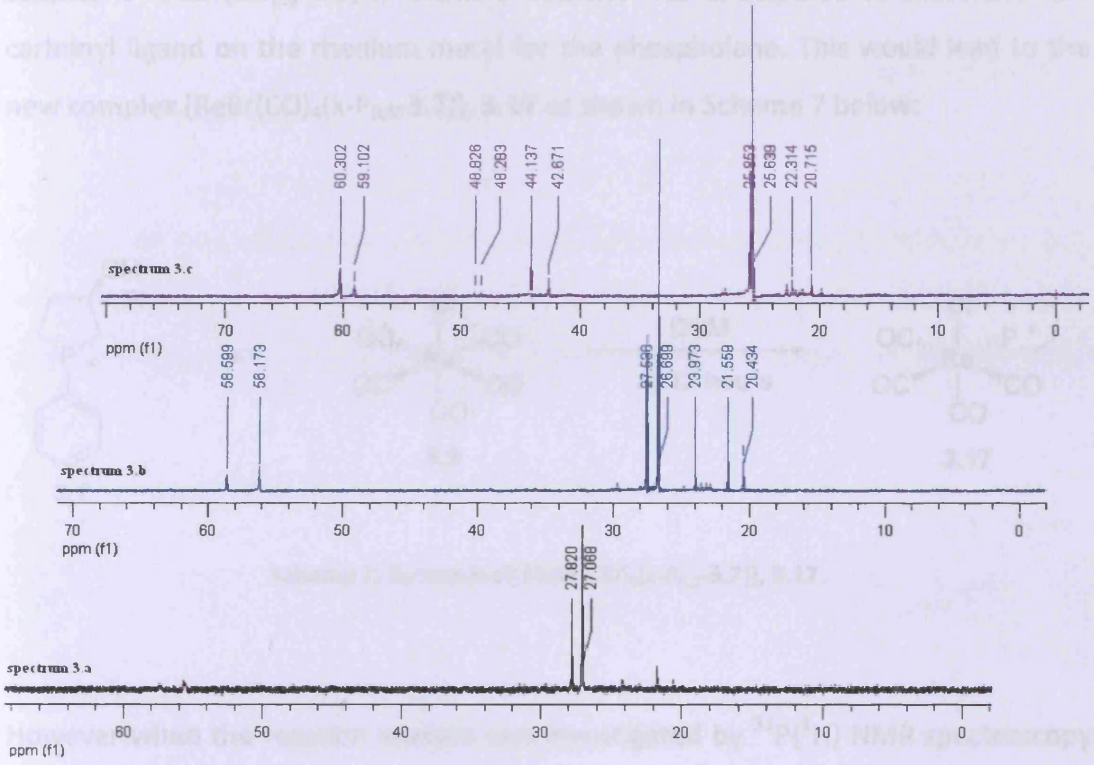

Spectrum 3: $^{31}P\{^{1}H\}$ NMR stack spectra showing the evolution of the various complexes from the 1:1 reaction of $[Mo(pip)_2(CO)_4]$ and **3.7** through time from spectrum 3.a to 3.c.

These results indicates that preferentially two ligands coordinate to the metal centre and the 2:1 stoichiometric reaction appears to be the one which can afford potentially better results leaving potentially no uncoordinated molecules of molybdenum metal precursor.

3.2.2.2 Attempts to coordinate 3(*R*)-hydroxy-phenylphospholane, **3.7**, to $ReBr(CO)_5$, **3.9**.

Addition of one molecular equivalent of 3(*R*)-hydroxy-phenylphospholane, **3.7**, to a solution of $ReBr(CO)_5$, **3.9**, in dichloromethane was anticipated to substitute one carbonyl ligand on the rhenium metal for the phospholane. This would lead to the new complex $[ReBr(CO)_4(k\text{-}P_{R,S}\text{-}\mathbf{3.7})]$, **3.17** as shown in Scheme 7 below:

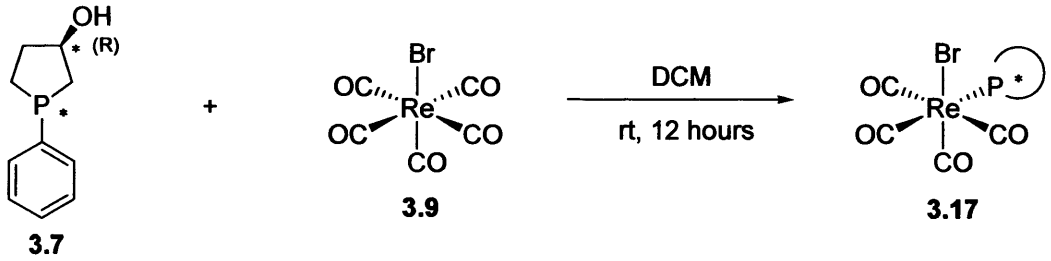

Scheme 7: Synthesis of $[ReBr(CO)_4(k\text{-}P_{R,S}\text{-}\mathbf{3.7})]$, **3.17**.

However when the reaction mixture was investigated by $^{31}P\{^1H\}$ NMR spectroscopy many signals were present suggesting a complex mixture of products.

Attempts to purify the crude product mixture by flash column chromatography or recrystalisation were unsuccesful and lead to an unclean mixture of diastereomers. The $^{31}P\{^1H\}$ NMR shows resonances at δ_P -0.2 ppm, δ_P 4.4 ppm, δ_P 43.9 ppm, δ_P 45.5 ppm, δ_P 90.2 ppm and δ_P 0.1 ppm, δ_P 4.1 ppm, δ_P 43 ppm, δ_P 45.9 ppm, δ_P 90.9 ppm respectively for the major and the minor species. The large downfield shifts observed in the spectrum are in accordance with the coordination of the phosphine on the metal centre but attempts to isolate the desired compound $[ReBr(CO)_4(k\text{-}P_{R,S}\text{-}\mathbf{3.7})]$, **3.17**,were unsuccessful.

Photolysis of the starting material $ReBr(CO)_5$, **3.9**, in toluene in the presence of the phospholane ligand, **3.7**, was carried out in order to further encourage displacement of a carbonyl ligand with the phosphorus atom of the phospholane ligand. As

observed before the reaction did not provide satisfactory results and this approach on the rhenium metal precursor **3.9** was abandoned.

3.2.2.3 Coordination chemistry of 3(*R*)-hydroxy-phenylphospholane, **3.7**, with a manganese metal precursor.

Addition of one molecular equivalent of 3(*R*)-hydroxy-phenylphospholane, **3.7**, added to a solution of $Mn(OTf)(CO)_5$, **3.10**, in dichloromethane afforded the complex $[Mn(CO)_5(k\text{-}P_{R,S}\text{-}\mathbf{3.7})]OTf$, **3.18**, (Scheme 8) as a pale yellow-orange solid (Scheme 8).

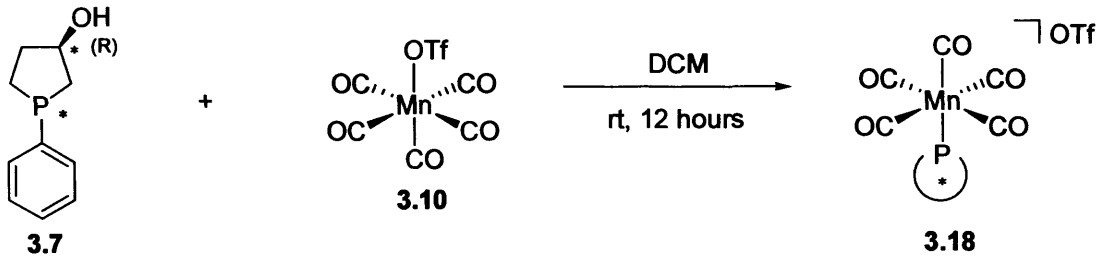

Scheme 8: Synthesis of $[Mn(CO)_5(k\text{-}P_{R,S}\text{-}\mathbf{3.7})]OTf$, **3.18**.

In 1987, 3,4-disubstituted chiral phosphines, comprising chloro, methoxy or dimethylamino substituents, having relatively electron-rich phosphorus centres were reported by Brunner et al.[19] These were complexed with manganese (as well as rhodium) and used as catalysts in the hydrogenation of alpha-N-acetoamido-cinnamic acid.

The reaction was followed *in situ* by $^{31}P\{^1H\}$ NMR spectroscopy which showed the growth of two new resonances at δ_P 42.7 ppm for the major isomer and δ_P 41.4 ppm for the minor isomer in a 70:30 ratio. Flash column chromatography was conducted in a gradient fashion from 100 % 40/60 petroleum ether which eluted the unwanted side-products through a mixture of 40/60 petroleum ether/diethyl ether to 100 %

THF which eluted the desired compound. Despite the fact that the unreacted and other unwanted products were left over by this method, the two isomers (assessed by $^{31}P\{^{1}H\}$ NMR spectroscopy) were not separated and complex **3.18** was characterised by a combination of ^{1}H, $^{13}C\{^{1}H\}$ and $^{31}P\{^{1}H\}$ NMR spectroscopy and elemental analysis (see Experimental).

The ^{1}H NMR spectrum was used for the determination of the diastereomeric ratio. At 500 MHz, the most reliable resonance for this purpose was the one assigned to the proton located on the chiral carbon atom $*C_3$ of the heterocycle. The other hydrogen atoms of the five-membered ring and of the phenyl group provided many resonances which overlap each other rendering their assignment difficult. The ^{1}H NMR spectrum showed broad resonances at δ_H 7.6 ppm and δ_H 7.4 ppm for the major isomer and δ_H 7.5 ppm and δ_H 7.3 ppm for the minor isomer corresponding to the hydrogen atoms of the aromatic ring. A singlet observed at δ_H 5.4 ppm corresponds to the proton of the hydroxyl group of the major isomer since the correlation in the $^{1}H/^{13}C$ heteronuclear spectrum was not observed. The signal of the corresponding proton signal for the minor isomer could not been assigned. Two broad doublets at δ_H 4.4 ppm (br d, $^{1}J_{H\text{-}C}$ = 15.8 Hz, $*C_3\mathbf{H}$) and δ_H 4.5 ppm (br d, $^{1}J_{H\text{-}C}$ = 15.9 Hz, $*C_3\mathbf{H}$) were assigned to the proton located on the chiral carbon atom of the major isomer and the minor isomer respectively in a 60:40 ratio which was confirmed by two-dimensional (2D) $^{1}H/^{13}C$ heteronuclear chemical shift correlation spectrum (Spectrum 4). The rest of the spectrum was fully assigned (see Experimental for full detail).

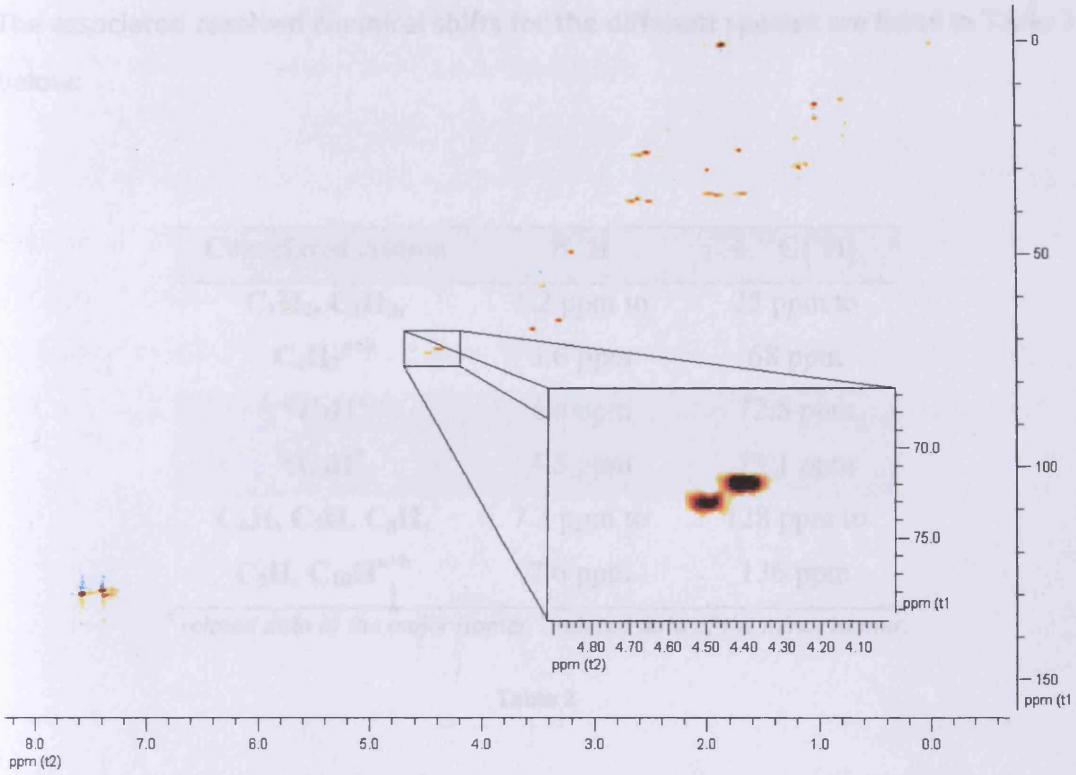

Spectrum 4: Two-dimensional (2D) $^{1}H/^{13}C$ heteronuclear chemical shift correlation spectrum of **3.18** focusing on the correlation at the $*C_3$ atom.

The $^{13}C\{^{1}H\}$ NMR spectrum, although broadened, allowed the major and minor diastereomers of the compound to be assigned. The two-dimensional (2D) $^{1}H/^{13}C$ spectrum confirmed the resonance of the chiral carbon atom of the five-membered ring for which a broad singlet at δ_C 72.5 for the major isomer and a broad singlet at δ_C 73.1 for the minor isomer of **3.18** were observed in the ^{13}C NMR spectrum. The rest of the ^{13}C NMR spectrum was fully assigned for the major and the minor isomers (see Experimental for full detail). In general the resonances for the carbon on the phospholane ring were observed between δ_C 25 ppm to δ_C 68 ppm, while the carbons of the aromatic ring showed resonances in the region from δ_C 128 ppm to δ_C 136 ppm. Due to the directly bonded ^{55}Mn quadrupolar nucleus, the spectrum was broad and the resonances corresponding to the carbonyl ligands could not be identified.

The associated resolved chemical shifts for the different species are listed in Table 2 below:

Correlated Atoms	δ ^{1}H	δ $^{13}C\{^{1}H\}$
C_1H_2, C_2H_2,	1.2 ppm to	25 ppm to
$C_4H_2^{a+b}$	3.6 ppm	68 ppm
$*C_3H^{a}$	4.4 ppm	72.5 ppm
$*C_3H^{b}$	4.5 ppm	73.1 ppm
C_6H, C_7H, C_8H,	7.3 ppm to	128 ppm to
C_9H, $C_{10}H^{a+b}$	7.6 ppm	136 ppm

[a] related data of the major isomer. [b] related data of the minor isomer.

Table 2

Identification of **3.18** was supported by mass spectrometric measurement which afforded the molecular ion at (m/z: 317.04 amu) as well as satisfactory elemental analysis (see Experimental). Attempts to grow single crystals of the new manganese complex were unsuccessful, leading, in each case, regardless of the technique used, to the formation of clusters which were ineffective for X-Ray crystallography.

Complex **3.18** was handled, purified and analysed as an air- and moisture-stable compound with no noticeable sign of decomposition, even after several weeks when handled this way. Important to notice that the compound showed some sign of discoloration when exposed to light for a long period of time, indicating possible decomposition of the complex.

3.2.2.4 Coordination chemistry of 3(*R*)-hydroxy-phenylphospholane, **3.7**, with Group 8 metal precursors **3.11** and **3.12.**

Addition of two molecular equivalents of 3(*R*)-hydroxy-phenylphospholane, **3.7**, to a solution of [RuCl(cymene)μ-Cl]$_2$, **3.11**, and one equivalent of **3.7** to a solution of [FeCp'(CO)$_2$(MeCN)]PF$_6$, **3.12**, in dichloromethane afforded the complex [Ru(cymene)Cl$_2$(k-P$_{R,S}$-**3.7**)], **3.19**, as a red-orange solid (Scheme 9) and the complex [FeCp'(CO)$_2$(k-P$_{R,S}$-**3.7**)]PF$_6$, **3.20**, as an orange-yelow solid (Scheme 10) respectively.

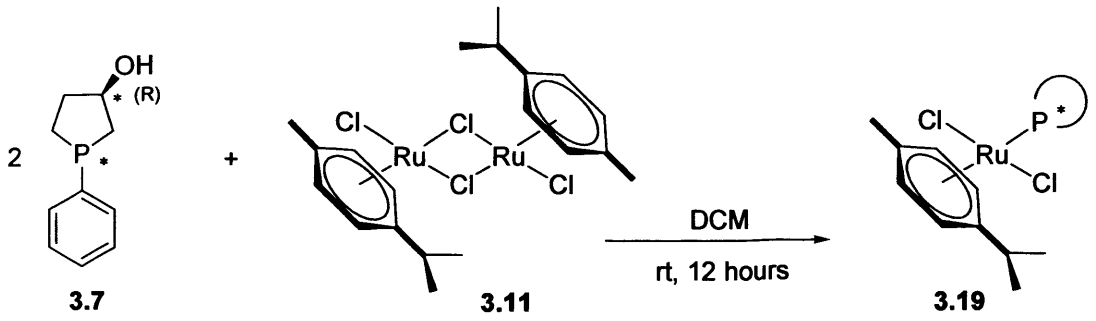

Scheme 9: Synthesis of [Ru(cymene)Cl$_2$(k-P$_{R,S}$-**3.7**)], **3.19.**

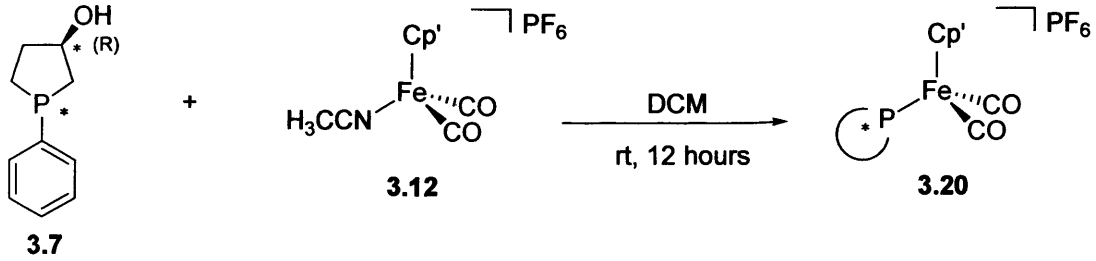

Scheme 10: Synthesis of [FeCp'(CO)$_2$(k-P$_{R,S}$-**3.7**)]PF$_6$, **3.20.**

Both reactions were followed *in situ* by $^{31}P\{^1H\}$ NMR spectroscopy which showed the rise of two new resonances at δ_P 35.1 ppm for the major isomer and δ_P 34.0 ppm for the minor isomer respectively for complex **3.19** (Spectrum 5) and two new resonances at δ_P 60.9 ppm for the major isomer and δ_P 60.7 ppm for the minor

isomer along with the septet of the PF_6^- counter ion at δ_P -143.0 ppm for complex **3.20** (Spectrum 6).

The ^1H NMR spectrum of the crude product of the ruthenium reaction showed some trace of the unreacted cymene precursor, **3.11**, and classical purification techniques were not sufficient to purify the desired complex **3.19**. Therefore, flash column chromatography was conducted in a gradient fashion from 100 % diethyl ether in which the desired product was eluted through 100 % methanol to 100 % THF in which the unwanted side products were eluted. By this process, the excess $[RuCl(cymene)\mu\text{-}Cl]_2$, **3.11**, was discarded (assessed by ^1H NMR spectroscopy) but as mentioned previously, the two isomers (assessed by $^{31}P\{^1H\}$ NMR spectroscopy) were not separated.

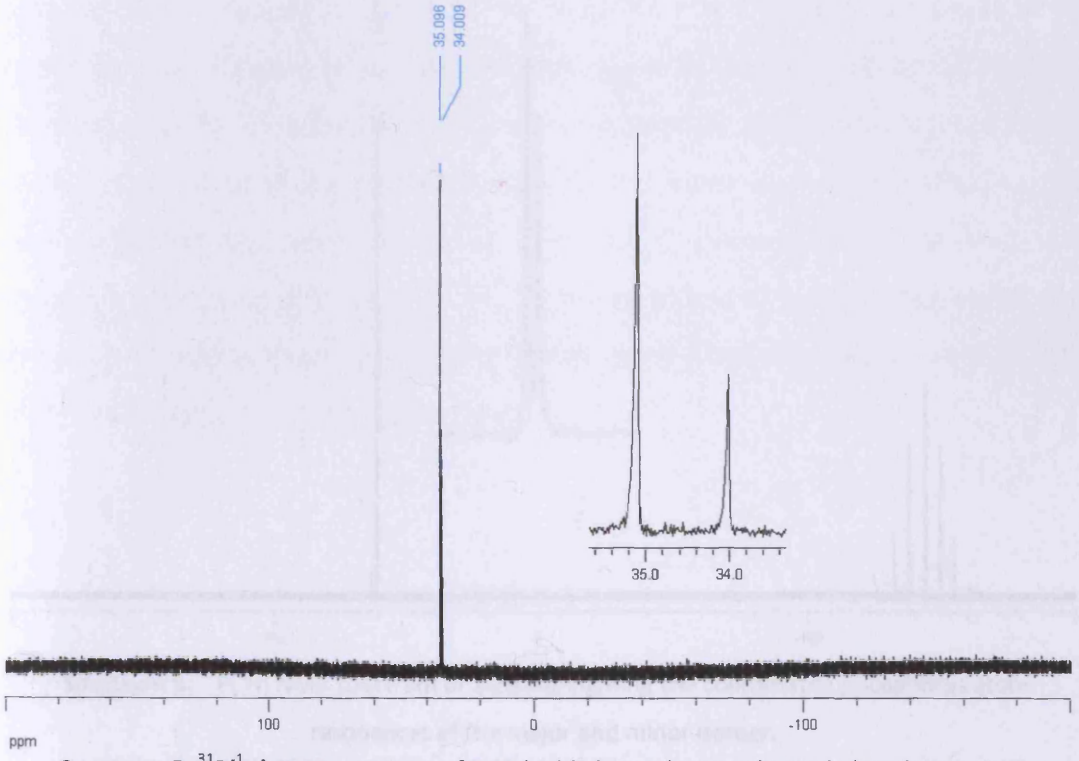

Spectrum 5: $^{31}P\{^1H\}$ NMR spectrum of **3.19** highlighting the coordinated phosphorus atom resonances of the major and minor isomer.

As before, flash column chromatography was conducted on complex **3.20** in a gradient fashion fom 100 % 40/60 petroleum ether which eluted the unwanted side-products as a dark brown solution through 100 % diethyl ether whereupon a yellow color band started to eluted, which was accelerated by gradually adding 100% dichloromethane and finally 100% THF to give the desired compound which was eluted as a bright yellow solution. Once again the chromatography was effective at purifying the desired compound **3.20** but no separation of the two isomers (assessed by $^{31}P\{^{1}H\}$ NMR spectroscopy) was observed. Therefore, the complexes **3.19** and **3.20** were characterised as a diastereomeric mixtures by a combinaison of ^{1}H, ^{13}C and $^{31}P\{^{1}H\}$ NMR spectroscopy and elemental analysis (see Experimental).

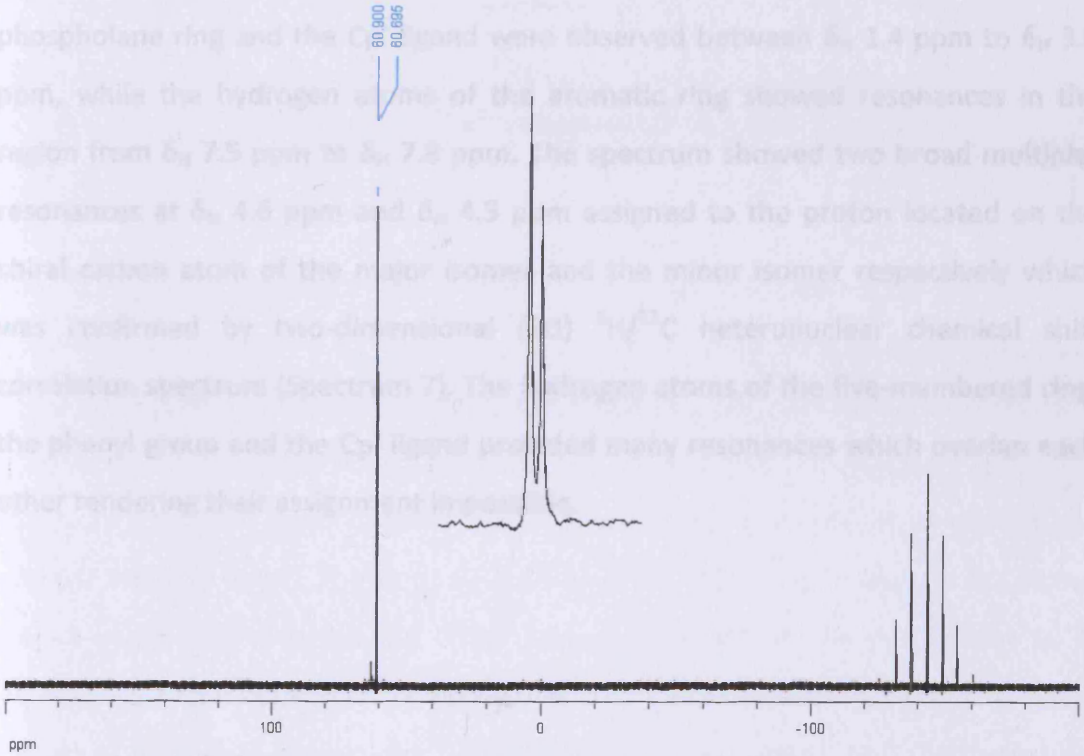

Spectrum 6: $^{31}P\{^{1}H\}$ NMR spectrum of **3.20** highlighting the coordinated phosphorus atom resonances of the major and minor isomer.

The ^{1}H NMR spectrum was used for the determination of the diastereomeric ratio. As before, the most reliable resonance for this purpose was the one assigned to the proton located on the chiral carbon atom $*C_3$ of the heterocycle. In general the

resonances for the proton atoms on the phospholane ring and the cymene ligand were observed between δ_H 0.9 ppm to δ_H 3.8 ppm, while the hydrogen atoms of the aromatic ring showed resonances in the region from δ_H 5 ppm to δ_H 7.8 ppm. The spectrum showed a broad doublet resonance at δ_H 4.3 ppm (br d, $^1J_{H\text{-}C}$ = 24.7 Hz, *C_3**H**) and an apparent broad doublet of multiplet at δ_H 4.5 ppm (br dm, $^1J_{H\text{-}C}$ = 15.3 Hz, *C_3**H**) assigned to the proton located on the chiral carbon atom of the major isomer and the minor isomer respectively, which was confirmed by two-dimensional (2D) $^1H/^{13}C$ heteronuclear chemical shift correlation spectrum. The hydrogen atoms of the five-membered ring, the phenyl group and the cymene ligand provided many resonances which were again overlaping each other rendering their assignment impossible.

Concerning the iron complex **3.20**, the resonances for the proton atoms on the phospholane ring and the Cp' ligand were observed between δ_H 1.4 ppm to δ_H 3.6 ppm, while the hydrogen atoms of the aromatic ring showed resonances in the region from δ_H 7.5 ppm to δ_H 7.8 ppm. The spectrum showed two broad multiplet resonances at δ_H 4.6 ppm and δ_H 4.5 ppm assigned to the proton located on the chiral carbon atom of the major isomer and the minor isomer respectively which was confirmed by two-dimensional (2D) $^1H/^{13}C$ heteronuclear chemical shift correlation spectrum (Spectrum 7). The hydrogen atoms of the five-membered ring, the phenyl group and the Cp' ligand provided many resonances which overlap each other rendering their assignment impossible.

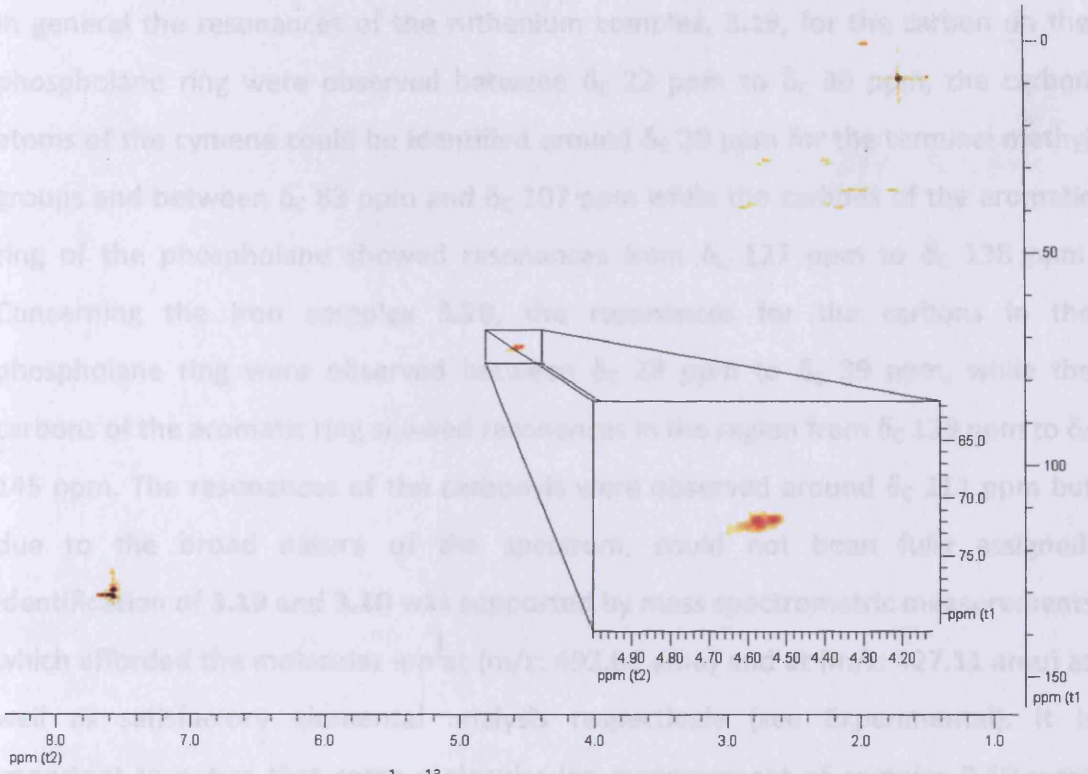

Spectrum 7: Two-dimensional (2D) $^{1}H/^{13}C$ heteronuclear chemical shift correlation spectrum of **3.20** focusing on the correlation at the $*C_3$ atom.

The $^{13}C\{^{1}H\}$ NMR spectrum provided relatively good resolution from which major and minor diastereomers of the compound were assigned for both complexes, **3.19** and **3.20**. However, the corresponding iron complex, **3.20**, spectrum appeared to be broadened rendering his full assignment difficult. The two-dimensional (2D) $^{1}H/^{13}C$ spectrum confirmed the resonance of the chiral carbon atom of the five-membered ring for which a broad singlet at δ_C 69.9 ppm for the major isomer and a broad singlet at δ_C 72.6 ppm for the minor isomer of **3.19** and a broad singlet at δ_C 71.70ppm for the major isomer and a broad singlet at δ_C 72.4 ppm for the minor isomer of **3.20** were seen in the $^{13}C\{^{1}H\}$ NMR spectrum respectively. The rest of the ^{13}C NMR spectrum of **3.19** and **3.20** was assigned for the major and the minor isomers (see Experimental for full detail). However, the low intensity of the signals arising from the minor isomer of complex **3.20** did not allow distinguishing all the corresponding resonances.

In general the resonances of the ruthenium complex, **3.19**, for the carbon on the phospholane ring were observed between δ_C 22 ppm to δ_C 36 ppm, the carbon atoms of the cymene could be identified around δ_C 20 ppm for the terminal methyl groups and between δ_C 83 ppm and δ_C 107 ppm while the carbons of the aromatic ring of the phospholane showed resonances from δ_C 127 ppm to δ_C 138 ppm. Concerning the iron complex **3.20**, the resonances for the carbons in the phospholane ring were observed between δ_C 28 ppm to δ_C 39 ppm, while the carbons of the aromatic ring showed resonances in the region from δ_C 129 ppm to δ_C 145 ppm. The resonances of the carbonyls were observed around δ_C 211 ppm but due to the broad nature of the spectrum, could not been fully assigned. Identification of **3.19** and **3.20** was supported by mass spectrometric measurements which afforded the molecular ion at (m/z: 492.01 amu) and at (m/z: 427.11 amu) as well as satisfactory elemental analysis respectively (see Experimental). It is important to notice that some molecular ion measurement of complex **3.19** were observed around (m/z: 992.26 amu) which was not clearly reliable as a direct derivative of our ruthenium complex but may indicate that some sort of polymerisation occurs *in situ*. Attempts to grow single crystals of the ruthenium complex or either the iron complex were unsuccessful leading, in each case, regardless of the technique used, to the formation of clusters which were useless for X-Ray crystallography. Complex **3.19** and **3.20** were handled, purified and analysed as air- and moisture-stable compounds which from no sign of decomposition was noticed, even after several weeks.

3.2.2.5 Coordination chemistry of 3(*R*)-hydroxy-phenylphospholane, **3.7**, with a rhodium metal precursor.

Addition of one molar equivalent of 3(*R*)-hydroxy-phenylphospholane, **3.7**, added to a solution of $[Rh(cod)\mu\text{-}Cl]_2$, **3.13**, in dichloromethane afforded the complex $[Rh(cod)Cl(k\text{-}P_{R,S}\text{-}\mathbf{3.7})]$, **3.21**, as a pale yellow-orange solid (Scheme 11).

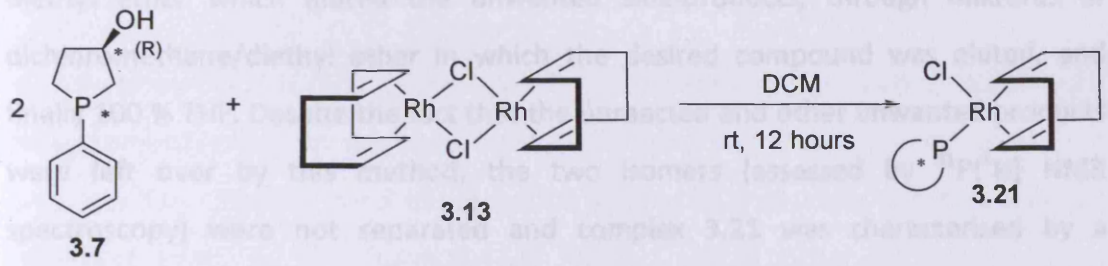

Scheme 11: Synthesis of [Rh(cod)Cl(k-$P_{R,S}$-**3.7**)], **3.21**.

The reaction was followed *in situ* by ^{31}P NMR spectroscopy which showed the rise of two new resonances at δ_P 27.1 ppm (d, $^1J_{Rh-P}$ = 148.3 Hz) for the major isomer and δ_P 27.0 ppm (d, $^1J_{Rh-P}$ = 146.9 Hz). for the minor isomer (Spectrum 8). Theses values correlate closely with those observed for previously published chiral phospholane compounds complexed with rhodium[20] as for [(COD)Rh(1,3-bis((2*R*,5*R*)-2,5-dimethylphospholano)-propane)]PF_6.and [(COD)Rh((2*R*,5*R*)-2,5-dimethyl-1-phenylphospholane)$_2$] SbF_6 which showed a doublet at δ_P 27.7 ppm (d, $^1J_{Rh-P}$ = 139.6 Hz) and δ_P 43.8 ppm (d, $^1J_{Rh-P}$ = 143.4 Hz) respectively.

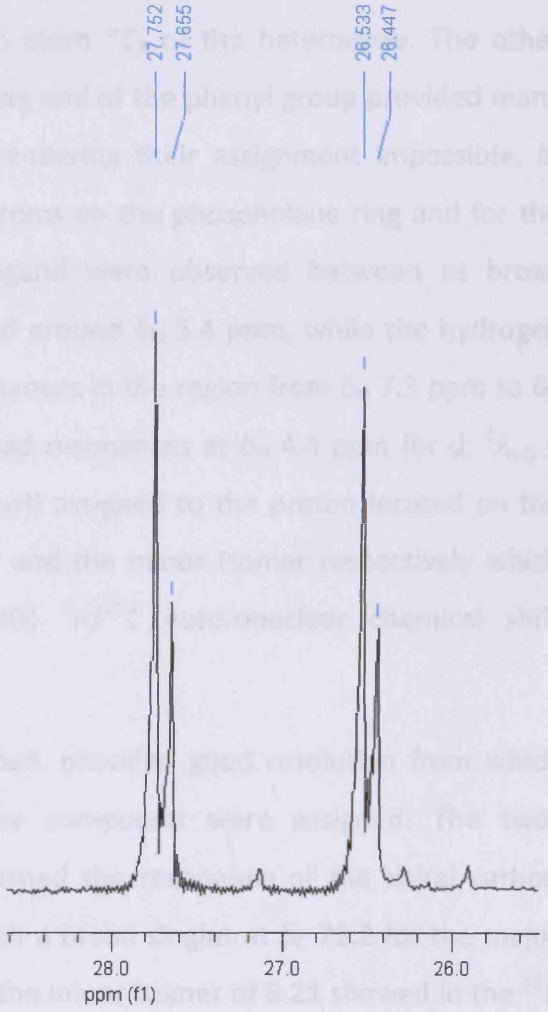

Spectrum 8: ^{31}P NMR spectrum of **3.21**.

Flash column chromatography was conducted in a gradient fashion from 100 % diethyl ether which eluted the unwanted side-products, through mixtures of dichloromethane/diethyl ether in which the desired compound was eluted, and finally 100 % THF. Despite the fact that the unreacted and other unwanted products were left over by this method, the two isomers (assessed by $^{31}P\{^{1}H\}$ NMR spectroscopy) were not separated and complex **3.21** was characterised by a combination of ^{1}H, ^{13}C and $^{31}P\{^{1}H\}$ NMR spectroscopy and elemental analysis (see Experimental).

The ^{1}H NMR spectrum was used for the determination of the diastereomeric ratio. At 500 MHz, the most reliable resonance for this purpose was the one assigned to the proton located on the chiral carbon atom $*C_3$ of the heterocycle. The other hydrogen atoms of the five-membered ring and of the phenyl group provided many resonances which overlap each other rendering their assignment impossible. In general the resonances for the proton atoms on the phospholane ring and for the proton atoms of the cyclooctadiene ligand were observed between as broad multiplets δ_H 0.8 ppm to δ_H 3.8 ppm and around δ_H 5.4 ppm, while the hydrogen atoms of the aromatic ring showed resonances in the region from δ_H 7.3 ppm to δ_H 7.6 ppm. The spectrum showed two broad resonances at δ_H 4.4 ppm (br d, $^{1}J_{H\text{-}C}$ = 24.1 Hz, $*C_3\mathbf{H}$)and δ_H 4.6 ppm (br m, $*C_3\mathbf{H}$) assigned to the proton located on the chiral carbon atom of the major isomer and the minor isomer respectively which was confirmed by two-dimensional (2D) $^{1}H/^{13}C$ heteronuclear chemical shift correlation spectrum.

The ^{13}C NMR spectrum, even if broadened, provided good resolution from which major and minor diastereomers of the compound were assigned. The two-dimensional (2D) $^{1}H/^{13}C$ spectrum confirmed the resonance of the chiral carbon atom of the five-membered ring for which a broad singlet at δ_C 72.2 for the major isomer and a broad singlet at δ_C 73.4 for the minor isomer of **3.21** showed in the ^{13}C NMR spectrum. The rest of the ^{13}C NMR spectra was fully assigned for the major and the minor isomers (see Experimental for full detail). In general the resonances for the carbon on the phospholane ring and the cyclooctadiene were observed between δ_C 23 ppm to δ_C 36.8 ppm as well as a doublet at δ_C 78.7 ppm (br d, cod), while the

carbons of the aromatic ring showed resonances in the region from δ_C 128 ppm to δ_C 131 ppm.

Identification of **3.21** was unfortunately not confirmed by mass spectrometric measurement neither by elemental analysis. Attempts to grow single crystals of the new rhodium complex were unsuccessful, leading in each case, regardless of the technique used, to the formation of clusters which were useless for X-Ray crystallography. Complex **3.21** was handled, purified and analysed as air- and moisture-stable compound which from no sign of decomposition was noticed (assessed by $^{31}P\{^1H\}$ NMR spectroscopy), even after several weeks.

3.2.2.6 Coordination chemistry of 3(*R*)-hydroxy-phenylphospholane, **3.7**, with Group 10 metal precursors platinum and palladium.

Addition of two molar equivalents of the 3(*R*)-hydroxy-phenylphospholane, **3.7**, ligand to a solution of dichloro(1,5-cyclooctadiene)platinum(II), **3.14**, in dichloromethane afforded the complex *cis*-[(k-$P_{R,S}$-**3.7**)$_2$ $PtCl_2$], **3.22**, as an air-stable white solid (Scheme 12).

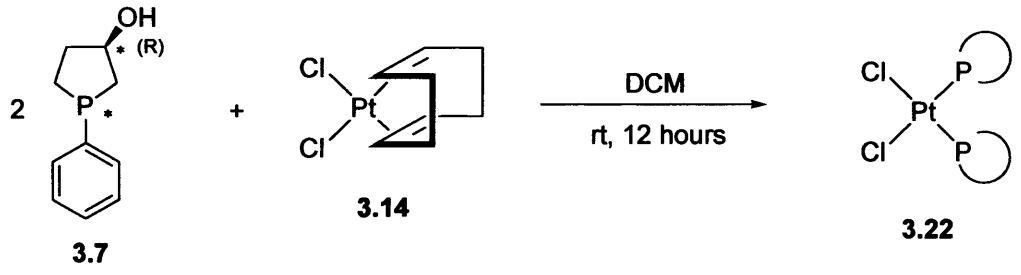

Scheme 12: Synthesis of *cis*-[(k-$P_{R,S}$-**3.7**)$_2$ $PtCl_2$], **3.22**.

Using the same condition reaction as described above but this time with dichloro(1,5-cyclooctadiene)palladium(II), **3.15**, afforded the complex *cis*-[(k-$P_{R,S}$-**3.7**)$_2$ $PdCl_2$], **3.23**, as an air-stable orange solid (Scheme 13).

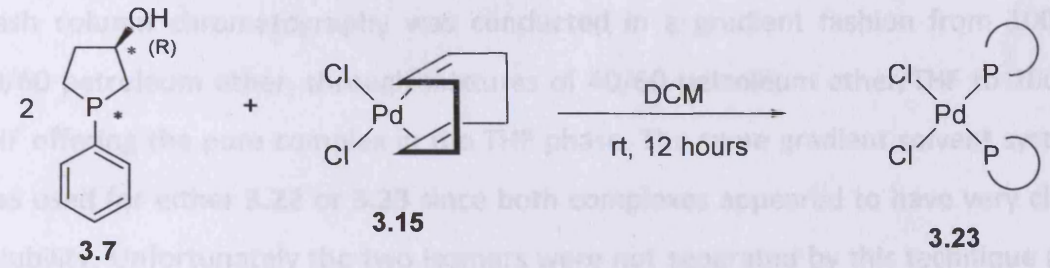

Scheme 13: Synthesis of *cis*-[(k-$P_{R,S}$-**3.7**)$_2$ $PdCl_2$], **3.23**.

Both of the reactions were followed by $^{31}P\{^1H\}$ NMR spectroscopy and the reactions were considered to be complete when the signal for the starting material, **3.7**, had disappeared. Two singlet resonances with their platinum satellites were observed in the ^{31}P NMR spectrum of the crude compound containing **3.22** in a 80:20 ratio at δ_P 13.8 ppm (s, $^1J_{Pt\text{-}P}$ = 3560 Hz), for the major isomer and δ_P 13.4 ppm (s, $^1J_{Pt\text{-}P}$ = 3559 Hz) for the minor isomer respectively (Spectrum 10). The $^{31}P\{^1H\}$ NMR spectrum of the solution containing the complex **3.23** showed two resonances in a 90:10 ratio at δ_P 47.1 ppm for the major isomer and δ_P 46.3 ppm for the minor isomer respectively (Spectrum 9). These values correlate closely to the thoses observed for previously published compounds complexed with platinum[21] and palladium[22] showing a singlet at δ_P 14.7 ppm (s, $^1J_{Pt\text{-}P}$ = 3524 Hz) and δ_P 32.4 ppm respectively.

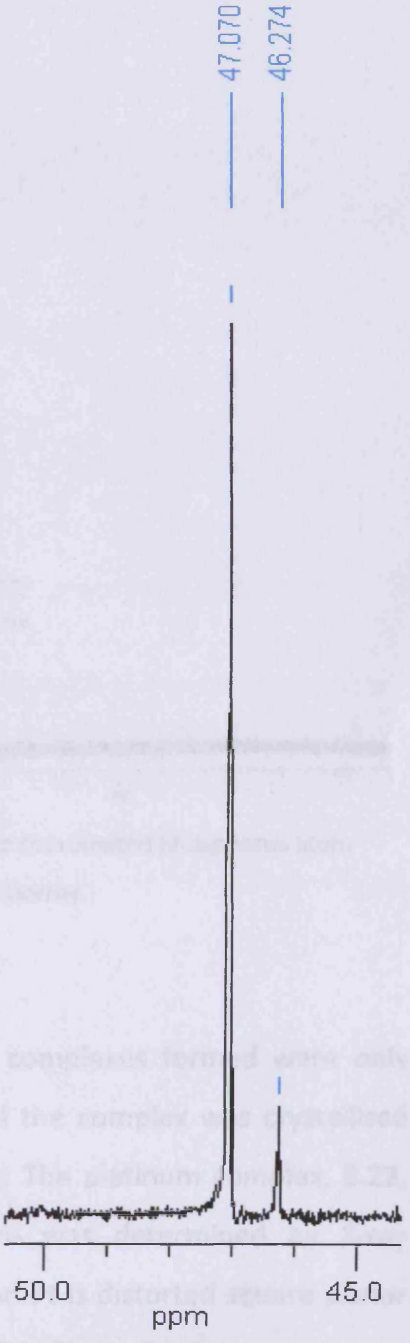

Spectrum 9: $^{31}P\{^1H\}$ NMR spectrum of **3.23** highlighting the coordinated phosphorus atom resonances of the major and minor isomer.

Flash column chromatography was conducted in a gradient fashion from 100 % 40/60 petroleum ether, through mixtures of 40/60 petroleum ether/THF to 100 % THF offering the pure complex in the THF phase. The same gradient solvent system was used for either **3.22** or **3.23** since both complexes appeared to have very close solubility. Unfortunately the two isomers were not separated by this technique and complexes **3.22** and **3.23** were then characterised respectively by spectroscopic methods, mass spectrometry and elemental analysis as a mixture of diastereomers.

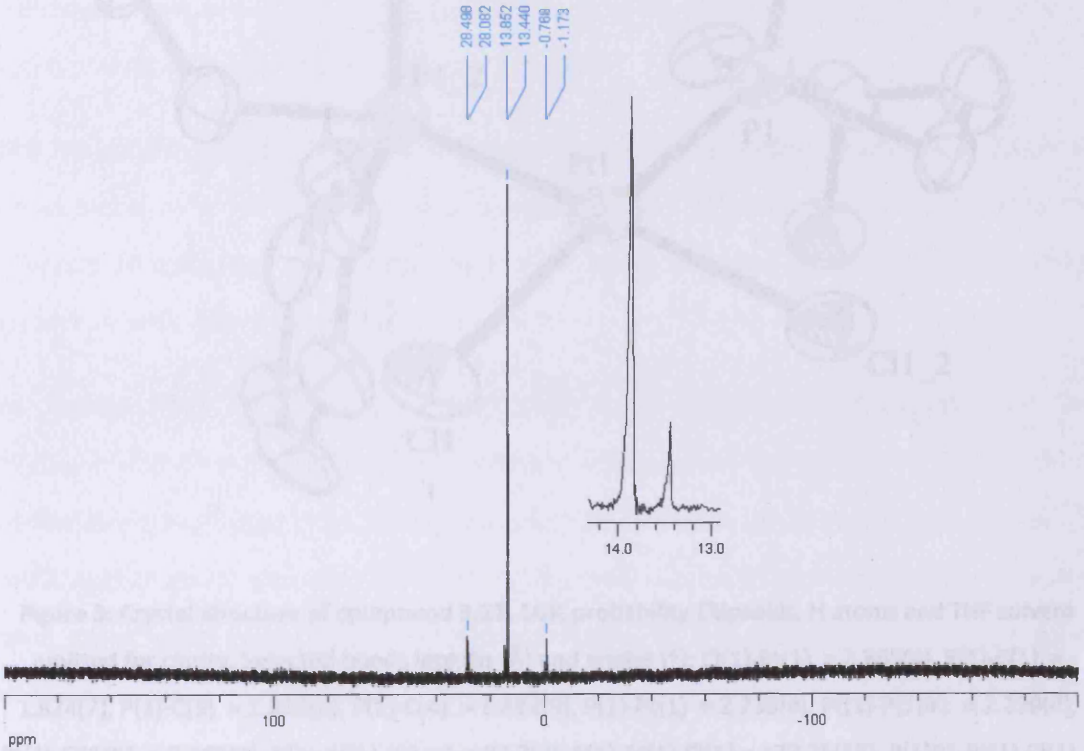

Spectrum 10: $^{31}P\{^{1}H\}$ NMR spectrum of **3.22** highlighting the coordinated phosphorus atom resonances of the major and minor isomer.

As mentioned before, the platinum and palladium complexes formed were only poorly soluble in various classical polar solvents and the complex was crystallised from DMSO by slow vapor diffusion of diethyl ether. The platinum complex, **3.22**, offered white needles crystals and their structure was determined by X-ray crystallography. The coordination environment around Pt is distorted square planar as shown by selected metrical data for compound **3.22** in Figure 3 below.

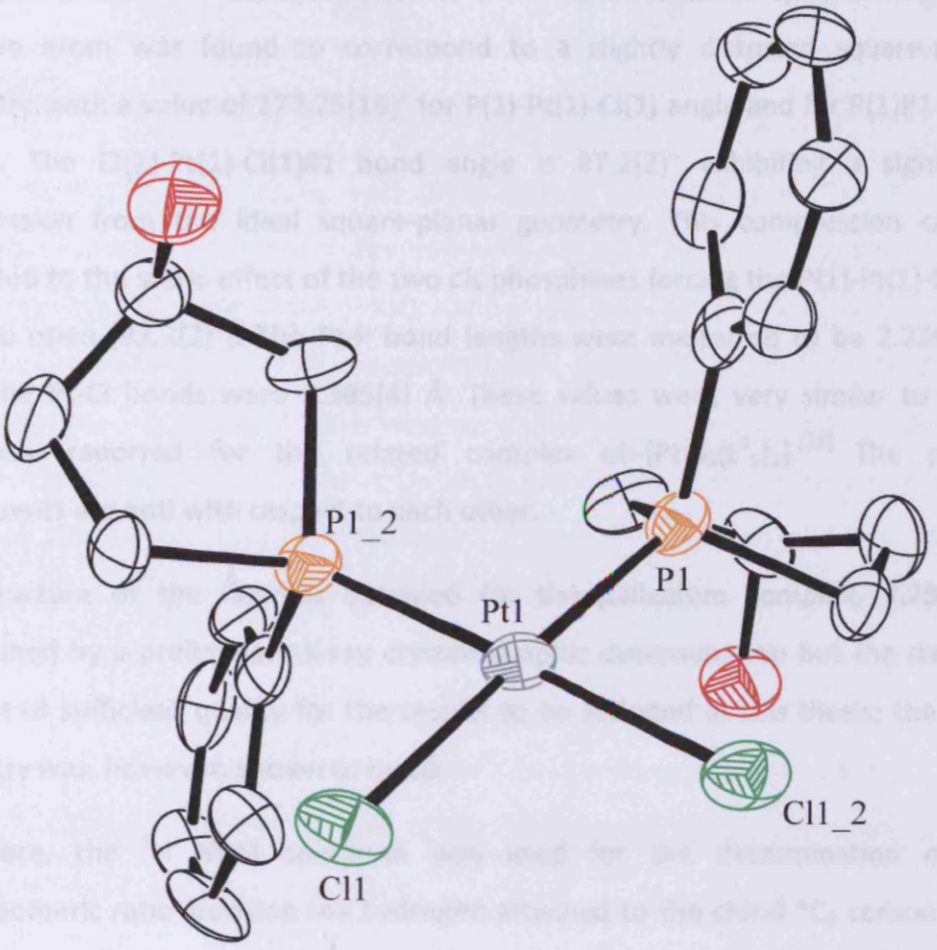

Figure 3: Crystal structure of compound **3.22**, 50% probability Ellipsoids, H atoms and THF solvent omitted for clarity. Selected bonds lengths (Å) and angles (º): Cl(1)-Pt(1) = 2.365(4), P(1)-C(1) = 1.824(7), P(1)-C(5) = 1.826(9), P(1)-C(4) = 1.832(9), P(1)-Pt(1) = 2.239(4), Pt(1)-P(1)#1 = 2.239(4), Pt(1)-Cl(1)#1 = 2.365(4), P(1)-Pt(1)-P(1)#1 = 92.2(2), P(1)-Pt(1)-Cl(1) = 177.25(18), P(1)#1-Pt(1)-Cl(1) = 90.32(8), P(1)-Pt(1)-Cl(1)#1 = 90.32(8), P(1)#1-Pt(1)-Cl(1)#1 = 177.25(18), Cl(1)-Pt(1)-Cl(1)#1 = 87.2(2) (#1 = -x+2,y,-z+2).

The molecule possesses a C_2 axis in the Cl-Pt-Cl plane that bisects Cl-Pt-Cl, and the two halves of the molecule are related by this. The coordination sphere around the platinum atom was found to correspond to a slightly distorted square-planar geometry, with a value of 177.25(18)° for P(1)-Pt(1)-Cl(1) angle and for P(1)#1-Pt(1)-Cl(1)#1. The Cl(1)-Pt(1)-Cl(1)#1 bond angle is 87.2(2)° exhibiting a significant compression from the ideal square-planar geometry. This compression can be attributed to the steric effect of the two *cis* phosphines forcing the P(1)-Pt(1)-P(1)#1 angle to open [92.2(2)°]. The Pt-P bond lengths were measured to be 2.239(4) Å while the Pt-Cl bonds were 2.365(4) Å. These values were very similar to those previously reported for the related complex *cis*-$[PtCl_2(L^a{}_5)_2]$.[21] The phenyl substituents are anti with respect to each other.

The structure of the needles obtained for the palladium complex, **3.23**, was determined by a preliminary X-ray crystallographic determination but the data set was not of sufficient quality for the results to be included in this thesis; the gross geometry was, however, shown to be *cis*.

As before, the ^1H NMR spectrum was used for the determination of the diastereomeric ratio studying the hydrogen attached to the chiral $*C_3$ carbon atom of the five-membered ring. Unfortunately, the ^1H NMR spectrum as well as the ^{13}C NMR spectrum of the palladium complex, **3.23**, were extremely broad rendering their assignment impossible. This was attributed to the presence of the mixture of isomers coupled to a very small scale of the eluted desired compound after the flash column chromatography, the palladium complex being, as mentioned before, poorly soluble in various classical polar solvents was very slowly eluted after the addition of several quantities of 100 % THF and the increase in polarity at this stage was an impossible choice since unwanted products may co-elute under these condition.

Concerning the platinum complex, **3.22**, the hydrogen atoms of the five-membered ring and of the phenyl group provided many resonances which overlap each other rendering their assignment difficult. In general the resonances for the proton atoms on the phospholane ring were observed between δ_H 1.7 ppm to δ_H 3.5 ppm, while the hydrogen atoms of the aromatic ring showed resonances in the region from δ_H

7.4 ppm to δ_H 7.9 ppm. The spectrum showed only one broad doublet resonance at δ_H 4.4 ppm (br d, $^1J_{H\text{-}C}$ = 19.4 Hz, *C_3**H**)assigned to the proton located on the chiral carbon atom of the major isomer which was confirmed by two-dimensional (2D) $^1H/^{13}C$ heteronuclear chemical shift correlation spectrum.

The ^{13}C NMR spectrum of **3.22**, even if broadened, provided good resolution from the major diastereomer of the compound were assigned. However, the low intensity of the signals arising from the minor isomer did not allow distinguishing all the corresponding resonances (see Experimental for detail). The two-dimensional (2D) $^1H/^{13}C$ spectrum confirmed the resonance of the chiral carbon atom of the five-membered ring for which a broad singlet at δ_C 71.1 for the major isomer and a broad singlet at δ_C 73.1 for the minor isomer of **3.22** were showed in the $^{13}C\{^1H\}$ NMR spectrum. The phospholane region as well as the aromatic ring region showed the appropriate correlation but there could not be cleary assigned due to the broadened nature of the data. In general the $^{13}C\{^1H\}$ NMR spectrum showed that the resonances for the carbon on the phospholane ring were observed between δ_C 25 ppm to δ_C 42 ppm, while the carbons of the aromatic ring showed resonances in the region from δ_C 126 ppm to δ_C 134 ppm.

Identification of **3.22** was supported by mass spectrometric measurements which afforded the molecular ion at (m/z = 608.09 amu) as well as satisfactory elemental analysis (see Experimental). Complex **3.23** afforded the molecular ion at (m/z = 519.05 amu) but unfortunately did not provide satisfactory elemental analysis.

Complexes **3.22** and **3.23** were handled, purified and analysed as air- and moisture-stable compounds which from no sign of decomposition was noticed (assessed by $^{31}P\{^1H\}$ NMR spectroscopy), even after several weeks.

3.3 Conclusion

A new chiral, rigid phospholane ligand **3.7** has been successfully synthesised by a 4 step synthesis in relatively good yield but the separation of the mixture of diastereomers obtained was not achieved. All attempts to coordinate this new chiral ligand, **3.7**, to molybdenum or rhenium gave mixtures from which it did not prove possible to obtain crystals.

The complexes $[Mn(CO)_5(k\text{-}P_{R,S}\text{-}\mathbf{3.7})]OTf$, **3.18**, $[Ru(cymene)Cl(k\text{-}P_{R,S}\text{-}\mathbf{3.7})]$, **3.19**, $[FeCp'(CO)_2(k\text{-}P_{R,S}\text{-}\mathbf{3.7})]PF_6$, **3.20**, $[Rh(cod)Cl(k\text{-}P_{R,S}\text{-}\mathbf{3.7})]$, **3.21**, were successfully prepared and characterised. It did not prove possible to separate the two diastereomers for any of theses systems.

The *cis*-$[(k\text{-}P_{R,S}\text{-}\mathbf{3.7})_2\ PtCl_2]$, **3.22**, and *cis*-$[(k\text{-}P_{R,S}\text{-}\mathbf{3.7})_2\ PdCl_2]$, **3.23**, complexes were succesfully synthesised and characterised by spectroscopic methods and their structure determined by X-Ray crystallography showing in both cases a *cis* geometry.

3.4 Experimental

3.4.1 Methods and materials

Unless otherwise stated all manipulations were carried out using standard Schlenk techniques, under an atmosphere of dry nitrogen. All solvents were dried and degassed by refluxing over standard drying agents under a nitrogen atmosphere. The starting materials $[Mo(pip)_2(CO)_4]$, **3.8**, (pip=piperidine), $Re(CO)_5Br$, **3.9**, $Mn(OTf)(CO)_5$, **3.10**, $[RuCl(cymene)\mu\text{-}Cl]_2$, **3.11**, $[FeCp'(CO)_2(MeCN)]PF_6$, **3.12**, ($Cp'=C_5Me_5$), $[Rh(cod)\mu\text{-}Cl]_2$, **3.13**, $[PtCl_2(cod)]$, **3.14**, and $[PdCl_2(cod)]$, **3.15**, were prepared according to literature methods.[16, 23, 24] (*S*)-Bromosuccinic acid, **3.2**, (*S*)-2-bromo-1,4-butanediol, **3.3**, (*R*)-2-(oxiran-2-yl)ethyl-4-methylphenylsulfonate, **3.4**, and (*R*)-2-(2-iodoethyl)oxirane, **3.5**, were prepared by modification of literature preparation.[13, 14, 15] Commercial reagents were used as supplied without further purification unless otherwise stated. All Phosphines and phospholanes ligands were stored under dry nitrogen atmosphere at room temperature. All complexes were stable to air and were stored as solids in air at room temperature. Column chromatography was carried out using Merk Kieselgel 60 H silica or Matrex silica 60. Analytical thin layer chromatography was carried out using aluminium-backed plates coated with Merck Kieselgel 60 GF_{254} that were visualised under UV light (at 254 and/or 360 nm). Deuterated solvents were dried over 3 or 4 Å molecular sieves and degassed by freeze-pump-thaw methods. The NMR spectra were recorded on a Bruker DPX-500 instrument at 500 MHz (^1H), 125.75 MHz (^{13}C) and 202.75 MHz (^{31}P), Bruker DPX-400 instrument at 400 MHz (^1H) and 100 MHz (^{13}C), Jeol Lamda Eclipse 300 at 121.65 MHz (^{31}P) and 75.57 MHz (^{13}C). ^1H and ^{13}C chemical shifts are quoted in ppm relative to residual solvent resonances, and ^{31}P chemical shifts are quoted in ppm relative to external 85% H_3PO_4; *J* values were recorded in Hz and multiplicities were expressed by the usual conventions (s=singlet, d=doublet, t=triplet, app=apparent, m=multiplet). *In vacuo* refers to evaporation at reduced pressure using a rotary evaporator and diaphragm pump, followed by removal of trace

volatiles using a vacuum (oil) pump. Infra-red spectra were recorded on a JASCO FT/IR-660 plus Spectrometer and the samples were prepared under N_2 as a KBr disk or as solution. Mass spectra of all the samples have been collected by direct injection into a Waters LCT Premier XE mass spectrometer fitted with an ESCI source.

Elemental analyses were performed by MEDAC LTD, UK, Analytical and Chemical Consultancy Services.

3.4.2 Syntheses

3.4.2.1 Synthesis of (*S*)-Bromosuccinic acid, **3.2**.

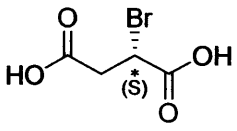

A 2 L round bottom flask equipped with a mechanical stirrer and a thermometer was charged with (L) + aspartic acid, **3.1**, (20.22 g; 0.15 mol) and potassium bromide (8.10 g; 0.68 mol). Sulphuric acid (1 M, 400 ml) was added and the solution was cooled to -5 °C. A solution of sodium nitrite (19.12 g; 0.28 mol) in H_2O (40 ml) was added via an addition funnel being careful to maintain the temperature below 0 °C during the 50 minutes addition period. The resulting brown mixture was stirred for 2 hours at -5 °C and then extracted with EtoAc (4 x 200 ml). The combined EtoAc extracts were dried over Na_2SO_4, filtered, and concentrated *in vacuo* to afford the desired product, **3.2**, as a white solid. Yield: 88 %. Spectroscopic and physical properties agree with those reported in ref. 15.

3.4.2.2 Synthesis of (*S*)-2-bromo-1,4-butanediol, **3.3**.

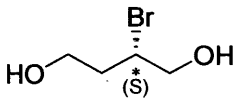

In a 1 L round bottom flask equipped with a mechanical stirrer, bromosuccinic acid, **3.2**, (8.81 g; 44.7 mmol) was suspended in THF (70 ml). The mixture was cooled to 0 °C in an ice bath and BH_3-THF (134 ml, 1 M; 0.134 mol) was added *via* a cannula over a 20 minute period. After the addition, the cooling bath was removed and the reaction was stirred for 4 hours. The excess borane was quenched by the addition of THF/H_2O (18 ml, 1:1) then calcinated K_2CO_3 (30 g) was added. This mixture was stirred, then filtered and the solid residue was washed with Et_2O (3 x 15 ml). The combinated filtrate and Et_2O washes were concentrated *in vacuo* to a mixture of a yellow oil and borate salts. The oil was then redissolved in Et_2O (2 x 40 ml) and filtered away from the borate salts. The filtrate was dried over MgSO4, filtered and evaporated to an oil which was chromatographed on silica gel (1:1, acetone/ dichloromethane) to give the desired product **3.3**. Purification by flash column (2:1, acetone/ dichloromethane) was runed two times and afforded a pure bright orange-yellow viscous oil. Yield: 92 %. Spectroscopic and physical properties agree with those reported in ref. 15.

3.4.2.3 Synthesis of (*R*)-2-(oxiran-2-yl)ethyl-4-methylphenylsulfonate, **3.4**.

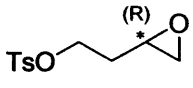

A 2.5 g portion of NaH (60 % in oil, 83 mmol) was washed free of oil with 3x5 ml portions of 40/60 petroleum ether, the residual 40/60 petroleum ether were evaporated and the residue was diluted with of anhydrous THF (15 ml). The resulting suspension was cooled to -10 °C and a soultion of 1.15 g (7 mmol) of bromobutanediol, **3.3**, in 15 ml of anhydrous THF was added dropwise over 10 minutes period. The resulting mixture was stirred for 30 minutes at -10 °C and 2.5 g of solid *p*-toluenesulfonylchloride (13 mmol) was added. After 4 hours at -10 °C the mixture was diluted with Et_2O (50 ml) and filtered through a pad of SiO_2.

Concentration of the filtrate *in vacuo* and purification by flash column (SiO_2; Et_2O/(40/60) petroleum ether 4:1) afforded 2.12 g of the desired product, **3.4**, as a bright yellow oil. Yield: 91 %. Spectroscopic and physical properties agree with those reported in ref. 15.

3.4.2.4 Synthesis of (*R*)-2-(2-iodoethyl)oxirane, **3.5**.

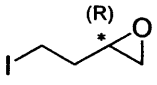

A solution of 0.76 g (3.1 mmol) of 2-(oxiran-2-yl)ethyl-4-methylphenylsulfonate, **3.4**, in 35 ml of acetone was combined with 0.47 g of solid NaI (3.1 mmol) and the mixture was heated at reflux for 2 hours. After cooling to room temperature, the mixture was diluted with 15 ml of Et_2O and filtered through a pad of Celite. The filtrate was concentrated *in vacuo* to afford 0.37 g of the desired product, **3.5**, as a colourless oil. Yield: 96 %. Spectroscopic and physical properties agree with those reported in ref. 15.

3.4.2.5 Synthesis of phenylphosphine, **3.6**.

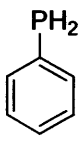

Dichlorophenylphosphine (48.9 g; 0.27 mol) in ether (125 ml) was added dropwise with stirring to a flask containing lithium aluminium hydride (10 g; 0.27 mol) in diethyl ether (200 ml). Stirring was continued for 1 hour, water (26 ml) added and the mixture refluxed for 2 hours. The liquid was then filtered; excess of solvent removed by distillation and the residual liquid dried over anhydrous calcium chloride, decanted, and distilled to afford phenyphosphine, **3.6**, as a colourless liquid. Yield: 56 %.

3.4.2.6 Synthesis of 3(*R*)-hydroxy-phenylphospholane, **3.7**.

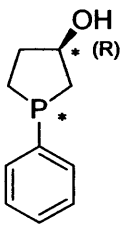

To a solution of n-BuLi (1.134; 18mmol) in THF (20 ml) was added phenylphosphine, **3.6**, (1ml; 9mmol) over 15 min period at -78 °C. The reaction mixture was stirred at -78 °C for 20 min before being warmed up to 0 °C and added dropwise to a solution of 2-(oxiran-2-yl) ethyl-4-methylphenylsulfonate, **3.4** (1.99g; 9mmol) in THF (15 ml) at -78 °C. The resultant solution was stirred at -78 °C for 60 min then warmed up to room temperature and allowed to stir for an additional 4 hours. NaCl/H_2O degassed solution was added and the organic phase extracted. The mixture was washed with dichloromethane (5 x 30 ml), the different organic extracts were collected and dried over $MgSO_4$. The solution was filtered and the solvent removed under reduced pressure to leave a bright yellow viscous oil as the desired product, **3.7**. Yield: 89 %. (major) ^{1}H NMR δ ppm ($CDCl_3$) = 1.2-2.4 (br m, 6 H, C_1H_2, C_2H_2, C_4H_2), 4.1 (br s, 1 H, OH), 4.4 (br s, 1 H, *C_3H_2), 7-7.8 (br m, 4 H, C_6H, C_7H, C_8H, C_9H). ^{13}C NMR δ ppm ($CDCl_3$) = 23.0 (d, 1 C, C_1H_2), 36.0 (d, 2 C, C_2H_2, C_4H_2), 74.6 (d, $^1J_{C\text{-}H}$ = 4 Hz, *C_3H), 127.4 (s, 1 C, C_8H), 128.3 (app d, 2 C, C_7H, C_9H), 130.2 (d, 2 C, C_6H, $C_{10}H$), 141.6 (d, 1 C, C_5). ^{31}P{^{1}H} NMR δ ppm ($CDCl_3$) = -18.2 (s). (minor) ^{1}H NMR δ ppm ($CDCl_3$) = 1-2.4 ppm (br m, 6 H, C_1H_2, C_2H_2, C_4H_2), 3.8 ppm (br s, 1 H, OH), 4.4 ppm (app m, 1 H, *C_3H_2), 7-7.8 ppm (m br, 4 H, C_6H, C_7H, C_8H, C_9H). ^{13}C NMR δ ppm ($CDCl_3$) = 23.5 (d, 1 C, C_1H_2), 35.1 (d, 1 C, C_4H_2), 36.0 (d, 1 C, C_2H_2), 74.9 (d, $^1J_{C\text{-}H}$ = 2.1 Hz, *C_3H), 127.6 (s, 1 C, C_8H), 128.3 (app d, 2 C, C_7H, C_9H), 130.7 (d, 2 C, C_6H, $C_{10}H$), 141.9 (d, 1 C, C_5). ^{31}P{^{1}H} NMR δ ppm ($CDCl_3$) = -20.2 (s). (major+minor) (TOF-MS, ES+): m/z (%) = 181.08 (100) $[M]^+$

3.4.2.7 Preparation of [Mo(k-$P_{R,S}$-**3.7**)$_2$(CO)$_4$], **3.16**.

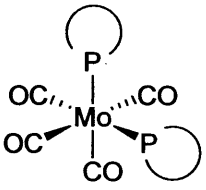

To a solution of [Mo(pip)$_2$(CO)$_4$], **3.8**, (46 mg; 0.12 mmol) in dichloromethane (10 ml) was added a solution of, **3.7**, (44 mg; 0.24 mmol) in dichloromethane (10 ml). The resulting yellow solution was stirred for 12 hours and the solvent removed under reduced pressure. Attempts to purify the product by flash column chromatography were unsuccessful offering an unclean crude product, **3.16**. Yield: 82 %.

3.4.2.8 Preparation of [ReBr(CO)$_4$(k-$P_{R,S}$-**3.7**)], **3.17**.

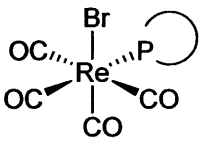

To a solution of ReBr(CO)$_5$, **3.9**, (99.2 mg, 0.24 mmol) in dichloromethane (10 ml) was added a solution of, **3.7**, (44 mg; 0.24 mmol) in dichloromethane (10 ml). The resulting yellow solution was stirred for 12 hours and the solvent removed under reduced pressure offering a mixture of compound. Attempts to purify the product by flash column chromatography, as well as classic solvent method were unsuccessful.

3.4.2.9 Preparation of [Mn(CO)$_5$(k-$P_{R,S}$-**3.7**)]OTf, **3.18**.

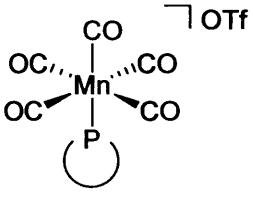

To a solution of Mn(OTf)(CO)$_5$, **3.10**, (84 mg; 0.24 mmol) in dichloromethane (10 ml) was added a solution of, **3.7**, (44 mg; 0.24 mmol) in dichloromethane (10 ml). The resulting yellow solution was stirred for 12 hours and the solvent removed under reduced pressure to afford the desired product, **3.18**. The crude mixture was purified by flash column chromatography firstly washed with 100 % 40/60

petroleum ether then miture of 40/60 petroleum ether/Et_2O followed by 100 % THF. The different desired phases were combined and solvent removed *in vacuo* to give a mixture of diastereomers of, **3.18**, as off-white air-stable powders. Yield: 91 %. (major) ^1H NMR δ ppm ($CDCl_3$) = 1.2 (br s, 1 H, **CH**), 1.9 (br s, 1 H, **CH**), 1.9 (br s, 1 H, **CH**), 2.5 (br s, 1 H, **CH**), 3.2 (br s, 1 H, **CH**), 3.6 (br s, 1 H, **CH**), 4.4 ppm (br d, $^1J_{H-C}$ = 15.8 Hz, *C_3**H**), 5.4 (br s, 1 H, **OH**), 7.4 (br m, 3 H, C_7**H**, C_8**H**, C_9**H**), 7.6 (br m, 2 H, C_6**H**, C_{10}**H**). ^{13}C NMR δ ppm ($CDCl_3$) = 25.8 (d, $^1J_{C-H}$ = 26.9 Hz, **C**$_1H_2$), 35.5 (s), 37.4 (d, $^1J_{C-H}$ = 26.4 Hz, **C**$_2H_2$, **C**$_4H_2$), 65.3 (s), 72.0 (s, 1 C, ***C**$_3H_2$), 128.9 (d, $^1J_{C-H}$ = 9.7 Hz, **C**$_7$H, **C**$_9$H), 129.7 (d, $^1J_{C-H}$ = 8.1 Hz, **C**$_6$H, **C**$_{10}$H), 130.2 (s, 1 C, **C**$_8$H), 136.4 (d, $^1J_{C-P}$ = 2.7 Hz, **C**$_5$). $^{31}P\{^1H\}$ NMR δ ppm ($CDCl_3$) = 42.7 (s). (minor) ^1H NMR δ ppm ($CDCl_3$) = 1.2 (br s, 1 H, **CH**), 1.7 (br s, 1 H, **CH**), 2.0 (br s, 1 H, **CH**), 2.6 (br s, 1 H, **CH**), 2.9 (br s, 1 H, **OH**), 3.2 (br s, 1 H, **CH**), 3.5 (br s, 1 H, **CH**), 4.5 ppm (br d, $^1J_{H-C}$ = 15.9 Hz, *C_3**H**), 7.3 (br m, 3 H, C_7**H**, C_8**H**, C_9**H**), 7.5 (br m, 2 H, C_6**H**, C_{10}**H**). ^{13}C NMR δ ppm ($CDCl_3$) = 26.4 (d, $^1J_{C-H}$ = 26.3 Hz, **C**$_1H_2$), 35.9 (s), 37.8 (d, $^1J_{C-H}$ = 27.7 Hz, **C**$_2H_2$, **C**$_4H_2$), 67.4 (s), 73.1 (s, 1 C, ***C**$_3H_2$), 129.2 (d, $^1J_{C-H}$ = 8.9 Hz, **C**$_7$H, **C**$_9$H), 129.8 (d, $^1J_{C-H}$ = 2.5 Hz, **C**$_6$H, **C**$_{10}$H), 130.1 (s, 1 C, **C**$_8$H), 136.7 (d, $^1J_{C-P}$ = 5.6 Hz, **C**$_5$). $^{31}P\{^1H\}$ NMR δ ppm ($CDCl_3$) = 41.4 (s). Anal. Calc. for $C_{15}H_{13}O_6MnP$ (375.17) = C,48.02; H,3.49. Found = C,48.76; H,4.21 %.(TOF-MS, ES+): m/z (%) = 317.04 (100) $[M-2CO-2H]^+$

3.4.2.10 Preparation of [Ru(cymene)Cl_2(k-$P_{R,S}$-**3.7**)], **3.19**.

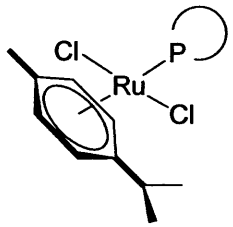

To a solution of [RuCl(cymene)μ-Cl]$_2$, **3.11**, (74.8 mg; 0.12 mmol) in dichloromethane (10 ml) was added a solution of, **3.7**, (44 mg; 0.24 mmol) in dichloromethane (10 ml). The resulting red-orange solution was stirred for 12 hours and the solvent removed under reduced pressure to afford the desired product, **3.19**. The crude mixture was purified by flash column chromatography firstly washed with 100 % diethyl ether then 100 % methanol followed by 100 % THF. The diethyl ether phases were combined and solvent removed *in vacuo* to give a mixture of diastereomers of,

3.19, as off-white air-stable powder. Yield: 88 %. (major) ^{1}H NMR δ ppm ($CDCl_3$) = 1.0 (s), 1.1 (s), 1.2 (s), 1.4 (s), 1.8 (s), 2.1 (br s), 2.6 (br m), 2.7 (t, 5.4 Hz), 3.4 (q, 7.0 Hz), 4.3 (br d, $^{1}J_{H\text{-}C}$ = 24.7 Hz, *C_3**H**), 5.1 (br d, 6.5 Hz), 5.1 (s), 7.4 (br m), 7.7 (br m). ^{13}C NMR δ ppm ($CDCl_3$) = 20.5 (s), 22.3 (d, $^{1}J_{C\text{-}H}$ = 29 Hz, **C**$_1$H$_2$), 29.1 (app s), 35.58 (d, $^{1}J_{C\text{-}H}$ = 29 Hz, **C**$_2$H$_2$), 35.1 (s, **C**$_4$H$_2$), 69.9 (s, *C_3H), 83.4 (d, 4.8 Hz), 84 (d, 4.8 Hz), 87.9 (br s), 93.7 (s), 106.8 (s), 127.6 (d, $^{1}J_{C\text{-}H}$ = 9.7 Hz, **C**$_6$H, **C**$_{10}$H), 128.4 (d, $^{1}J_{C\text{-}H}$ = 6.5 Hz, **C**$_7$H, **C**$_9$H), 129.1 (s, **C**$_8$H), 135.2 (d, $^{1}J_{C\text{-}P}$ = 36 Hz, **C**$_5$). ^{31}P{^{1}H} NMR δ ppm ($CDCl_3$) = 35.1 (s). (minor) ^{1}H NMR δ ppm ($CDCl_3$) = 0.9 (s), 1.0 (s), 1.1 (s), 1.8 (s), 2.2 (br s), 2.5 (br m), 2.7 (t, 5.4 Hz), 3.6 (q, 7.0 Hz), 4.5 (br d, $^{1}J_{H\text{-}C}$ = 15.4 Hz, *C_3**H**), 5.0 (br d, 7.2 Hz), 5.1 (s), 7.4 (br m), 7.8 (br m). ^{13}C NMR δ ppm ($CDCl_3$) = 16.7 (s), 22.3 (d, $^{1}J_{C\text{-}H}$ = 29 Hz, **C**$_1$H$_2$), 28.4 (s), 34.0 (d, $^{1}J_{C\text{-}H}$ = 31 Hz, **C**$_2$H$_2$), 34.7 (s, **C**$_4$H$_2$), 72.6 (s, *C_3H), 83.7 (d, 4.8 Hz), 83.8 (d, 4.8 Hz), 87.9 (br s), 93.4 (s), 106.6 (s), 127.3 (d, $^{1}J_{C\text{-}H}$ = 9.7 Hz, **C**$_6$H, **C**$_{10}$H), 128.3 (d, $^{1}J_{C\text{-}H}$ = 6.5 Hz, **C**$_7$H, **C**$_9$H), 128.6 (s, **C**$_8$H), 138.1 (d, $^{1}J_{C\text{-}P}$ = 36 Hz, **C**$_5$). ^{31}P{^{1}H} NMR δ ppm ($CDCl_3$) = 34.0 (s). IR (CH_2Cl_2) = ν(OH) = 3699s cm^{-1}. Anal. Calc. for $RuPC_{20}H_{26}OCl$ (449.92) = C,53.39; H,5.82. Found = C,53.83; H,6.67 %. (TOF-MS, ES+): m/z (%) = 492.01 (100) [M-acetonitrile]$^{+}$.

3.4.2.11 Preparation of [FeCp'(CO)$_2$(k-P$_{R,S}$-**3.7**)]PF$_6$, **3.20**.

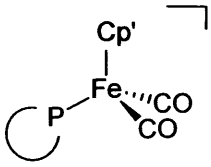

To a solution of [FeCp'(CO)$_2$(MeCN)]PF$_6$, **3.12**, (0.1g; 0.24 mmol) in dichloromethane (10 ml) was added a solution of, **3.7**, (44 mg; 0.24 mmol) in dichloromethane (10 ml). The resulting dark red-brown solution was stirred for 12 hours and the solvent removed under reduced pressure to afford the desired product, **3.20**. The crude mixture was purified by flash column chromatography firstly washed with 100 % 40/60 petroleum ether then mixture of 40/60 petroleum ether/Et_2O), 100 % dichloromethane, followed by 100 % THF. The THF phases were combined and solvent removed *in vacuo* to give a mixture of diastereomers of, **3.20**, as off-white air-stable powder. Yield: 93 %. Recrystallisation from methanol was so far

unsuccessful leading to the formation of clusters only. ^{1}H NMR δ ppm ($CDCl_3$) = 1.0-3.8 (br m), (major) 4.6 (br m, *C_3**H**), (minor) 4.5 (br m, *C_3**H**), 7.5-7.7 (br m). ^{13}C NMR δ ppm ($CDCl_3$) = 28.1 (d, $^{1}J_{C-H}$ = 30.2 Hz), 35.0 (s), 39.0 (d, $^{1}J_{C-H}$ = 30.6 Hz), 71.7 (s), 129.4 (d, $^{1}J_{C-H}$ = 9.9 Hz), 130.6 (d, $^{1}J_{C-H}$ = 2.7 Hz), 131.2 (d, $^{1}J_{C-H}$ = 2.7 Hz), 144.7 (s, **C$_5$**), 211.6 (br s, CO). ^{31}P{^{1}H} NMR δ ppm ($CDCl_3$) = 60.9 (s). (minor) ^{13}C NMR δ ppm ($CDCl_3$) = 28.9 (d, $^{1}J_{C-H}$ = 31 Hz), 34.9 (s), 38.3 (d, $^{1}J_{C-H}$ = 31.1 Hz), 72.2 (s, ***C$_3$**H), 129.4 (d, $^{1}J_{C-H}$ = 10.1 Hz), 130.6 (d, $^{1}J_{C-H}$ = 3.1 Hz), 131.2 (d, $^{1}J_{C-H}$ = 2.7 Hz), 144.0 (s, **C$_5$**). ^{31}P{^{1}H} NMR δ ppm ($CDCl_3$) = 60.7 (s). IR (CH_2Cl_2) = γ(OH) = 3576s cm^{-1}, γ(CO) = 2033s and 1983s cm^{-1}. Anal. Calc. for $FePO_3C_{22}H_{28}$ (427.27) = C,61.84; H,6.68. Found = C,60.88; H,6.43 %. (TOF-MS, ES+): m/z (%) = 427.11 (100) $[M]^+$

3.4.2.12 Preparation of [Rh(cod)Cl(k-P$_{R,S}$-**3.7**)], **3.21**.

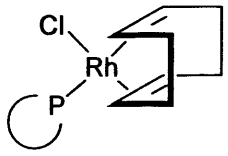

To a solution of [Rh(cod)μ-Cl]$_2$, **3.13**, (60 mg; 0.12 mmol) in dichloromethane (10 ml) was added a solution of, **3.7**, (44 mg; 0.24 mmol) in dichloromethane (10 ml). The resulting yellow solution was stirred for 12 hours and the solvent removed under reduced pressure to afford the desired product, **3.21**. The crude mixture was purified by flash column chromatography firstly washed with 100 % Et_2O then mixture of dichloromethane /Et_2O followed by 100 % THF. The different desired phases were combined and solvent removed *in vacuo* to give a mixture of diastereomers of, **3.21**, as off-white air-stable powder. Yield: 92 %. ^{1}H NMR δ ppm ($CDCl_3$) = 0.8-2.8 (br m), 3.0 (s), 3.1 (s), 3.6 (s), 3.8 (app br d), 4.2 (s), (major) 4.4 (br d, $^{1}J_{H-C}$ = 24.1 Hz, *C_3**H**), 5.3 (br s), 7.3(br m), (minor) 4.6 (br m), 5.5 (s), 7.6 (br m). (major) ^{13}C NMR δ ppm ($CDCl_3$) = 23.0-36.8 (br m), 72.2 (s), 78.7 (d, 13.9 Hz), 104.7 (br s), 128.4 (s), 128.6 (s), 129.6 (s), 131.1 (d, 9.5 Hz). ^{31}P NMR δ ppm ($CDCl_3$) = 27.1 (d, $^{1}J_{Rh-P}$ = 148.3 Hz). (minor) ^{13}C NMR δ ppm ($CDCl_3$) = 23.0-36.8 (br m), 73.4 (s), 78.7 (d, 13.9 Hz), 104.4 (br s), 128.4 (s), 128.7 (s), 129.5 (s), 130.5 (d, 8.6 Hz). ^{31}P NMR δ ppm ($CDCl_3$) = 27.0 (d, $^{1}J_{Rh-P}$ = 146.9 Hz).

3.4.2.13 Preparation of *cis*-[(k-$P_{R,S}$-**3.7**)$_2$ $PtCl_2$], **3.22**.

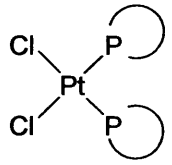

To a solution of [$PtCl_2$(cod)], **3.14**, (45.7 mg; 0.12 mmol) in dichloromethane (10 ml) was added a solution of, **3.7**, (44 mg; 0.24 mmol) in dichloromethane (10 ml). The resulting colourless solution was stirred for 12 hours and the solvent removed under reduced pressure to afford the desired product, **3.22**. The crude mixture was purified by flash column chromatography firstly washed with 100 % 40/60 petroleum ether, through mixtures of 40/60 petroleum ether/THF to 100 % THF. The different desired phases were combined and solvent removed *in vacuo* to give a mixture of diastereomers of, **3.22**, as off-white air-stable powder. Yield: 96 %. X-Ray quality crystals were grown by slow diffusion of Et_2O into a saturated DMSO solution. (major) ^{1}H NMR δ ppm ($CDCl_3$) = 1.7-3.5 (br m), 4.4 (d, $^1J_{H\text{-}C}$ = 19.4 Hz, *C_3**H**), 5.1 (s, **OH**), 7.4-7.5 (br m). ^{13}C NMR δ ppm ($CDCl_3$) = 34.9 (s), 35.2 (s), 37.9 (br m), 71.1 (s, ***C**$_3$H), 129.2 (app t), 131.6(s), 132.7 (app t). (minor) ^{1}H NMR δ ppm ($CDCl_3$) = 1.7-3.5 (br m), 5.2 (s, **OH**), 7.8-7.9 (br m). ^{13}C NMR δ ppm ($CDCl_3$) = 34.9 (s), 35.2 (s), 37.6 (br m), 71.3 (s, ***C**$_3$H), 129.2 (app t), 131.6(s), 132.7 (app t). ^{31}P NMR δ ppm ($CDCl_3$) = 13.4 (s, $^1J_{Pt\text{-}P}$ = 3559 Hz). Anal. Calc. for $PtC_{20}H_{26}O_2P_2Cl_2$ (626.35) = C,38.35; H,4.18. Found = C,37.78; H,4.38 %. (TOF-MS, ES+): m/z (%) = 608.09 (100) $[M\text{-}OH]^+$

3.4.2.14 Preparation of *cis*-[(k-$P_{R,S}$-**3.7**)$_2$ $PdCl_2$], **3.23**.

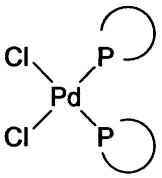

To a solution of [$PdCl_2$(cod)], **3.15**, (34.8 mg; 0.12 mmol) in dichloromethane (10 ml) was added a solution of, **3.7**, (44 mg; 0.24 mmol) in dichloromethane (10 ml). The resulting yellow solution was stirred for 12 hours and the solvent removed under reduced pressure to afford the desired product, **3.23**. The crude mixture was purified by flash column chromatography firstly washed with 100 % 40/60 petroleum ether, through mixtures of 40/60 petroleum ether/THF to 100 % THF. The different desired phases were

combined and solvent removed *in vacuo* to give a mixture of diastereomers of, **3.23**, as off-white air-stable powder. Yield: 92 %. X-Ray crystals were grown by slow diffusion of Et_2O into a staturated DMSO solution. (major) $^{31}P\{^1H\}$ NMR δ ppm ($CDCl_3$) = 47.1 (s). (minor) $^{31}P\{^1H\}$ NMR δ ppm ($CDCl_3$) = 46.3 (s). (TOF-MS, ES^+): m/z (%): 519.05 (100) $[M\text{-}OH]^+$

3.4.3 X-ray Crystal Structure Analyses

A summary of crystal data, data collection parameters and model refinement parameters is given in Appendix 2. All single crystal X-ray data was collected at 150K on a Bruker/Nonius Kappa CCD diffractometer using graphite monochromated Mo-Kα radiation (λ = 0.71073 Å), equipped with an Oxford Cryostream cooling apparatus. The data was corrected for Lorentz and polarization effects and for absorption using SORTAV.[25] Structure solution was achieved by direct methods and refined by full-matrix least-squares on F^2 (SHELX-97)[26] with all non hydrogen atoms assigned anisotropic displacement parameters. Hydrogen atoms attached to carbon atoms were placed in idealised positions and allowed to ride on the relevant carbon atom. Molecular structures in the Figures were drawn with Ortep 3.0 for Windows (version 1.08).[27]

3.5 References

[1] For recent reviews, see: S. Gladioli, A. Dore, D. Fabbri, O. De Lucci, M. Manassero, *Tetrahedron: Asymmetry*, **1994**, *5*, 511; K. Junge, G. Oehme, A. Monsees, T. H. Riermeier, U. Dingerdissen, M. Beller, *Tetrahedron Lett.*, **2002**, *43*, 4977; S. Enthaler, B. Hagemann, K. Junke, G. Erre, M. Beller, *Eur. J. Org. Chem.*, **2006**, 2912.

[2] M. J. Burk, *Acc. Chem. Res.*, **2000**, *33*, 363.

[3] J. Holz, M. Quirmbach, U. Schmidt, D. Heller, R. Stürmer, A. Börner, J. Org. Chem. 1998, 63, 8031; W. Li, Z. Zhang, X.Demging, X. Zhang, *Tetrahedron Lett.*, **1999**, *40*, 6701.

[4] J. Holz, O. Zayas, H. Jiao, W. Baumann, A. Spannenberg, A. Monsees, T. H. Riermeier, J. Almena, R. Kadyrov, A Börner, *Chem. Eur. J.*, **2006**, *12*, 5001.

[5] C. A. Tolman, *Chem. Rev.*, **1977**, *77*, 313.

[6] N.Fey, A. C. Tsipis, S. E. Harris, J. N. Harvey, A. Guy Orpen, R. A. Mansson, *Chem. Eur. J.*, **2005**, 12(1), 291.

[7] F. Lagasse, H. Kagan, *Chem. Pharm. Bull.*, **2000**, *48*, 315.

[8] A Marinetti, J.-P. Genet, *C. R. Chim.*, **2003**, *6*, 507.

[9] W. Tang, X. Zhang, *Chem. Rev*, **2003**, *103*, 3029 and references cited therein.

[10] T. P. Clark, C. R. Landis, *Tetrahedron: Asymmetry*, **2004**, *15*, 2123 and references cited therein.

[11] K. Nozaki, M. Lakshmi-Kantam, T. Horiuchi, H. Takaya, *J. Mol. Catal. A: Chem.*, **1997**, *118*, 247.

[12] S. Feldgus, C. R. Landis, *J. Am. Chem Soc.*, **2000**, *122*, 12714.

[13] C. D. Donner, *Tetrahedron Lett.*, **2007**, *48*, 8888.

[14] J. E. Robinson, M. A Brimble, *Chem. Comm.*, **2005**, 1560.

[15] J. A. Frick, B. Klassen, A Bathe, J. M. Abramson, H. Rapoport, *Synthesis*, **1992**, *7*, 621

[16] E. Reixach, Thesis, Cardiff University (Cardiff), **2006**.

[17] J. G. Verkade, L. D. Quin, *Methods in Stereochemical Analysis*, Vol. 8 (Eds.: J. G. Verkade, L. D. Quin), Deerfield Beach, Florida, **1987**.

[18] W. Zhang, Thesis, Cardiff University (Cardiff), **2006**.

[19] Brunner, *J Org. Chem.*, **1987**, *328*, 71-80.

[20] M. J. Burk, (Du pont de Nemours, E. I., and Co, USA) U.S., **1991**.

[21] R. Angharad Baber, M. F. Haddow, Ann J. Middleton, A. Guy Orpen, Paul G. Pringle, *Organometallics*, **2007**, *26*, 713.

[22] S. J Coles, P. G. Edwards, M. B. Husthouse, K. M. A. Malik, J. L. Thick, R. P Tooze, *J. Chem. Soc., Dalton Trans.*, **1997**, 1821.

[23] R. H. Reimann, E. Singleton, *J. Organomet. Chem.*, **1973**, *59*, C24.

[24] L. D. Freedman, C. O. Doak, *J. Am. Chem. Soc.*, **1952**, *74*, 3414.

[25] R. H. Blessing, *Acta Crystallogr.*, Sect A **1995**, *51*, 33.

[26] G. M. Sheldrick, SHELX-97, Program for Crystal Structures Analysis, University of Göttingen, Germany **1998**.

[27] L.J. Farrugia, *J. Appl. Cryst.*, **1997**, *30*, 565.

Chapter 4
Tribenzannulated mixed arsino-phosphino macrocycles complexes by template synthesis

4.1 Introduction

Macrocycles having rigid unsaturated hydrocarbon backbones have attracted interest due to their properties and possible application in catalysis. The first example of a tribenzannulated trisphosphorus macrocycle was synthesised by using a template method with di-*ortho*-fluorophenylbisphosphinobenzene, **4.e**, as a bidentate phosphine with replacable leaving groups (F^-) and phenylphosphine, **4.c**, as the monodentate phosphine (Scheme 1).[1]

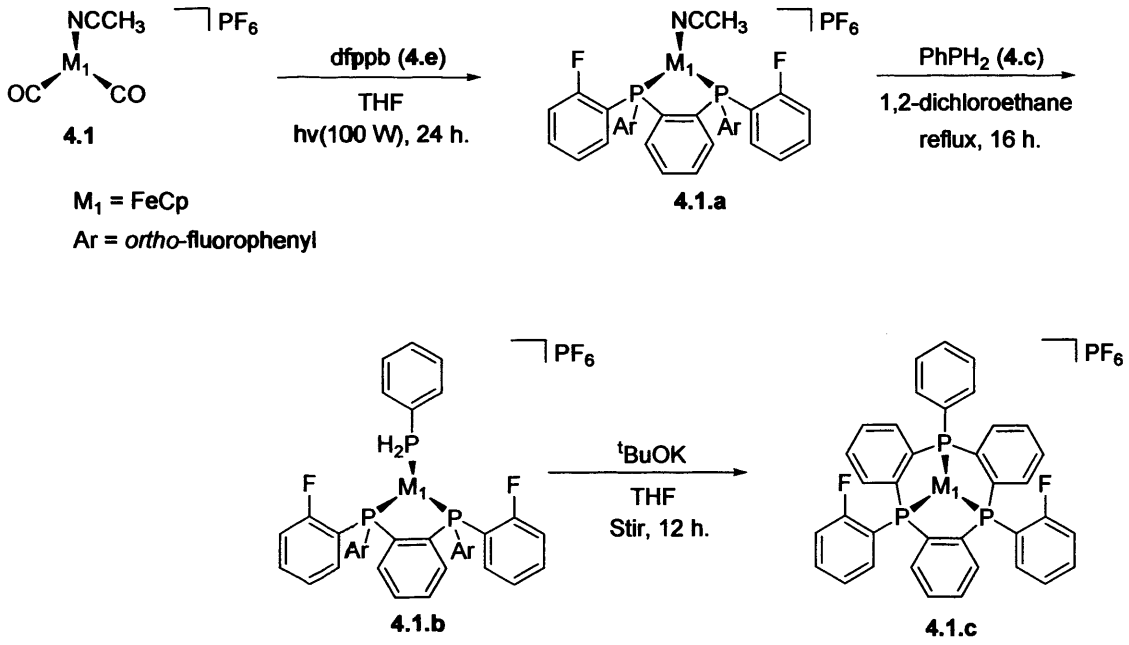

Scheme 1: Tribenzannulated triphosphorus macrocycle, **4.1.c**, synthesis by $FeCp^+$ template method.

The strategy in this template is to allow the base-promoted closure of a very rigid 9-membered macrocycle bearing *ortho*-phenylene backbone functions by nucleophilic substitution of fluoride on adjacent aryl groups by coordinated phosphide (Scheme 2).

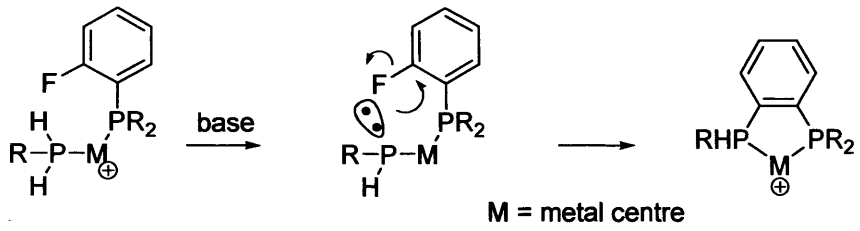

Scheme 2: Base promoted substitution of *ortho*-fluoride.

The generated lone pair on the phosphide is readily available for nucleophilic attack as there is no possibility for π-donation to the 18 electron Fe(II) centre. Other triphosphorus macrocycles have been synthesised in a similar way including one derived from di-*ortho*-fluorophenylbisphosphinoethane, **4.f**, as the bidentate phosphine (Scheme 3).

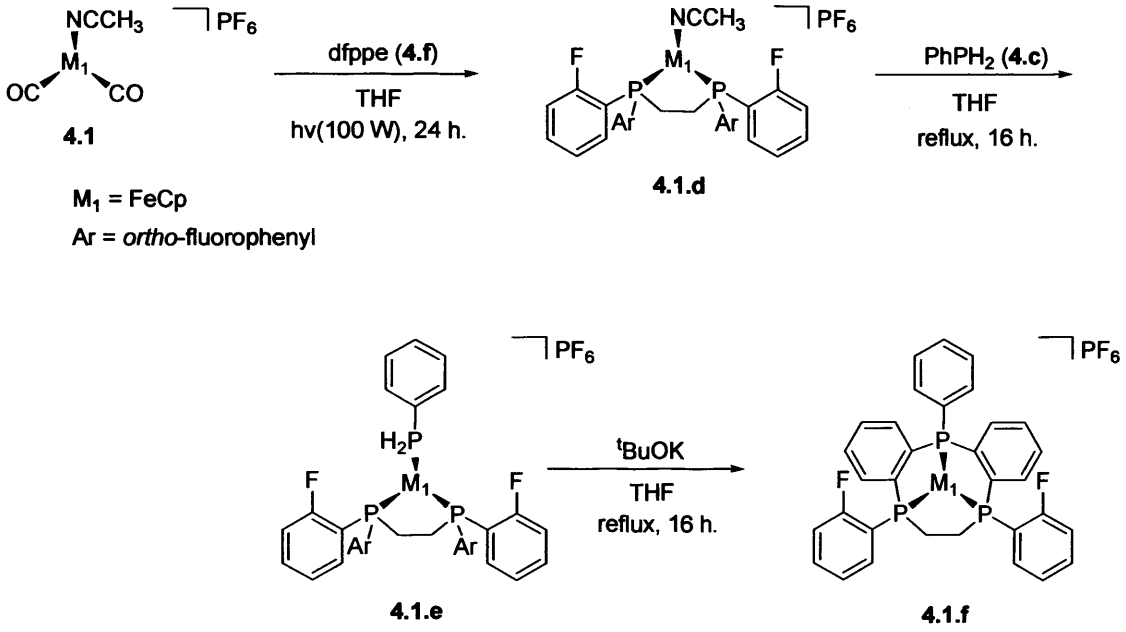

Scheme 3: Tribenzannulated triphosphorus macrocycle, **4.1.f**, synthesis by $FeCp^+$ template method.

More recently, the synthesis of a template synthesised triarsenic macrocycle, **4.1.g**, has been reported[2] using a method similar to that previously described (Figure 1).

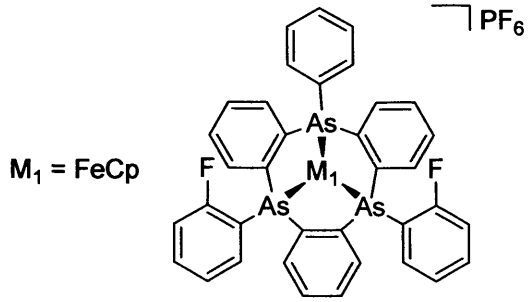

4.1.g

Figure 1: Tribenzannulated triarsenic macrocycle.

To date, the triarsenic template synthesised macrocycle is unique and to our knowledge, as previously related in the Introduction Chapter, the only other example of a triarsenic macrocycle is the 11-membered system made by Kyba *et al.*[3] under high dilution conditions.

As mentioned in Chapter 1, one of the aims of using mixed donor ligands is their potential hemilability and in the continuity of the synthesis of the triphosphorus and the triarsenic complexes, making mixed donor macrocycles comprising both phosphine and arsenic atoms was an obvious next step. Previous examples of both diarsine monophosphine complexes as well as diphosphine monoarsine complexes on $Cp'Fe^+$ and $CpFe^+$ metal templates have been made in our laboratories and in a desire to expand our work on piano-tool structures containing inert facially capping ligands *trans* to three labile ligands the use of other metal precursors as alternative templates has been explored as detailed here.

This chapter will focus on two new synthetic approaches. The first approach (referred to as method 1 in this Chapter) uses 1,2-bis(arsino)benzene, **4.a**, and tris(*o*-fluoro)phenylphosphine, **4.d**, on a number of different template metal precursors (Scheme 4). The idea was to generate the macrocycle by dehydrofluorinative cyclisation as described above.

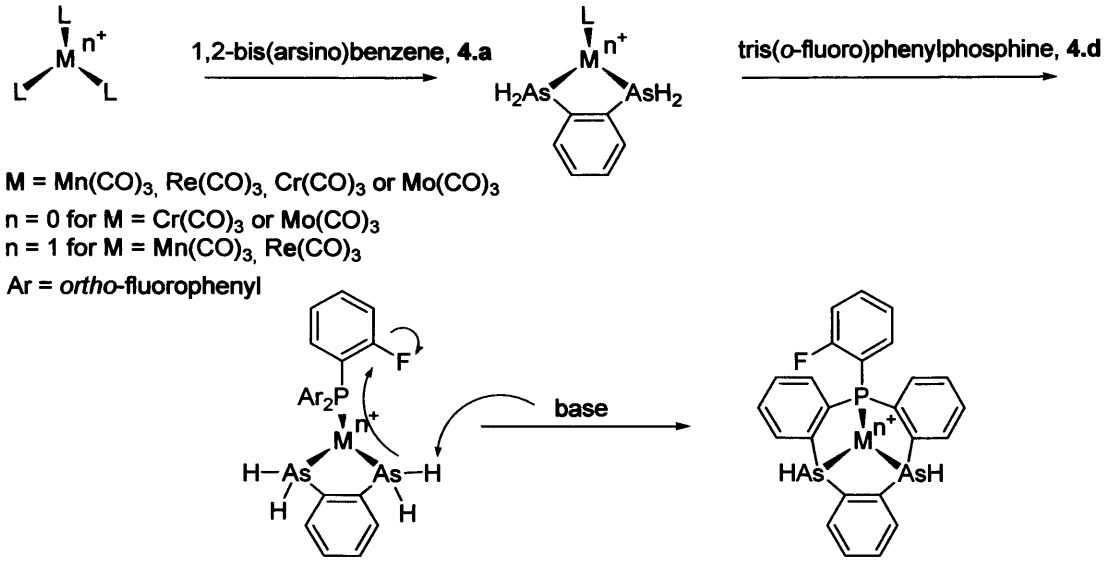

Scheme 4: Predicted scheme for the template synthesis of a new bisarsino-monophosphine macrocycle based on *fac*-X(L)$_3$ metal precursors.

The second approach (referred as method 2 in this Chapter), directly inspired by the previous work, was developed by using *ortho*-fluorophenyl aryl moieties (Ar) attached to the bisarsinobenzene fragment, followed by substitution of phenylphoshine, **4.c**. The C-F bond activation in the *ortho*-position of fluorophenylarsine in the coordination sphere of the transition metal was then used in order to generate the desired macrocycle. The strategy involved is going to be described in detail in the next section.

4.2 Results and discussion

4.2.1 Synthesis of a tribenzannulated 9-membered diarsino-monophosphino macrocycle based on the *fac*-tricarbonylmanganese template by method 1

Treatment of $MnBr(CO)_5$, **4.2**, $Mn(OTf)(CO)_5$, **4.3**, $[Mn(CO)_3(NCCH_3)_3]PF_6$, **4.4**, or $[Mn(CO)_3(acetone)_3]PF_6$, **4.5**, with a molar equivalent of 1,2-bis(arsino)benzene, **4.a**, was anticipated to give complexes with the diarsine coordinated as a bidentate ligand to the metal. Previous attempts in our laboratory to coordinate 1,2-bis(arsino)benzene to $Cp'Fe^+$ and $CpFe^+$ metal template precursors were unsuccessful and, therefore, the synthesis and isolation of these new complexes based on a manganese template (as well as rhenium, chromium and molybdenum as described in the following sections) would be of value in developing a better understanding of the arsenic chemistry, although to our knowledge such ligands remain unknown. The idea was then to introduce tris-*ortho*-fluorophenylphosphine, **4.d**, to displace the remaining labile ligand *cis* to the bisarsinobenzene ligand on the manganese centre and finally form the desired macrocycle by dehydrofluorinative cyclisation as described in Scheme 4.

Unfortunately, we were unable to isolate and characterise a complex containing the primary arsine coordinated to the metal centre. The following reaction scheme (Scheme 5) shows the different approaches that were attempted in order to obtain the desired tribenzannulated 9-membered macrocycle product around a manganese template.

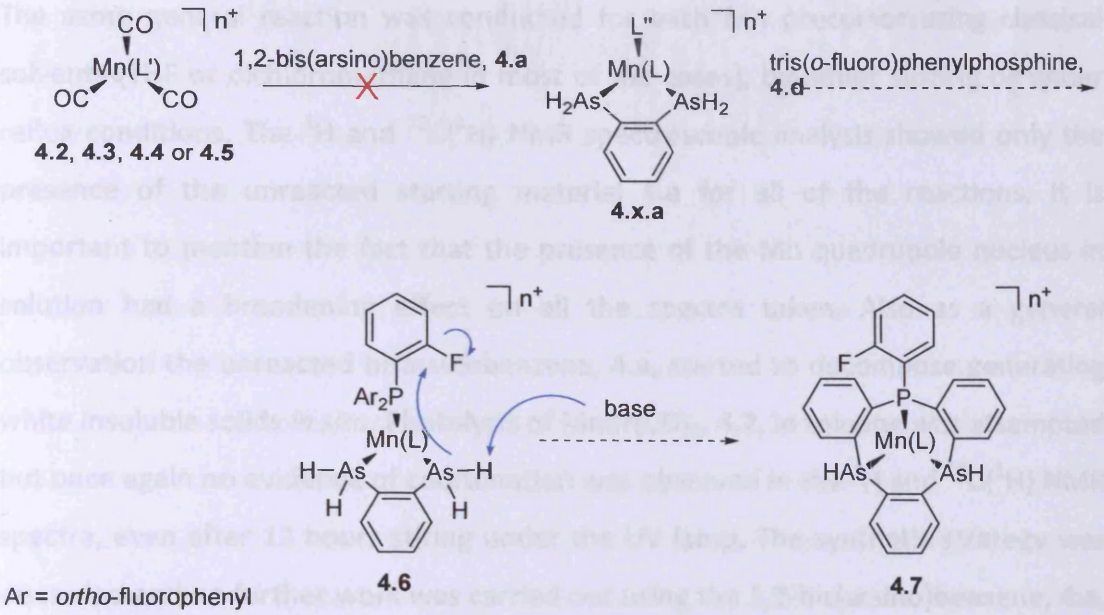

Ar = *ortho*-fluorophenyl
L = $(CO)_3$
L' = $(CO)_2Br$, $(CO)_2OTf$, $(NCCH_3)_3$ or $(ace)_3$
L" = Br, OTf, n = 0
L" = $(NCCH_3)$, (ace), n = 1
x = **2**, **3**, **4** or **5**

Scheme 5: predicted scheme to synthesise *fac*-9-membered diarsino-monophosphino tricarbonylmanganese macrocycle **4.7** by method 1.

As shown in Scheme 5, introduction of the 1,2-bis(arsino)benzene, **4.a**, to the metal precursors, **4.2, 4.3, 4.4** or **4.5**, did not provide the desired products, **4.x.a**. Based on a similar reaction starting with $MnBr(CO)_5$, **4.2**, with 1,2-bis(phosphino)benzene in dichloromethane (see Chapter 2), but using in this case the readily available 1,2-bis(arsino)benzene ligand was unsuccessful and the ^{1}H and $^{13}C\{^{1}H\}$ NMR spectra of the crude product did not show any sign of coordination even after several hours of heating. The different spectra obtained of the recovered material showed only resonances corresponding to the starting material, **4.a**.

Since the attempted coordination of **4.a** to $MnBr(CO)_5$ was unsuccessful we decided to change the substituents on the manganese metal precursor in order to increase the reactivity from $Mn(OTf)(CO)_5$, **4.3**, $[Mn(CO)_3(NCCH_3)_3]PF_6$, **4.4**, to $[Mn(CO)_3(acetone)_3]PF_6$, **4.5**.

The same general reaction was conducted for each Mn precursor using classical solvents (THF or dichloromethane in most of the cases), by either stirring or under reflux conditions. The ^{1}H and $^{13}C\{^{1}H\}$ NMR spectroscopic analysis showed only the presence of the unreacted starting material **4.a** for all of the reactions. It is important to mention the fact that the presence of the Mn quadrupole nucleus in solution had a broadening effect on all the spectra taken. Also as a general observation the unreacted bisarsinobenzene, **4.a**, started to decompose generating white insoluble solids *in situ*. Photolysis of $MnBr(CO)_5$, **4.2**, in toluene was attempted but once again no evidence of coordination was observed in the ^{1}H and $^{13}C\{^{1}H\}$ NMR spectra, even after 12 hours stiring under the UV lamp. The synthetic strategy was discarded and no further work was carried out using the 1,2-bis(arsino)benzene, **4.a**, to coordinate to a manganese template.

4.2.2 Synthesis of a tribenzannulated 9-membered diarsino-monophosphino macrocycle based on the *fac*-tricarbonylmanganese template by method 2

The failure to isolate complexes containing 1,2-bis(arsino)benzene, **4.a**, prompted a change in approach to the more familiar chemistry with 1,2-bis(*o*-fluorophenyl)arsinobenzene.

Treatment of $[Mn(CO)_3(NCCH_3)_3]PF_6$, **4.4**, with a molar equivalent of 1,2-bis(di-2-fluorophenyl)arsinobenzene (dfpab), **4.b**, in dichloromethane leads to an air-stable off-white solid complex, **4.8**, which was isolated as its PF_6^- salt (Scheme 6).

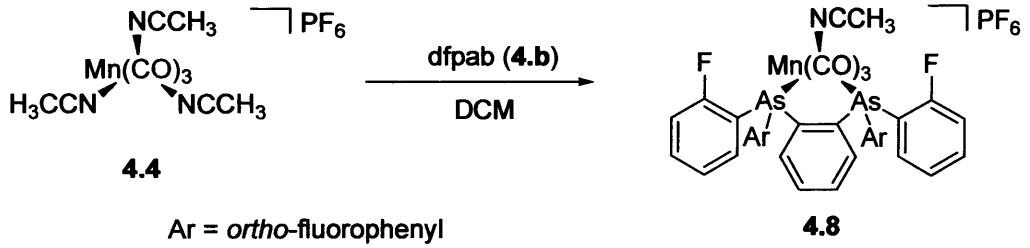

4.4

Ar = *ortho*-fluorophenyl

4.8

Scheme 6: Synthesis of complex, **4.8**.

The substitution of two $NCCH_3$ ligands from **4.4** by dfpab, **4.b**, is relatively slow and takes several hours to reach completion. The product obtained was purified by washing with diethyl ether. The reaction was followed by ^{19}F NMR spectroscopy which showed the disappearance of a resonance at δ_F -102.6 ppm corresponding to the free dfpab, **4.b**, and the growth of a new resonance at δ_F -98.8 ppm which indicates coordination of the dfpab, **4.b**, to the metal centre. The reaction was complete after 10 hours. The ^{31}P NMR spectrum showed only the septet resonance of the PF_6^- at δ_P -145.4 ppm. Identification of, **4.8**, was supported by mass spectrometric measurements which afforded the molecular ion at (m/z: 785.9 amu). The ^1H NMR spectrum also confirmed that coordination occurred but, due to the ^{55}Mn quadrupole moment, the spectrum was broadened and the only reliable information was the integration of the resonances (between δ_H 6.8 and 7.8 ppm) corresponding to the 20H of the aromatic hydrogens compared to the integration of the remaining three H's of the $NCCH_3$ at δ_H 1.3 ppm which is also observed as a slightly broad singlet (Spectrum 1).

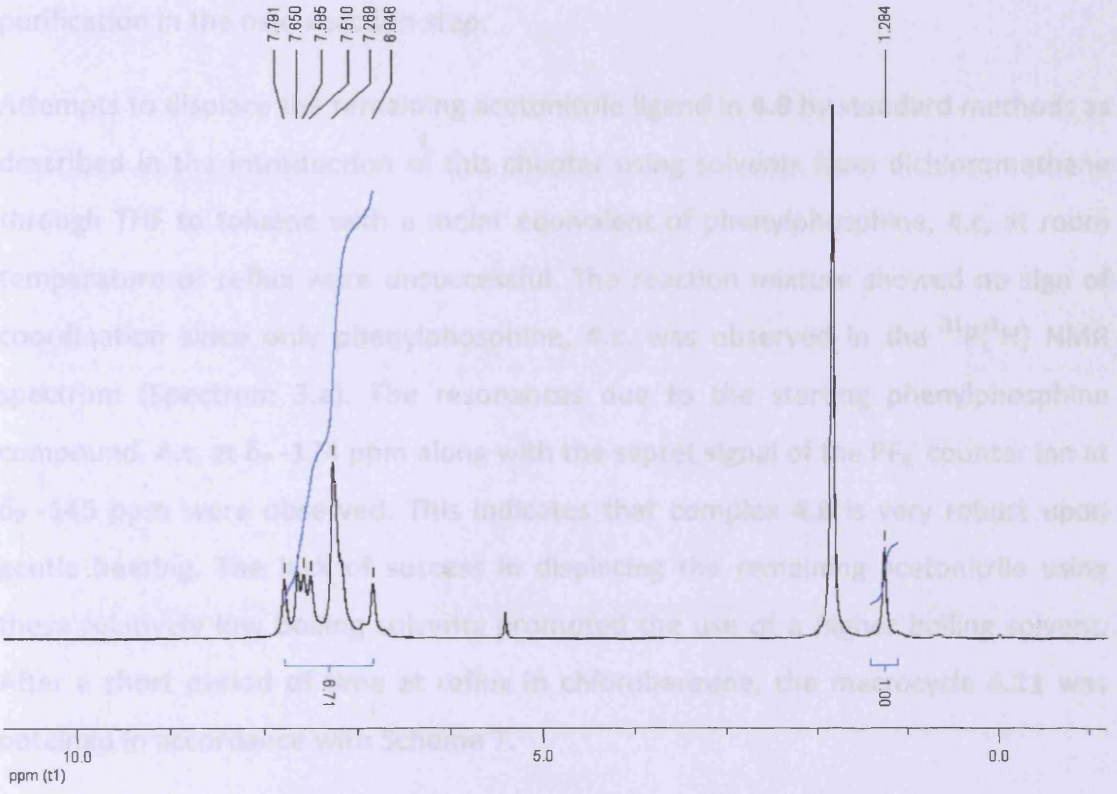

Spectrum 1: ^1H NMR spectrum of complex, **4.8**, in d^6-acetone showing the integration of the aromatic/acetonitrile protons of 20:3.

The $^{13}C\{^1H\}$ NMR spectrum was also broad due to the quadrupole moment of the manganese and the CO resonances were not observed. The rest of the spectrum was fully assigned (see Experimental) with many resonances occurring in the aromatic region between δ_C 115 ppm and δ_C 136 ppm as well as the fluorinated carbon resonances of the *ortho*-fluorophenyl aryl moieties at δ_C 163.6 ppm (doublet, $^1J_{C\text{-}F}$ = 168 Hz, **C**F) .The configuration of **4.8** is fac,*cis*- on the manganese centre in which the dfpab, **4.b**, ligand is *cis* to the $NCCH_3$ ligand and the CO ligands are in a facial arrangement as confirmed by the IR spectrum which shows strong γ(CO) absorption bands at 1931 (w) and 1968 (m) in accordance with the stereochemistry of the complex, **4.8.** The band at 2305 (s) is assigned to the CN stretch of the acetonitrile ligand.

Elemental analatical data was consistent with the proposed structure of the new complex (see Experimental section).

Attempts to recrystalise **4.8** by vapour diffusion at room temperature and at -35 °C were unsuccessful and consequently the compound was used without further purification in the next reaction step.

Attempts to displace the remaining acetonitrile ligand in **4.8** by standard methods as described in the introduction of this chapter using solvents from dichloromethane through THF to toluene with a molar equivalent of phenylphosphine, **4.c**, at room temperature or reflux were unsuccessful. The reaction mixture showed no sign of coordination since only phenylphosphine, **4.c**, was observed in the $^{31}P\{^1H\}$ NMR spectrum (Spectrum 3.a). The resonances due to the starting phenylphosphine compound, **4.c**, at δ_P -124 ppm along with the septet signal of the PF_6^- counter ion at δ_P -145 ppm were observed. This indicates that complex **4.8** is very robust upon gentle heating. The lack of success in displacing the remaining acetonitrile using these relatively low boiling solvents prompted the use of a higher boiling solvent. After a short period of time at reflux in chlorobenzene, the macrocycle **4.11** was obtained in accordance with Scheme 7.

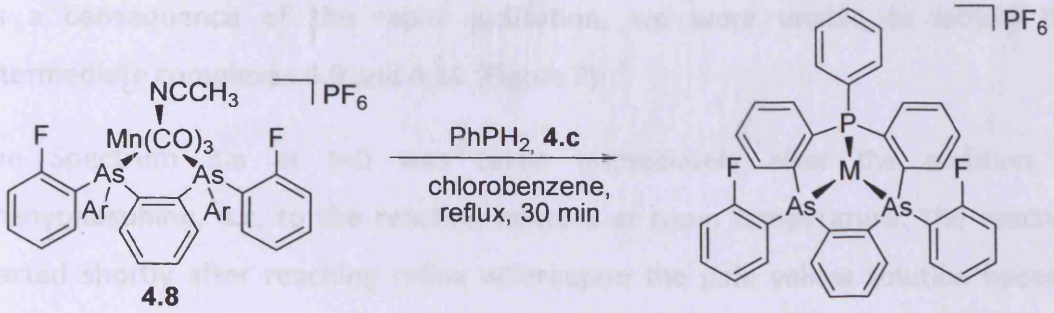

4.8 **4.11**

Ar = *ortho*-fluorophenyl
M = $Mn(CO)_3$

Scheme 7: Preparation of complex, **4.11**.

The substitution reaction was very rapid, did not require the addition of base, and was monitored by ^{31}P NMR spectroscopic methods as detailed in Spectrum 3.

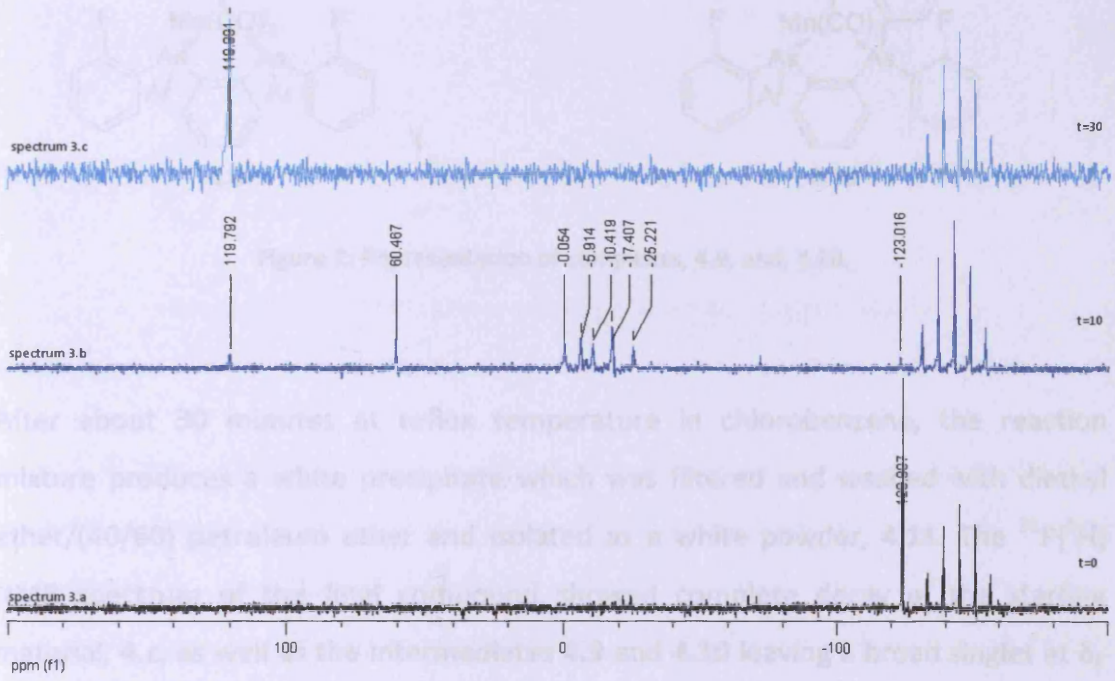

Spectrum 3: Stack spectrum, 3a-c, showing the *in situ* evolution of **4.11** with time (t=time in minutes).

As a consequence of the rapid cyclisation, we were unable to isolate the intermediate complexes **4.9** and **4.10** (Figure 2).

The Spectrum 3.a at t=0 was taken immediately after the addition of phenyphosphine, **4.c**, to the reaction mixture at room temperature. The reaction started shortly after reaching reflux whereupon the pale yellow solution became opaque and the $^{31}P\{^{1}H\}$ NMR spectrum taken at this stage (Spectrum 3.b) showed the presence of several broad resonances between δ_P -26 ppm and δ_P 0 ppm and one at δ_P 60.5 ppm corresponding to the different intermediates including **4.9** and **4.10** as shown in Figure 2 as well as the growth of a broad small resonance at δ_P 119.8 ppm. The starting material resonance at δ_P -124.4 ppm corresponding to the phenylphosphine, **4.c**, has decreased appreciably at this stage.

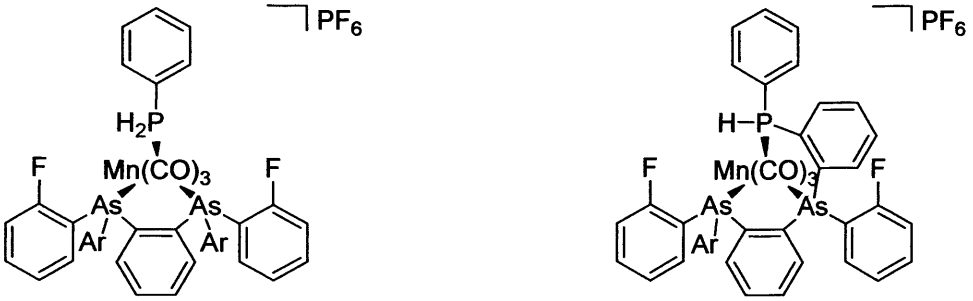

Figure 2: Representation of complexes, **4.9**, and, **4.10**.

After about 30 minutes at reflux temperature in chlorobenzene, the reaction mixture produces a white precipitate which was filtered and washed with diethyl ether/(40/60) petroleum ether and isolated as a white powder, **4.11**. The $^{31}P\{^{1}H\}$ NMR spectrum of the final compound showed complete decay of the starting material, **4.c**, as well as the intermediates **4.9** and **4.10** leaving a broad singlet at δ_P 120 ppm along with the septet of the PF_6^- counter ion at δ_P -144.4 ppm. (Spectrum 3.c).

The ^{19}F NMR spectrum recorded near completion showed a dominant resonance at δ_F -99.9 ppm for the desired compound **4.11**. During the formation of the C-P bond, two C-F bonds on the starting material, **4.8**., are lost leaving only two remaining C-F bonds for the macrocyclic compound **4.11** as shown in Spectra 4.a and 4.b.

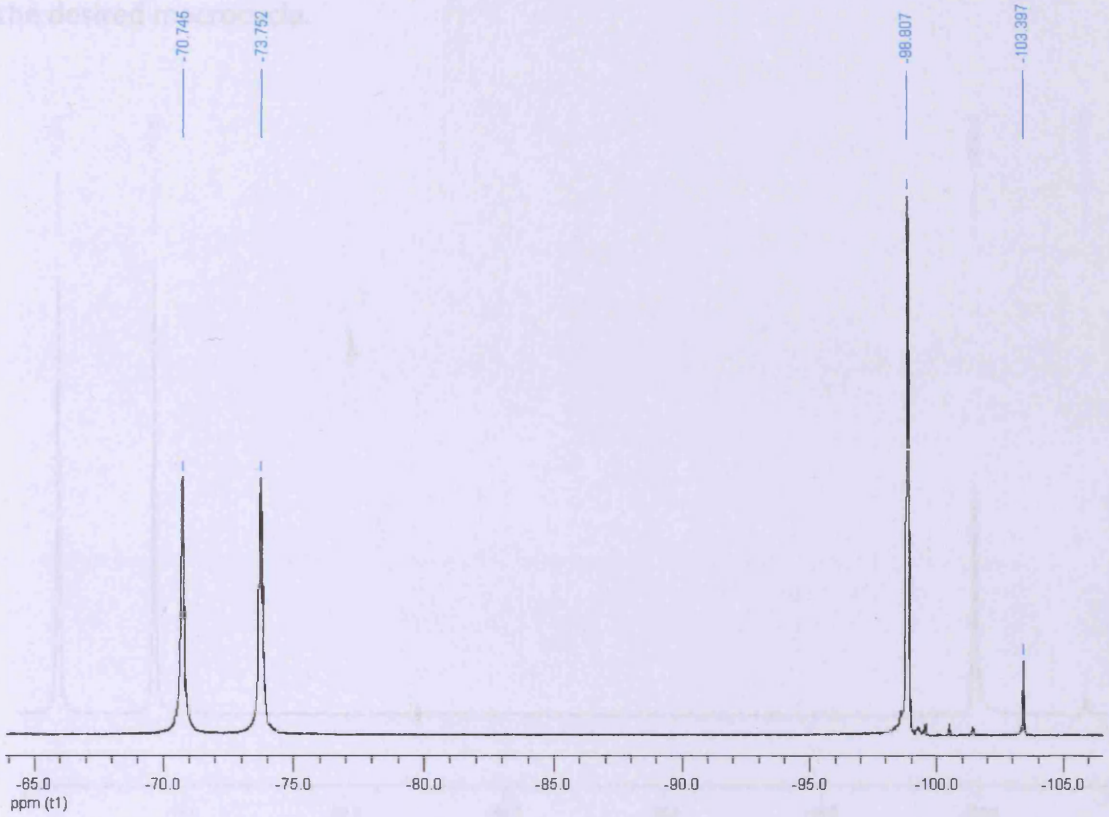

Spectrum 4a: ^{19}F NMR spectrum of compound **4.8**. See text for details.

Theses values correlate closely to the thoses observed for previously published tribenzannulated 9-membered trisphosphamacrocycles complexed with manganese,[4] $(CO)_3$Mn-1,4-bis(2-fluorophenyl)-7-phenyl-[b,e,h]tribenzo-1,4,7-triphosphacyclononane hexafluorophosphate, which showed a resonance at δ_P 109 ppm on the $^{31}P\{^1H\}$ NMR spectrum. The observed resonance was described as complex due to P-P and P-F coupling and quadrupolar broadening. The ^{19}F NMR spectrum showed a resonance at δ_F -96.4 ppm, wich correlates with complex **4.11** described above. Another previously reported[2] compound based on the same

diarsine monophosphine ligand, dfpab, was reported but this time using a iron template. The $^{31}P\{^{1}H\}$ NMR spectrum of $[CpFe(As(C_6H_4F)(C_6H_4)As(C_6H_4F)(C_6H_4)\text{-}P(C_6H_5)(C_6H_4)][PF_6]$ showed a singlet at δ_P 134.6 ppm and the corresponding ^{19}F NMR spectrum showed a single at δ_F -100.1 ppm along the doublet of the PF_6^- resonance observed at δ_F -73.5 ppm (d, $^{1}J_{P\text{-}F}$ = 714.4 Hz). In contrast, the reaction was conducted in THF and potassium *tert*-butoxide was added to allow the formation of the desired macrocycle.

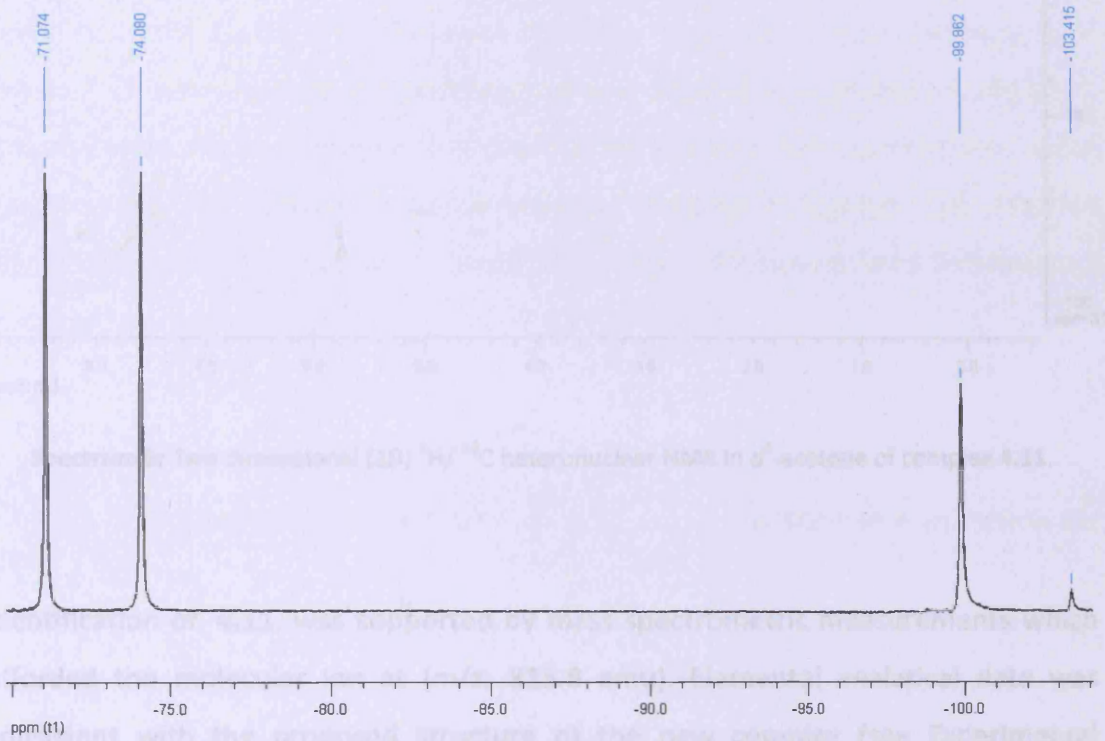

Spectrum 4b: ^{19}F NMR spectrum of compound **4.11**. See text for details.

The $^{13}C\{^{1}H\}$ NMR and ^{1}H NMR spectra of the isolated compound were broad and largely uninformative and, in an effort to obtain a better understanding of these data, a two-dimensional $^{1}H/^{13}C$ heteronuclear NMR was taken (Spectrum 5). Some of the correlations between the proton and carbon atoms are evident but individual assignment remains impossible.

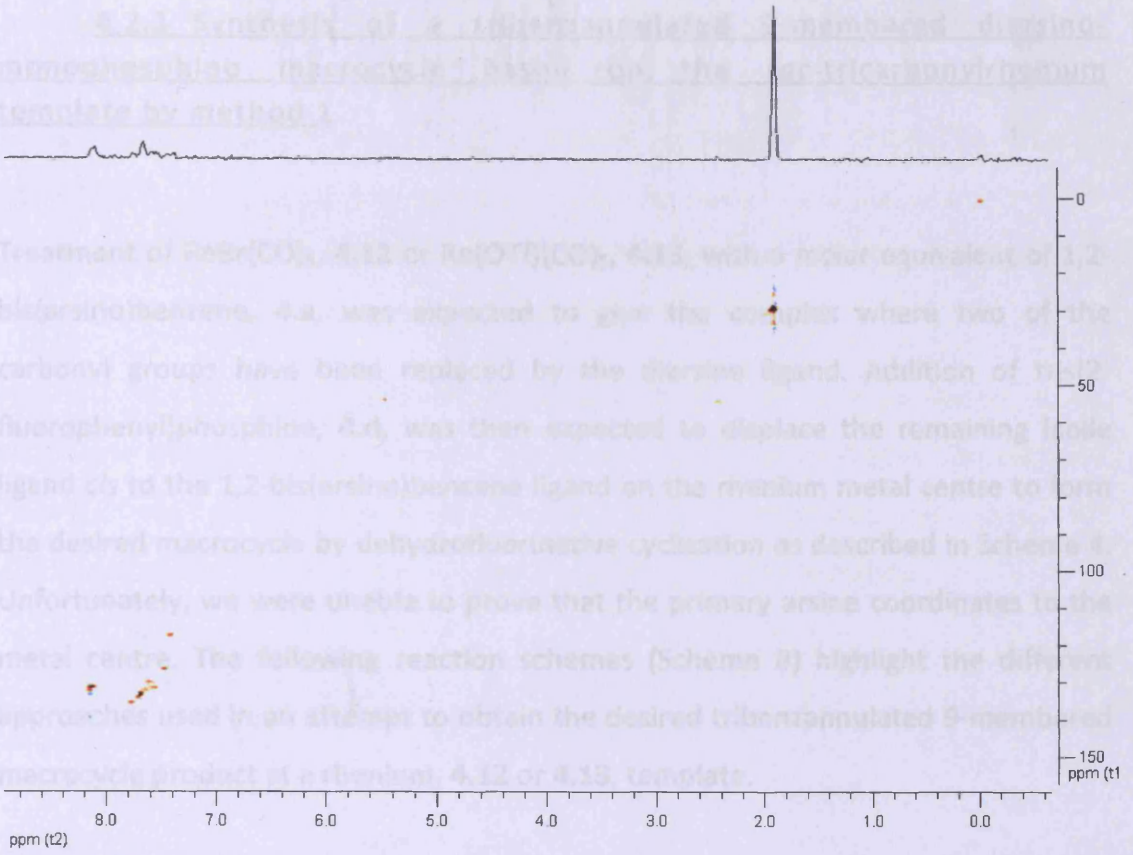

Spectrum 5: Two dimensional (2D) $^{1}H/\ ^{13}C$ heteronuclear NMR in d^{6}-acetone of complex **4.11**.

Identification of, **4.11**, was sopported by mass spectrometric measurements which afforded the molecular ion at (m/z: 815.8 amu). Elemental analatical data was consistant with the proposed structure of the new complex (see Experimental section). To date, all attempts to recrystalize complex **4.11** have proved unsuccessful.

4.2.3 Synthesis of a tribenzannulated 9-membered diarsino-monophosphino macrocycle based on the *fac*-tricarbonylrhenium template by method 1

Treatment of $ReBr(CO)_5$, **4.12** or $Re(OTf)(CO)_5$, **4.13**, with a molar equivalent of 1,2-bis(arsino)benzene, **4.a**, was expected to give the complex where two of the carbonyl groups have been replaced by the diarsine ligand. Addition of tris(2-fluorophenyl)phosphine, **4.d**, was then expected to displace the remaining labile ligand *cis* to the 1,2-bis(arsino)benzene ligand on the rhenium metal centre to form the desired macrocycle by dehydrofluorinative cyclisation as described in Scheme 4. Unfortunately, we were unable to prove that the primary arsine coordinates to the metal centre. The following reaction schemes (Scheme 8) highlight the different approaches used in an attempt to obtain the desired tribenzannulated 9-membered macrocycle product at a rhenium, **4.12** or **4.13**, template.

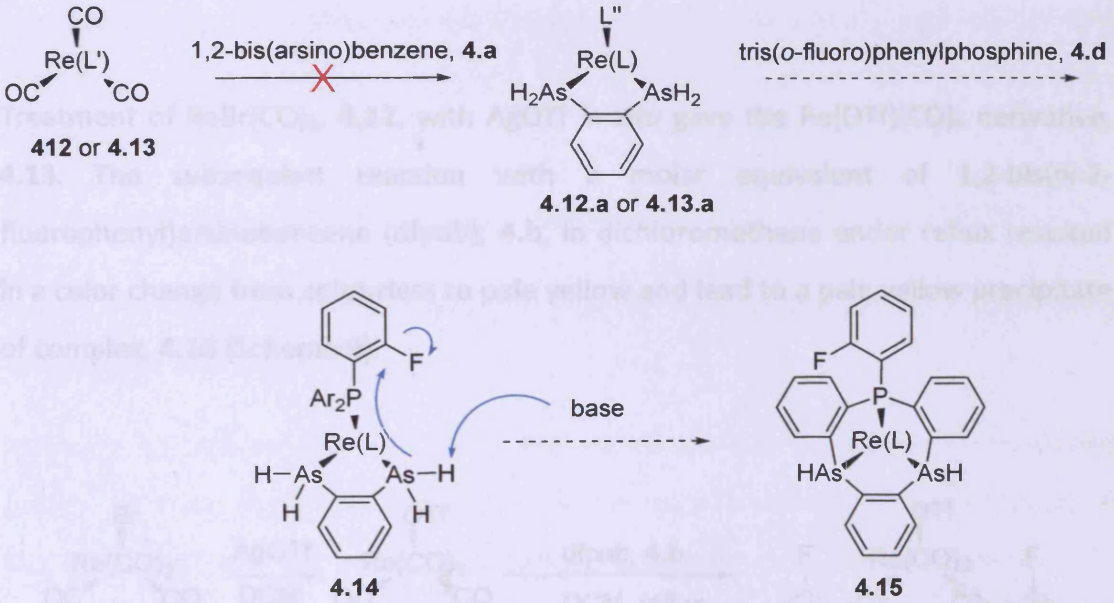

Ar = *ortho*-fluorophenyl
L = $(CO)_3$
L' = $(CO)_2Br$ or $(CO)_2OTf$
L" = Br or OTf

Scheme 8: predicted scheme to synthesise *fac*-9-membered diarsino-monophosphino tricarbonylrhenium macrocycle, **4.15**, by method 1.

As observed for the series of Mn precursors using method 1, the ^{1}H and $^{13}C\{^{1}H\}$ NMR spectra as well as IR data showed that no coordination of the 1,2-bis(arsino)benzene ligand to the rhenium metal centre occurs. Starting from $ReBr(CO)_5$, **4.12** or $Re(OTf)(CO)_5$, **4.13**, in dichloromethane or THF did not provide the desired product respectively **4.12.a** and **4.13.a**. The NMR and IR spectra obtained of the recovering material showed only unreacted starting material **4.a**.

Photolysis (UV, 12 h.) of a solution of $ReBr(CO)_5$, **4.12**, with 1,2-bis(arsino)benzene, **4.a**, in toluene also did not result in the formation of the product **4.12.a**. The synthetic strategy was discarded and no further work was carried out using the diprimarybisarsinobenzene, **4.a**, to coordinate to a rhenium template.

4.2.4 Synthesis of a tribenzannulated 9-membered diarsino-monophosphino macrocycle based on the *fac*-tricarbonylrhenium template by method 2

Treatment of $ReBr(CO)_5$, **4.12**, with AgOTf *in situ* gave the $Re(OTf)(CO)_5$ derivative, **4.13**. The subsequent reaction with a molar equivalent of 1,2-bis(di-2-fluorophenyl)arsinobenzene (dfpab), **4.b**, in dichloromethane under reflux resulted in a color change from colourless to pale yellow and lead to a pale yellow precipitate of complex, **4.16** (Scheme 9).

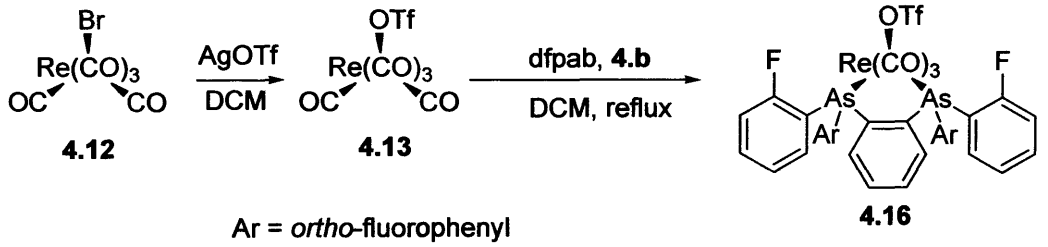

Scheme 9: Preparation of complex, **4.16**.

The substitution of two carbonyl ligands of $ReBr(CO)_5$, **4.12**, by dfpab did not occur even under refluxing conditions and the addition of a molar equivalent of AgOTf *in situ* is required for the reaction to occur. This leads to the formation of the complex, **4.16**, which was washed by using cold diethyl ether and isolated as a pale yellow powder after all volatile materials were removed *in vacuo*.

The reaction was followed by ^{19}F NMR spectroscopy which shows a small shift from δ_F -103.4 ppm corresponding to the free dfpab ligand to δ_F -101.5 ppm for complex, **4.16**. The reaction is slow and took several hours under refluxing conditions in dichloromethane for completion. Mass spectroscopic analysis was not satisfactory since no distinct sign of the corresponding peak of the complex **4.16** was noticed. It appears that **4.16** polymerises in the mass spectrometer since resonances of a molecular weight much greater than expected were observed. Attempts to recrystallise **4.16** by vapour diffusion at room temperature and at -35 °C were unsuccessful

The $^{13}C\{^1H\}$ NMR and ^1H NMR spectra of the isolated compound were broad and not very informative since the resonances observed correlate closely with the starting material. A global downfield shift of a few ppm can be observed in both spectra which indicate coordination.

The IR spectrum showed strong ν(CO) absorption bands at 2015 (s) and 2070 (s)

Due to this unstable nature, for further reaction of **4.16**, the compound was used immediately and not stored.

Attempts to displace the remaining OTf ligand in **4.16** by using chlorobenzene solvent at reflux leads to the synthesis of the complex **4.16.a**. Characterisation of this compound was impossible as decomposition occurs too rapidly if treated with deuterated solvents. The only reliable data was the *in situ* ^{31}P NMR spectrum taken after 2 hours of reflux, which showed a triplet at δ_P -97 ppm (t, $^1J_{P-H}$ = 286 Hz) and the *in situ* IR spectrum which showed three strong bands corresponding to the carbonyl stretches at 1968s, 2011s and 2057s cm^{-1}.The lack of success to obtain the desired macrocycle prompted the use of a base as described in the introduction of

this Chapter. ^{t}BuOK was added in catalytic quantities and after about 40 minutes at reflux temperature in chlorobenzene, the reaction mixture produces a pale yellow/off-white precipitate which was filtered off and washed with diethyl ether/(40/60) petroleum ether and isolated as a yellow powder, **4.17**. Analysis of the reaction mixture by $^{31}P\{^{1}H\}$ NMR spectroscopy shows over time the growth of a resonance at δ_P 73.3 ppm while the resonance at δ_P -97 ppm corresponding to **4.16.a** decreases. Once the base is added to the solution mixture, the substitution reaction is very rapid and was considered to be achieved after 40 minutes (Scheme 10).

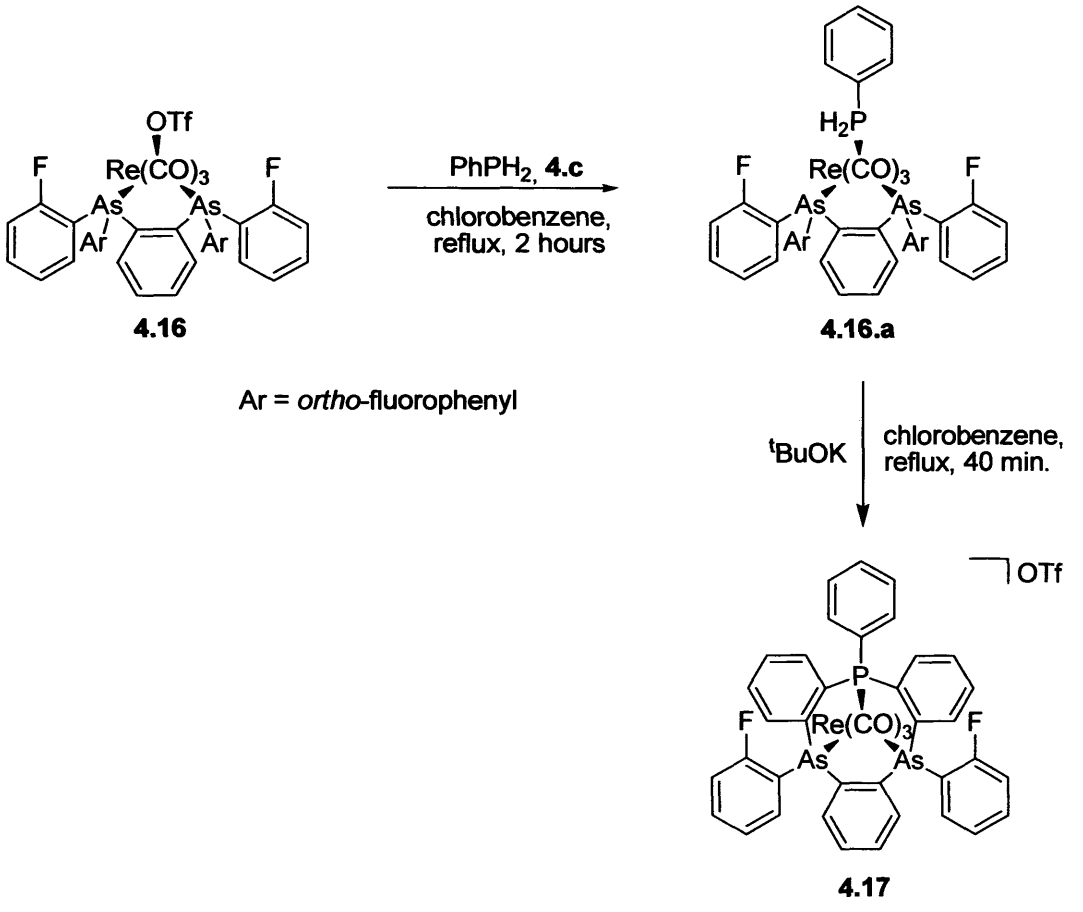

Scheme 10: Preparation of complex, **4.17**.

Unfortunately the $^{13}C\{^{1}H\}$ NMR and ^{1}H NMR spectra of the isolated compound **4.17** were broad and not very informative and individual assignment remains impossible.

The ^{19}F NMR spectrum recorded near completion showed a resonance at δ_F -100.2 ppm for the desired compound **4.17**.

To date, all attempts to recrystalize complex **4.17** have proved unsuccessful.

4.2.5 Synthesis of a tribenzannulated 9-membered diarsino-monophosphino macrocycle based on the *fac*-tricarbonylchromium and the *fac*-tricarbonylmolybdenum template by method 1

The difficulties encountered with the coordination of 1,2-bis(arsino)benzene to Mn(I) and Re(I) prompted an exploration of the chemistry with the zerovalent metals Cr(0) and Mo(0).

Treatment of $[Cr(CO)_3(NCCH_3)_3]$, **4.18**, or $[Mo(CO)_3(NCCH_3)_3]$, **4.19**, with a molar equivalent of 1,2-bis(arsino)benzene, **4.a**, was expected to give the complexes $[M(CO)_3(L)(MeCN)]$ as shown in Scheme 11. Subsequent addition of trisfluorophenylphosphine, **4.d**, to displace the remaining labile acetonitrile ligand *cis* to the bisarsinobenzene ligand would then ultimately produce the desired macrocycle, **4.21** by dehydrofluorinative cyclisation as described in Scheme 4.

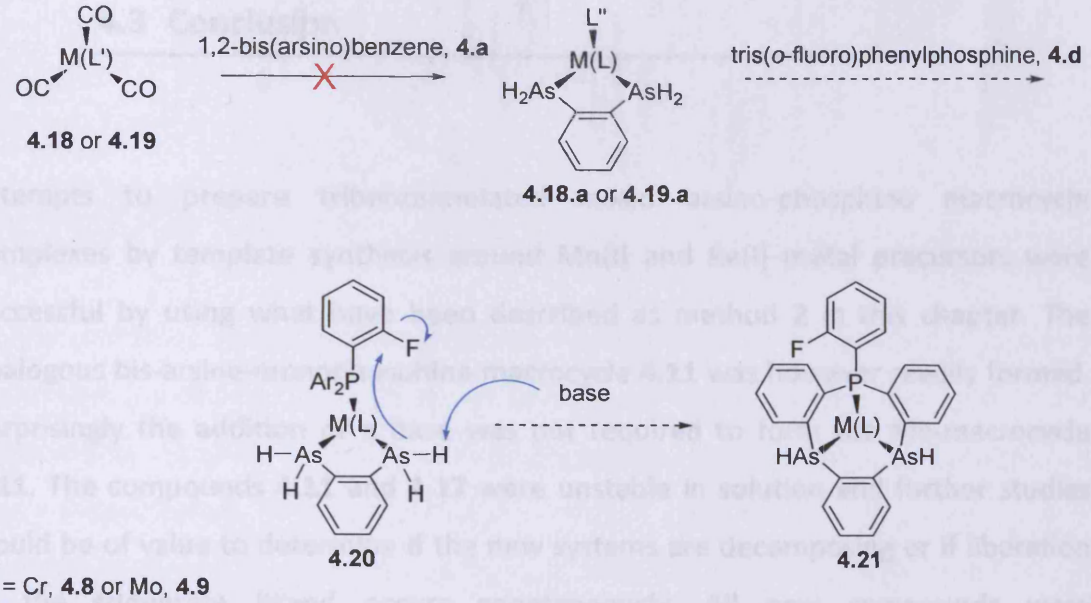

M = Cr, **4.8** or Mo, **4.9**
Ar = *ortho*-fluorophenyl
L = $(CO)_3$
L' = $(NCCH_3)_3$
L'' = $(NCCH_3)$

Scheme 11: predicted scheme to synthesise *fac*-9-membered diarsino-monophosphino tricarbonylchromium and tricarbonylmolybdenum macrocycle, **4.21**, by method

As observed for the series of Mn and Re precursors using method 1, the ^{1}H and $^{13}C\{^{1}H\}$ NMR as well as IR analysis showed that no coordination of the 1,2-bis(arsino)benzene ligand occurs to the chromium or the molybdenum metal centre. The different spectra obtained of the recovering material showed, as before, only unreacted starting material. Unfortunately we were unable to identify the primary arsine complex and no further studies in this area were pursued.

4.3 Conclusion

Attempts to prepare tribenzannulated mixed arsino-phosphino macrocycle complexes by template synthesis around Mn(I) and Re(I) metal precursors were successful by using what have been described as method 2 in this chapter. The analogous bis-arsine-monophosphine macrocycle **4.11** was however readily formed. Surprisingly the addition of a base was not required to form the Mn-macrocycle **4.11**. The compounds **4.11** and **4.17** were unstable in solution and further studies would be of value to determine if the new systems are decomposing or if liberation of the tridentate ligand occurs spontaneously. All new compounds were characterised by spectroscopic methods, but unfortunately no crystals suitable for X-Ray crystallography were obtained.

All attempts to introduce the 1,2-bis(arsino)benzene ligand by method 1 were unsuccessful and is approach was abandoned.

4.4 Experimental

4.4.1 Methods and materials

Unless otherwise stated all manipulations were carried out using standard Schlenk techniques, under an atmosphere of dry nitrogen. All solvents were dried and degassed by refluxing over standard drying agents under a nitrogen atmosphere. The compounds $Mn(OTf)(CO)_5$, **4.3**, $[Mn(CO)_3(NCCH_3)_3]PF_6$, **4.4**, $[Mn(CO)_3(acetone)_3]PF_6$, **4.5**, $ReBr(CO)_5$, **4.12**, $Re(OTf)(CO)_5$, **4.13**, $[Cr(CO)_3(NCCH_3)_3]$, **4.18**, $[Mo(CO)_3(NCCH_3)_3]$, **4.19**, and 1,2-bis(arsino)benzene were prepared according to literature methods.[5, 6, 7] $MnBr(CO)_5$, **4.2**, was obtained from Aldrich Chemical Company and used without further purification. Deuterated solvents were dried over 3 or 4 Å molecular sieves and degassed by freeze-thaw methods. The NMR spectra were recorded on a Bruker DPX-500 instrument at 500 MHz (^1H), 125.75 MHz (^{13}C) and 202.75 MHz (^{31}P), Bruker DPX-400 instrument at 400 MHz (^1H) and 100 MHz (^{13}C), Jeol Lamda Eclipse 300 at 121.65 MHz (^{31}P) and 75.57 MHz (^{13}C). ^1H and ^{13}C chemical shifts are quoted in ppm relative to residual solvent resonances, and ^{31}P chemical shifts are quoted in ppm relative to external 85 % H_3PO_4. Infra-red spectra were recorded on a JASCO FT/IR-660 plus Spectrometer and the samples were prepared under N_2 as a KBr disk or as solution. Mass spectra of all the samples have been collected by direct injection into a Waters LCT Premier XE mass spectrometer fitted with an ESCI source.

Elemental analyses were performed by MEDAC LTD, UK, Analytical and Chemical Consultancy Services.

4.4.2 Syntheses

4.4.2.1 Synthesis of $[Mn(CO)_3\{(o\text{-}C_6H_4F)_2AsC_6H_4As(o\text{-}C_6H_4F)_2\}(NCCH_3)]PF_6$, **4.8**.

To a solution of $[Mn(CO)_3(NCCH_3)_3]PF_6$, **4.4**, (200 mg; 0.49 mmol) in 20 ml of dichloromethane, dfpab, **4.b**, (297.9 mg; 0.49 mmol) was added with stirring. After 4 hours the solvent was evaporated *in vacuo* and the solid residue washed with cold Et2O/ (40/60) petroleum ether. The residual solvent was removed under reduced pressure to leave an off-white solid as the desired product, **4.8**. Yield: 94 %. ^{1}H NMR δ ppm ($CDCl_3$) = 1.28 (s, 3 H, CH_3), 6.8-7.8 (br m, 20 H, Ph). ^{13}C NMR δ ppm ($CDCl_3$) = 116.4 (br d), 117 (br d), 126.1 (s), 126.57 (s), 133.4 (br d), 134.2 (s), 134.9 (app br t), 135.6 (s), 163.6 (d, $^1J_{C\text{-}F}$ = 168 Hz). ^{31}P NMR δ ppm ($CDCl_3$) = -145.4 (PF_6). ^{19}F NMR δ ppm ($CDCl_3$) = -98.8 (s), -72.2 (d, $^1J_{P\text{-}F}$ = 225 Hz). IR (KBr) = γ(CN) = 2305s cm^{-1}, γ(CO) = 1931s and 1968s cm^{-1}. Anal. Calc. for $[C_{35}H_{23}O_3NAs_2F_4Mn^+][PF_6^-]$ (786.34) = C,45.14; H,2.49; N,1.50. Found = C,44.07; H,2.47; N,1.38 %. (TOF-MS, ES+): m/z (%) = 785.9 (100) $[M]^+$.

4.4.2.2 Synthesis of $[Mn(CO)_3\{(o\text{-}C_6H_4F)\ (C_6H_4)\ As\ (C_6H_4)\ As\ (C_6H_4)\ (o\text{-}C_6H_4F)\}\{P(C_6H_5)\}]\ PF_6$, **4.11**.

To a solution of **4.8** (50 mg; 0.053 mmol) in 20 ml of chlorobenzene, phenylphosphine (5.79 ml; 0.053 mmol) was added. After refluxing for 30 min, the solution change with the formation of an off-white precipitate. After filtering, the precipitate was washed with cold portion of 40/60 petroleum ether offering the desired compound **4.11**. as a white solid. Yield: 94 %. ^{1}H NMR δ ppm ($CDCl_3$) = 1.28 (s, 3 H, CH_3), 6.7-8 (br m, Ph). ^{13}C NMR δ ppm ($CDCl_3$) = 118.2 (s), 118.5 (s), 127.3 (d, 2.4 Hz), 130.7 (d, 11.2 Hz), 132.4 (d, 11.2 Hz), 132.5 (d, 6.4 Hz), 133.3 (s), 134.1 (d, 4.8 Hz), 134.3 (s), 134.6 (d, 3.2 Hz), 134.9 (s), 136.5 (d, 8 Hz), 137.0 (s), 137.4 (s),

137.6 (s), 142.3 (d, 38 Hz), 164.3 (d, $^{1}J_{C\text{-}F}$ = 247 Hz). ^{31}P NMR δ ppm ($CDCl_3$) = -142.8 (PF_6), 120 (s). ^{19}F NMR δ ppm ($CDCl_3$) = -99.9 (s), -72.6 (d, $^{1}J_{P\text{-}F}$ = 226 Hz). IR (KBr) = γ(CN) = 2305s cm^{-1}, γ(CO) = 1931s and 1968s cm^{-1}. Anal. Calc. for $[C_{35}H_{23}O_3NAs_2F_4Mn^{+}][PF_6^{-}]$ (815.36) = C,57.45; H,3.09. Found = C,56.95; H,2.81 %. (TOF-MS, ES+): m/z (%) = 815.85 (100) $[M]^{+}$.

4.4.2.3 Synthesis of $[Re(OTf)(CO)_3\{(o\text{-}C_6H_4F)_2As(C_6H_4)As(o\text{-}C_6H_4F)_2\}]$, **4.16**.

To a solution of $Re(OTf)(CO)_5$, **4.13**, (200 mg; 0.42 mmol) in 20 ml of dichloromethane, dfpab, **4.b**, (255.1 mg; 0.42 mmol) was added with stirring. After 4 hours the solvent was evaporated *in vacuo* and the solid residue washed with cold Et_2O/ (40/60) petroleum ether. The residual solvent was removed under reduced pressure to leave a pale yellow solid as the desired product, **4.16**. Yield: 91 %. ^{1}H NMR δ ppm ($CDCl_3$) = 7.7-8.5 (br m, Ph). ^{13}C NMR δ ppm ($CDCl_3$) = 116.2 (br d), 125 (br d), 126.3 (s), 131.2 (s), 132.7 (br d), 135.8 (s), 145.5 (s), 165.1 (d, $^{1}J_{C\text{-}F}$ = 239 Hz). ^{19}F NMR δ ppm ($CDCl_3$) = -101.6 (s). IR (chlorobenzene) = γ(CO) = 2015s and 2071s cm^{-1}.

4.4.2.4 Synthesis of $[Re(CO)_3\{(o\text{-}C_6H_4F)\ (C_6H_4)\ As\ (C_6H_4)\ As\ (C_6H_4)\ (o\text{-}C_6H_4F)\}\{P(C_6H_5)\}]$, **4.17**.

To a solution of **4.16** (50 mg; 0.048 mmol) in 20 ml of chlorobenzene, phenylphosphine (5.36 ml; 0.048 mmol) was added dropwise followed by addition of ^{t}BuOK (catalytic quantities). After refluxing for 30 min, the solution change with the formation of a yellow precipitate. After filtering, the precipitate was washed with cold portion of 40/60 petroleum ether offering the desired compound **4.17** as a pale

yellow-orange solid. Yield: 79 %. $^{31}P\{^{1}H\}$ NMR δ ppm ($CDCl_3$) = 73.3 (s). ^{19}F NMR δ ppm ($CDCl_3$) = -100.2 (s).

4.5 References

[1] T. Albers, P. G. Edwards, *Chem. Comm*, **2007**, 858.

[2] J. Johnstone, Thesis, Cardiff University (Cardiff), **2006**.

[3] E. P. Kyba, S. P. Chou, *J. Am. Chem. Soc.* **1980**, *102*, 7012.

[4] W. Zhang, Thesis, Cardiff University (Cardiff), **2006**.

[5] R. H. Reimann, E. Singleton, *J. Organomet. Chem.*, **1973**, *59*, C24.

[6] E. Reixach, Thesis, Cardiff University (Cardiff), **2006**.

[7] Carlton, Cook, *Inorg. Chem.*, **1971**, *10*, 2628.

Appendix 1
Tables of bond distances and angles

5.1 X-Ray crystallography data for the *trans*-isomer of complex 2.11 (see Chapter 2)

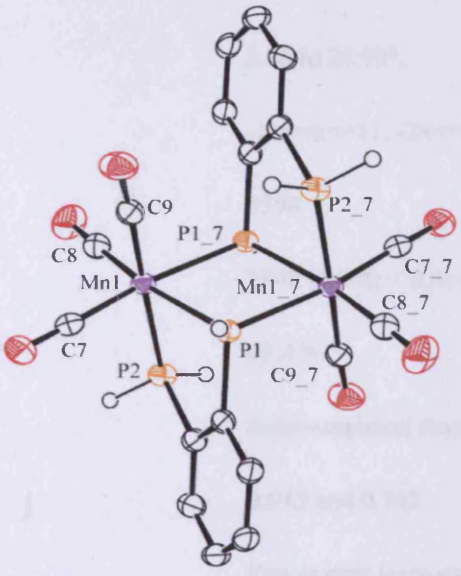

Table 1. Crystal data and structure refinement for c2c.

Identification code	ASPGE01	
Empirical formula	C22 H22 Mn2 O7 P4	
Formula weight	632.16	
Temperature	150(2) K	
Wavelength	0.71073 Å	
Crystal system	Monoclinic	
Space group	C2/c	
Unit cell dimensions	a = 9.3011(19) Å	α= 90°.
	b = 19.035(4) Å	β= 94.99(3)°.
	c = 14.797(3) Å	γ = 90°.
Volume	2609.8(9) Å^3	
Z	4	
Density (calculated)	1.609 Mg/m^3	

Absorption coefficient	1.253 mm^{-1}
F(000)	1280
Crystal size	0.25 x 0.25 x 0.10 mm^3
Theta range for data collection	3.50 to 26.99°.
Index ranges	-11<=h<=11, -24<=k<=24, -18<=l<=18
Reflections collected	5598
Independent reflections	2842 [R(int) = 0.0166]
Completeness to theta = 26.99°	99.4 %
Absorption correction	Semi-empirical from equivalents
Max. and min. transmission	0.943 and 0.763
Refinement method	Full-matrix least-squares on F^2
Data / restraints / parameters	2842 / 0 / 171
Goodness-of-fit on F^2	1.064
Final R indices [I>2sigma(I)]	R1 = 0.0251, wR2 = 0.0616
R indices (all data)	R1 = 0.0291, wR2 = 0.0636
Largest diff. peak and hole	0.520 and -0.250 $e.Å^{-3}$

Table 2. Atomic coordinates (x 10^4) and equivalent isotropic displacement parameters ($Å^2$x 10^3) for c2c. U(eq) is defined as one third of the trace of the orthogonalized U^{ij} tensor.

	x	y	z	U(eq)
Mn(1)	785(1)	2673(1)	517(1)	23(1)
P(1)	2485(1)	1794(1)	328(1)	22(1)
O(1)	-1087(2)	1801(1)	1582(1)	46(1)
C(1)	1540(2)	1082(1)	-303(1)	24(1)
P(2)	-288(1)	2174(1)	-763(1)	27(1)
O(2)	-1082(2)	3935(1)	414(1)	49(1)
C(2)	272(2)	1260(1)	-837(1)	25(1)
O(3)	2290(2)	3156(1)	2250(1)	45(1)
C(3)	-485(2)	753(1)	-1365(1)	30(1)
O(4)	5000	-1244(1)	-2500	51(1)
C(4)	18(2)	65(1)	-1346(1)	33(1)
C(5)	1270(2)	-111(1)	-825(1)	31(1)
C(6)	2043(2)	394(1)	-309(1)	28(1)
C(7)	-365(2)	2137(1)	1160(1)	30(1)
C(8)	-373(2)	3441(1)	444(1)	31(1)
C(9)	1739(2)	2971(1)	1568(1)	29(1)
C(10)	6025(2)	-809(1)	-2889(2)	51(1)
C(11)	5788(3)	-77(2)	-2566(2)	71(1)

Table 3. Bond lengths [Å] and angles [°] for c2c.

Mn(1)-C(7)	1.8084(19)
Mn(1)-C(9)	1.8123(19)
Mn(1)-C(8)	1.8125(18)
Mn(1)-P(2)	2.2710(7)
Mn(1)-P(1)	2.3361(6)
Mn(1)-P(1)#1	2.3518(7)
P(1)-C(1)	1.8264(17)
P(1)-Mn(1)#1	2.3518(7)
O(1)-C(7)	1.150(2)
C(1)-C(6)	1.392(2)
C(1)-C(2)	1.403(2)
P(2)-C(2)	1.8221(17)
O(2)-C(8)	1.147(2)
C(2)-C(3)	1.393(2)
O(3)-C(9)	1.146(2)
C(3)-C(4)	1.390(3)
O(4)-C(10)#2	1.421(2)
O(4)-C(10)	1.421(2)
C(4)-C(5)	1.382(3)
C(5)-C(6)	1.389(2)
C(10)-C(11)	1.496(3)
C(11)-C(11)#2	1.495(5)

C(7)-Mn(1)-C(9)	89.59(8)
C(7)-Mn(1)-C(8)	96.35(8)
C(9)-Mn(1)-C(8)	92.49(8)
C(7)-Mn(1)-P(2)	87.99(6)
C(9)-Mn(1)-P(2)	173.18(6)
C(8)-Mn(1)-P(2)	94.12(6)
C(7)-Mn(1)-P(1)	95.50(6)
C(9)-Mn(1)-P(1)	92.34(6)
C(8)-Mn(1)-P(1)	167.23(6)
P(2)-Mn(1)-P(1)	81.55(3)
C(7)-Mn(1)-P(1)#1	170.66(6)
C(9)-Mn(1)-P(1)#1	90.86(6)
C(8)-Mn(1)-P(1)#1	92.95(6)
P(2)-Mn(1)-P(1)#1	90.49(2)
P(1)-Mn(1)-P(1)#1	75.16(2)
C(1)-P(1)-Mn(1)	106.98(6)
C(1)-P(1)-Mn(1)#1	111.67(5)
Mn(1)-P(1)-Mn(1)#1	104.84(2)
C(6)-C(1)-C(2)	119.34(15)
C(6)-C(1)-P(1)	123.67(13)
C(2)-C(1)-P(1)	116.93(12)
C(2)-P(2)-Mn(1)	110.05(6)
C(3)-C(2)-C(1)	120.55(15)
C(3)-C(2)-P(2)	124.18(13)
C(1)-C(2)-P(2)	115.26(12)

C(4)-C(3)-C(2)	119.23(16)
C(10)#2-O(4)-C(10)	108.8(2)
C(5)-C(4)-C(3)	120.43(16)
C(4)-C(5)-C(6)	120.62(16)
C(5)-C(6)-C(1)	119.81(17)
O(1)-C(7)-Mn(1)	178.82(16)
O(2)-C(8)-Mn(1)	178.26(17)
O(3)-C(9)-Mn(1)	177.15(16)
O(4)-C(10)-C(11)	106.88(18)
C(11)#2-C(11)-C(10)	102.41(16)

Symmetry transformations used to generate equivalent atoms:

#1 -x+1/2,-y+1/2,-z #2 -x+1,y,-z-1/2

Table 4. Anisotropic displacement parameters ($Å^2 x\ 10^3$)for c2c. The anisotropic displacement factor exponent takes the form: $-2\pi^2[\ h^2 a^{*2} U^{11} + ... + 2\ h\ k\ a^*\ b^*\ U^{12}\ ]$

	U^{11}	U^{22}	U^{33}	U^{23}	U^{13}	U^{12}
Mn(1)	23(1)	18(1)	26(1)	-1(1)	1(1)	0(1)
P(1)	24(1)	18(1)	25(1)	1(1)	0(1)	1(1)
O(1)	56(1)	36(1)	50(1)	-5(1)	22(1)	-17(1)
C(1)	27(1)	21(1)	24(1)	2(1)	6(1)	-2(1)
P(2)	27(1)	22(1)	30(1)	0(1)	-4(1)	1(1)
O(2)	51(1)	35(1)	63(1)	1(1)	7(1)	20(1)
C(2)	30(1)	22(1)	24(1)	2(1)	5(1)	-2(1)
O(3)	56(1)	48(1)	29(1)	-5(1)	-3(1)	-15(1)
C(3)	33(1)	30(1)	26(1)	0(1)	2(1)	-7(1)
O(4)	51(1)	48(1)	55(1)	0	14(1)	0
C(4)	44(1)	26(1)	30(1)	-7(1)	11(1)	-11(1)
C(5)	40(1)	19(1)	36(1)	-2(1)	15(1)	-2(1)
C(6)	31(1)	22(1)	32(1)	1(1)	8(1)	0(1)
C(7)	34(1)	23(1)	34(1)	-7(1)	4(1)	-1(1)
C(8)	32(1)	28(1)	35(1)	-1(1)	4(1)	-1(1)
C(9)	34(1)	24(1)	31(1)	1(1)	7(1)	-4(1)
C(10)	44(1)	66(2)	47(1)	-1(1)	19(1)	3(1)
C(11)	64(2)	65(2)	88(2)	-4(2)	33(2)	-14(1)

Table 5. Hydrogen coordinates (x 10^4) and isotropic displacement parameters ($Å^2$x 10^3) for c2c.

	x	y	z	U(eq)
H(1)	3021(19)	1448(10)	1053(12)	30(5)
H(3)	-1334	876	-1734	36
H(4)	-503	-286	-1694	39
H(5)	1606	-583	-819	37
H(6)	2914	270	38	34
H(10A)	5885	-830	-3559	62
H(10B)	7018	-966	-2693	62
H(11A)	6377	20	-1989	85
H(11B)	6019	274	-3025	85
H(2A)	-1720(20)	2134(11)	-824(14)	40(6)
H(2B)	-80(20)	2431(11)	-1594(14)	43(6)

5.2 X-Ray crystallography data for the *cis*-isomer of complex 2.11 (see Chapter 2)

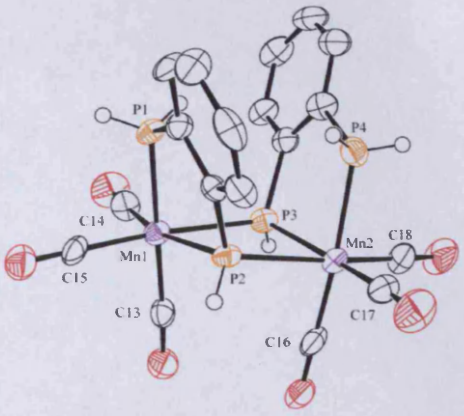

Table 6. Crystal data and structure refinement for pge0832b.

Identification code	pge0832b	
Empirical formula	C18 H14 Mn2 O6 P4	
Formula weight	560.05	
Temperature	150(2) K	
Wavelength	0.71073 Å	
Crystal system	Tetragonal	
Space group	I41/a	
Unit cell dimensions	a = 21.6710(4) Å	α= 90°.
	b = 21.6710(4) Å	β= 90°.
	c = 19.1310(4) Å	γ = 90°.
Volume	8984.5(3) $Å^3$	
Z	16	
Density (calculated)	1.656 Mg/m^3	
Absorption coefficient	1.441 mm^{-1}	
F(000)	4480	

Crystal size	0.30 x 0.26 x 0.20 mm^3
Theta range for data collection	3.01 to 27.48°.
Index ranges	-28<=h<=28, -19<=k<=19, -19<=l<=24
Reflections collected	8603
Independent reflections	5135 [R(int) = 0.0282]
Completeness to theta = 27.48°	99.7 %
Max. and min. transmission	0.7615 and 0.6718
Refinement method	Full-matrix least-squares on F^2
Data / restraints / parameters	5135 / 0 / 271
Goodness-of-fit on F^2	1.025
Final R indices [I>2sigma(I)]	R1 = 0.0401, wR2 = 0.0897
R indices (all data)	R1 = 0.0567, wR2 = 0.0968
Largest diff. peak and hole	0.558 and -0.575 $e.Å^{-3}$

Table 7. Atomic coordinates (x 10^4) and equivalent isotropic displacement parameters ($Å^2$x 10^3) for pge0832b. U(eq) is defined as one third of the trace of the orthogonalized U^{ij} tensor.

	x	y	z	U(eq)
C(1)	10603(1)	9755(1)	7531(1)	26(1)
C(2)	10159(1)	9758(1)	7005(1)	24(1)
C(3)	10350(1)	9729(1)	6307(1)	30(1)
C(4)	10973(2)	9682(1)	6151(2)	39(1)
C(5)	11410(1)	9682(2)	6677(2)	43(1)
C(6)	11232(1)	9722(1)	7366(2)	36(1)
C(7)	9638(1)	11229(1)	8638(2)	31(1)
C(8)	10044(1)	11476(1)	8145(2)	32(1)
C(9)	10543(1)	11837(1)	8363(2)	41(1)
C(10)	10622(1)	11958(2)	9067(2)	48(1)
C(11)	10218(2)	11722(2)	9558(2)	46(1)
C(12)	9728(1)	11353(1)	9346(2)	38(1)
C(13)	9440(1)	8827(1)	8402(2)	33(1)
C(14)	8463(1)	9494(1)	8392(2)	31(1)
C(15)	9257(1)	9712(1)	9400(2)	34(1)
C(16)	8614(1)	11604(2)	7216(2)	39(1)
C(17)	8971(1)	10827(1)	6178(2)	37(1)
C(18)	8190(1)	10471(1)	7142(2)	36(1)
O(1)	9529(1)	8310(1)	8361(1)	51(1)
O(2)	7948(1)	9381(1)	8366(1)	48(1)

O(3)	9236(1)	9775(1)	9994(1)	55(1)
O(4)	8413(1)	12089(1)	7290(1)	58(1)
O(5)	8980(1)	10817(1)	5581(1)	58(1)
O(6)	7715(1)	10241(1)	7144(1)	54(1)
P(1)	10313(1)	9800(1)	8423(1)	26(1)
P(2)	9351(1)	9840(1)	7261(1)	23(1)
P(3)	9042(1)	10698(1)	8321(1)	26(1)
P(4)	9875(1)	11295(1)	7235(1)	32(1)
Mn(1)	9280(1)	9649(1)	8455(1)	24(1)
Mn(2)	8941(1)	10840(1)	7125(1)	27(1)

Table 8. Bond lengths [Å] and angles [°] for pge0832b.

C(1)-C(2)	1.391(4)
C(1)-C(6)	1.401(4)
C(1)-P(1)	1.822(3)
C(2)-C(3)	1.399(4)
C(2)-P(2)	1.827(3)
C(3)-C(4)	1.387(4)
C(3)-H(3)	0.9500
C(4)-C(5)	1.383(5)
C(4)-H(4)	0.9500
C(5)-C(6)	1.377(4)
C(5)-H(5)	0.9500
C(6)-H(6)	0.9500
C(7)-C(12)	1.395(4)
C(7)-C(8)	1.397(4)
C(7)-P(3)	1.832(3)
C(8)-C(9)	1.400(4)
C(8)-P(4)	1.821(3)
C(9)-C(10)	1.383(5)
C(9)-H(9)	0.9500
C(10)-C(11)	1.382(5)
C(10)-H(10)	0.9500
C(11)-C(12)	1.389(4)
C(11)-H(11)	0.9500

C(12)-H(12)	0.9500
C(13)-O(1)	1.140(4)
C(13)-Mn(1)	1.818(3)
C(14)-O(2)	1.145(3)
C(14)-Mn(1)	1.805(3)
C(15)-O(3)	1.146(4)
C(15)-Mn(1)	1.813(3)
C(16)-O(4)	1.147(4)
C(16)-Mn(2)	1.809(3)
C(17)-O(5)	1.141(4)
C(17)-Mn(2)	1.813(3)
C(18)-O(6)	1.144(4)
C(18)-Mn(2)	1.814(3)
P(1)-Mn(1)	2.2625(8)
P(1)-H(1A)	0.9900
P(1)-H(1B)	0.9900
P(2)-Mn(1)	2.3262(7)
P(2)-Mn(2)	2.3556(8)
P(2)-H(2)	1.0000
P(3)-Mn(2)	2.3188(8)
P(3)-Mn(1)	2.3452(8)
P(3)-H(3A)	1.0000
P(4)-Mn(2)	2.2621(8)
P(4)-H(4A)	0.9900
P(4)-H(4B)	0.9900

C(2)-C(1)-C(6)	120.6(2)
C(2)-C(1)-P(1)	116.06(19)
C(6)-C(1)-P(1)	123.3(2)
C(1)-C(2)-C(3)	119.1(2)
C(1)-C(2)-P(2)	117.91(19)
C(3)-C(2)-P(2)	122.9(2)
C(4)-C(3)-C(2)	119.7(3)
C(4)-C(3)-H(3)	120.1
C(2)-C(3)-H(3)	120.1
C(5)-C(4)-C(3)	120.7(3)
C(5)-C(4)-H(4)	119.7
C(3)-C(4)-H(4)	119.7
C(6)-C(5)-C(4)	120.3(3)
C(6)-C(5)-H(5)	119.9
C(4)-C(5)-H(5)	119.9
C(5)-C(6)-C(1)	119.5(3)
C(5)-C(6)-H(6)	120.2
C(1)-C(6)-H(6)	120.2
C(12)-C(7)-C(8)	119.6(3)
C(12)-C(7)-P(3)	122.8(2)
C(8)-C(7)-P(3)	117.4(2)
C(7)-C(8)-C(9)	120.0(3)
C(7)-C(8)-P(4)	115.9(2)
C(9)-C(8)-P(4)	124.1(2)

C(10)-C(9)-C(8)	119.5(3)
C(10)-C(9)-H(9)	120.3
C(8)-C(9)-H(9)	120.3
C(11)-C(10)-C(9)	120.9(3)
C(11)-C(10)-H(10)	119.6
C(9)-C(10)-H(10)	119.6
C(10)-C(11)-C(12)	120.0(3)
C(10)-C(11)-H(11)	120.0
C(12)-C(11)-H(11)	120.0
C(11)-C(12)-C(7)	120.1(3)
C(11)-C(12)-H(12)	120.0
C(7)-C(12)-H(12)	120.0
O(1)-C(13)-Mn(1)	178.5(3)
O(2)-C(14)-Mn(1)	177.8(3)
O(3)-C(15)-Mn(1)	177.4(3)
O(4)-C(16)-Mn(2)	178.2(3)
O(5)-C(17)-Mn(2)	178.9(3)
O(6)-C(18)-Mn(2)	179.1(3)
C(1)-P(1)-Mn(1)	111.03(9)
C(1)-P(1)-H(1A)	109.4
Mn(1)-P(1)-H(1A)	109.4
C(1)-P(1)-H(1B)	109.4
Mn(1)-P(1)-H(1B)	109.4
H(1A)-P(1)-H(1B)	108.0
C(2)-P(2)-Mn(1)	108.03(8)

C(2)-P(2)-Mn(2)	114.96(9)
Mn(1)-P(2)-Mn(2)	104.33(3)
C(2)-P(2)-H(2)	109.8
Mn(1)-P(2)-H(2)	109.8
Mn(2)-P(2)-H(2)	109.8
C(7)-P(3)-Mn(2)	108.08(10)
C(7)-P(3)-Mn(1)	114.67(9)
Mn(2)-P(3)-Mn(1)	104.90(3)
C(7)-P(3)-H(3A)	109.7
Mn(2)-P(3)-H(3A)	109.7
Mn(1)-P(3)-H(3A)	109.7
C(8)-P(4)-Mn(2)	111.24(10)
C(8)-P(4)-H(4A)	109.4
Mn(2)-P(4)-H(4A)	109.4
C(8)-P(4)-H(4B)	109.4
Mn(2)-P(4)-H(4B)	109.4
H(4A)-P(4)-H(4B)	108.0
C(14)-Mn(1)-C(15)	93.11(13)
C(14)-Mn(1)-C(13)	90.09(13)
C(15)-Mn(1)-C(13)	97.71(13)
C(14)-Mn(1)-P(1)	174.09(10)
C(15)-Mn(1)-P(1)	92.46(10)
C(13)-Mn(1)-P(1)	87.21(9)
C(14)-Mn(1)-P(2)	91.86(9)
C(15)-Mn(1)-P(2)	165.24(10)

C(13)-Mn(1)-P(2)	96.17(9)
P(1)-Mn(1)-P(2)	83.22(3)
C(14)-Mn(1)-P(3)	87.58(9)
C(15)-Mn(1)-P(3)	91.73(10)
C(13)-Mn(1)-P(3)	170.38(9)
P(1)-Mn(1)-P(3)	94.22(3)
P(2)-Mn(1)-P(3)	74.59(3)
C(16)-Mn(2)-C(17)	97.10(14)
C(16)-Mn(2)-C(18)	92.83(14)
C(17)-Mn(2)-C(18)	92.47(14)
C(16)-Mn(2)-P(4)	86.73(10)
C(17)-Mn(2)-P(4)	93.89(10)
C(18)-Mn(2)-P(4)	173.63(10)
C(16)-Mn(2)-P(3)	93.64(10)
C(17)-Mn(2)-P(3)	168.70(10)
C(18)-Mn(2)-P(3)	90.51(9)
P(4)-Mn(2)-P(3)	83.18(3)
C(16)-Mn(2)-P(2)	168.09(10)
C(17)-Mn(2)-P(2)	94.79(10)
C(18)-Mn(2)-P(2)	86.06(9)
P(4)-Mn(2)-P(2)	93.06(3)
P(3)-Mn(2)-P(2)	74.53(3)

Symmetry transformations used to generate equivalent atoms:

Table 9. Anisotropic displacement parameters ($Å^2 x\ 10^3$)for pge0832b. The anisotropic displacement factor exponent takes the form: $-2\pi^2[\ h^2a^{*2}U^{11} + ... + 2\ h\ k\ a^*\ b^*\ U^{12}\ ]$

	U^{11}	U^{22}	U^{33}	U^{23}	U^{13}	U^{12}
C(1)	24(1)	30(1)	24(1)	2(1)	1(1)	1(1)
C(2)	25(1)	25(1)	21(1)	-1(1)	2(1)	0(1)
C(3)	38(2)	29(1)	22(1)	1(1)	1(1)	1(1)
C(4)	45(2)	42(2)	29(2)	1(1)	12(1)	2(1)
C(5)	30(2)	54(2)	47(2)	12(2)	13(1)	4(1)
C(6)	25(1)	50(2)	34(2)	8(1)	-1(1)	2(1)
C(7)	29(1)	27(1)	37(2)	-6(1)	-2(1)	3(1)
C(8)	28(1)	28(1)	39(2)	-8(1)	-4(1)	2(1)
C(9)	26(2)	41(2)	54(2)	-8(2)	-1(1)	-3(1)
C(10)	31(2)	50(2)	64(2)	-21(2)	-11(2)	-2(1)
C(11)	42(2)	47(2)	48(2)	-16(2)	-12(2)	6(2)
C(12)	39(2)	39(2)	37(2)	-9(1)	-3(1)	3(1)
C(13)	32(2)	38(2)	30(2)	4(1)	-4(1)	-3(1)
C(14)	31(2)	29(1)	34(2)	7(1)	2(1)	2(1)
C(15)	34(2)	41(2)	28(2)	4(1)	3(1)	3(1)
C(16)	36(2)	41(2)	39(2)	1(1)	-9(1)	4(1)
C(17)	36(2)	39(2)	35(2)	7(1)	-6(1)	0(1)
C(18)	34(2)	39(2)	35(2)	10(1)	-6(1)	4(1)
O(1)	65(2)	32(1)	58(2)	-2(1)	-12(1)	4(1)
O(2)	30(1)	51(1)	62(2)	19(1)	0(1)	-7(1)

O(3)	67(2)	77(2)	22(1)	1(1)	5(1)	4(1)
O(4)	63(2)	39(1)	73(2)	-11(1)	-23(1)	17(1)
O(5)	67(2)	77(2)	30(1)	6(1)	-5(1)	1(1)
O(6)	32(1)	65(2)	66(2)	28(1)	-14(1)	-11(1)
P(1)	24(1)	35(1)	20(1)	0(1)	-4(1)	2(1)
P(2)	22(1)	27(1)	20(1)	-1(1)	-4(1)	-1(1)
P(3)	24(1)	29(1)	26(1)	-3(1)	1(1)	2(1)
P(4)	31(1)	30(1)	34(1)	3(1)	1(1)	-4(1)
Mn(1)	24(1)	28(1)	20(1)	1(1)	0(1)	0(1)
Mn(2)	25(1)	29(1)	27(1)	3(1)	-4(1)	1(1)

Table 10. Hydrogen coordinates (x 10^4) and isotropic displacement parameters ($Å^2$x 10^3) for pge0832b.

	x	y	z	U(eq)
H(3)	10053	9743	5941	36
H(4)	11100	9648	5677	46
H(5)	11836	9655	6562	52
H(6)	11533	9726	7727	44
H(9)	10826	11998	8030	49
H(10)	10959	12206	9216	58
H(11)	10275	11812	10040	55
H(12)	9455	11185	9684	46
H(1A)	10411	10211	8621	32
H(1B)	10519	9484	8714	32
H(2)	9092	9536	6999	28
H(3A)	8641	10791	8557	31
H(4A)	10198	11016	7050	38
H(4B)	9883	11680	6956	38

5.3 X-Ray crystallography data for *cis*-[(k-$P_{R,S}$-3.7)$_2$ $PtCl_2$], 3.22, (see Chapter 3)

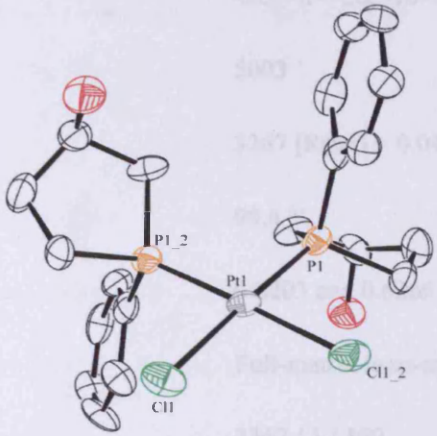

Table 11. Crystal data and structure refinement for pge0802t.

Identification code	pge0802t	
Empirical formula	C24 H38 Cl2 O4 P2 Pt S2	
Formula weight	782.59	
Temperature	150(2) K	
Wavelength	0.71073 Å	
Crystal system	Monoclinic	
Space group	C2	
Unit cell dimensions	a = 16.9588(12) Å	α= 90°.
	b = 8.3160(4) Å	β= 105.851(5)°.
	c = 11.0000(8) Å	γ = 90°.
Volume	1492.33(17) Å^3	
Z	2	
Density (calculated)	1.742 Mg/m^3	
Absorption coefficient	5.156 mm^{-1}	
F(000)	776	

Crystal size	0.10 x 0.04 x 0.04 mm^3
Theta range for data collection	1.92 to 27.59°.
Index ranges	-22<=h<=20, -10<=k<=10, -11<=l<=14
Reflections collected	5003
Independent reflections	3367 [R(int) = 0.0427]
Completeness to theta = 27.59°	99.4 %
Max. and min. transmission	0.8203 and 0.6266
Refinement method	Full-matrix least-squares on F^2
Data / restraints / parameters	3367 / 1 / 160
Goodness-of-fit on F^2	1.074
Final R indices [I>2sigma(I)]	R1 = 0.0870, wR2 = 0.2050
R indices (all data)	R1 = 0.0948, wR2 = 0.2174
Absolute structure parameter	0.00(3)
Largest diff. peak and hole	11.888 and -1.520 e.$Å^{-3}$

Table 12. Atomic coordinates (x 10^4) and equivalent isotropic displacement parameters ($Å^2$x 10^3) for pge0802t. U(eq) is defined as one third of the trace of the orthogonalized U^{ij} tensor.

	x	y	z	U(eq)
C(1)	8000(10)	4580(20)	8933(17)	38(4)
C(2)	7601(12)	2960(30)	8420(20)	57(6)
C(3)	8197(12)	2000(20)	7981(17)	44(4)
C(4)	9056(12)	2180(20)	8914(17)	42(4)
C(5)	8909(11)	3390(20)	11371(17)	41(4)
C(6)	8889(11)	1880(20)	11775(19)	46(4)
C(7)	8758(11)	1580(30)	12990(20)	48(4)
C(8)	8663(13)	2860(30)	13770(16)	51(5)
C(9)	8690(13)	4380(30)	13306(15)	51(5)
C(10)	8819(12)	4680(20)	12196(18)	45(4)
C(11)	5562(16)	4290(30)	3357(19)	58(5)
C(12)	5840(20)	1100(60)	3540(20)	88(11)
O(1)	8233(9)	2600(20)	6794(12)	53(3)
O(2)	6618(12)	3060(20)	5354(15)	71(5)
P(1)	9030(4)	4021(7)	9842(7)	31(2)
Cl(1)	10987(6)	7909(7)	10142(9)	48(2)
Pt(1)	10000	5886(2)	10000	30(1)
S(1)	6401(4)	2999(9)	3905(5)	65(2)

Table 13. Bond lengths [Å] and angles [°] for pge0802t.

C(1)-C(2)	1.55(3)
C(1)-P(1)	1.821(17)
C(2)-C(3)	1.47(3)
C(3)-O(1)	1.41(2)
C(3)-C(4)	1.54(3)
C(4)-P(1)	1.848(18)
C(5)-C(6)	1.34(3)
C(5)-C(10)	1.44(3)
C(5)-P(1)	1.83(2)
C(6)-C(7)	1.44(3)
C(7)-C(8)	1.40(3)
C(8)-C(9)	1.37(3)
C(9)-C(10)	1.32(2)
C(11)-S(1)	1.75(2)
C(12)-S(1)	1.83(5)
O(2)-S(1)	1.535(17)
P(1)-Pt(1)	2.233(7)
Cl(1)-Pt(1)	2.348(8)
Pt(1)-P(1)#1	2.233(7)
Pt(1)-Cl(1)#1	2.348(8)
C(2)-C(1)-P(1)	103.5(12)
C(3)-C(2)-C(1)	108.9(16)

O(1)-C(3)-C(2)	108.6(19)
O(1)-C(3)-C(4)	107.9(15)
C(2)-C(3)-C(4)	109.7(15)
C(3)-C(4)-P(1)	106.8(13)
C(6)-C(5)-C(10)	118.4(18)
C(6)-C(5)-P(1)	126.4(15)
C(10)-C(5)-P(1)	115.1(14)
C(5)-C(6)-C(7)	119.6(18)
C(8)-C(7)-C(6)	121.0(17)
C(9)-C(8)-C(7)	116.7(15)
C(10)-C(9)-C(8)	124(2)
C(9)-C(10)-C(5)	121(2)
C(1)-P(1)-C(5)	104.3(9)
C(1)-P(1)-C(4)	94.2(9)
C(5)-P(1)-C(4)	107.3(9)
C(1)-P(1)-Pt(1)	116.1(7)
C(5)-P(1)-Pt(1)	113.1(6)
C(4)-P(1)-Pt(1)	119.4(8)
P(1)-Pt(1)-P(1)#1	92.0(3)
P(1)-Pt(1)-Cl(1)	178.1(4)
P(1)#1-Pt(1)-Cl(1)	89.77(16)
P(1)-Pt(1)-Cl(1)#1	89.77(16)
P(1)#1-Pt(1)-Cl(1)#1	178.1(4)
Cl(1)-Pt(1)-Cl(1)#1	88.5(4)
O(2)-S(1)-C(11)	106.3(11)

O(2)-S(1)-C(12)	102.5(11)
C(11)-S(1)-C(12)	97.6(15)

Symmetry transformations used to generate equivalent atoms:

#1 -x+2,y,-z+2

Table 14. Anisotropic displacement parameters ($Å^2 x\ 10^3$)for pge0802t. The anisotropic displacement factor exponent takes the form: $-2\pi^2[\ h^2a^{*2}U^{11} + ... + 2\ h\ k\ a^*\ b^*\ U^{12}\ ]$

	U^{11}	U^{22}	U^{33}	U^{23}	U^{13}	U^{12}
C(1)	24(7)	47(9)	39(8)	3(7)	0(6)	5(6)
C(2)	32(9)	55(12)	74(14)	-11(10)	-4(9)	-13(8)
C(3)	46(10)	56(11)	35(8)	-6(7)	21(7)	-13(8)
C(4)	53(10)	35(8)	32(8)	-9(6)	1(7)	-1(7)
C(5)	33(8)	47(10)	35(8)	-2(7)	-3(6)	1(7)
C(6)	38(9)	40(9)	52(10)	-14(8)	1(8)	1(7)
C(7)	33(8)	54(9)	55(11)	21(8)	8(8)	-16(7)
C(8)	52(11)	88(15)	19(7)	10(8)	17(7)	9(10)
C(9)	61(12)	83(14)	17(7)	10(8)	25(7)	32(10)
C(10)	43(10)	51(10)	44(10)	7(8)	20(8)	11(8)
C(11)	78(15)	64(13)	32(9)	8(8)	18(9)	20(11)
C(12)	130(20)	80(30)	39(10)	4(15)	-2(11)	10(20)
O(1)	56(9)	72(9)	29(6)	4(6)	11(6)	-2(7)
O(2)	71(11)	87(13)	41(8)	1(7)	-7(7)	-7(9)
P(1)	30(3)	36(3)	24(3)	-1(2)	1(2)	4(2)
Cl(1)	65(5)	30(3)	53(4)	-6(3)	25(3)	-11(3)
Pt(1)	40(1)	24(1)	24(1)	0	7(1)	0
S(1)	54(3)	100(5)	38(3)	13(3)	9(2)	2(3)

Table 15. Hydrogen coordinates (x 10^4) and isotropic displacement parameters ($Å^2$x 10^3) for pge0802t.

	x	y	z	U(eq)
H(1A)	7698	5111	9477	46
H(1B)	8017	5321	8233	46
H(2A)	7436	2375	9096	68
H(2B)	7105	3148	7713	68
H(3)	8029	840	7906	53
H(4A)	9477	2275	8449	51
H(4B)	9186	1232	9479	51
H(6)	8961	1004	11259	55
H(7)	8736	508	13270	58
H(8)	8583	2676	14581	62
H(9)	8612	5258	13808	61
H(10)	8853	5768	11941	54
H(11A)	5749	5409	3475	87
H(11B)	5160	4095	3832	87
H(11C)	5309	4088	2457	87
H(12A)	6230	200	3780	133
H(12B)	5572	1045	2633	133
H(12C)	5433	1030	4015	133
H(1)	7838	3223	6507	79

Appendix 2
Reported failure attempts to synthesis Hybrid Phosphine-Carbene Ligands

6.1 Foreword

The aim of this project was to design and to synthesise mixed phosphine-carbene ligands. Such ligands may have potential as precursors in subsequent template assisted cyclisation and hence alternative strategies for the synthesis of phosphine-carbene macrocycles. As mentioned in Chapter 1 the design of a wide range of phosphines or phosphites, recently incorporating carbenes ligands have been used to control and influence catalyst behaviour in different ways like steric and electronic effects as well as rigidity and hemo-lability of the ligand.

Several chelating phosphine-imidazolium salts have been successfully synthesised by different synthetic routes which have increased the scope for the potential number of theses salts. Given this interest the synthesis of new asymmetric bidentate phosphine-imidazolium salts (Figure 1) but using primary phosphines and nucleophilic heterocylic carbenes (NHC), both functionalities which have large *trans* influences but different coordination properties, would be of value.

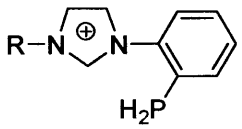

Figure 1: bidentate phosphine imidazolium salt (R= methyl or *iso*propyl).

Prior studies in the Edwards group have successfuly developed synthetic routes to alkyl and aryl phosphine substituted imidazolium salts (Figure 2) by the fluoride elimination method.[1, 2]

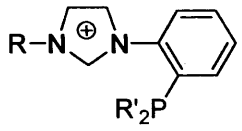

R' = ^{i}Pr, Ph

Figure 2

The work described in this appendix is based on establishing a synthetic methodology of novel mixed donor phosphine-NHC ligands and different attempts to substitute primary phosphines to the N-substituted 1-(2-fluorobenzene)imidazole derivatives were reported. Unfortunately all routes described in the next section were unsuccessful and the overall project was discarded after few month of research.

6.2 Results and discussion

6.2.1 Synthesis of the imidazolium precursors

A very effective synthesis route was adapted from the literature method for the formation for N-substituted imidazoles[3, 4] and required to build the imidazole ring from the corresponding amine. The synthesis of compound **6.1** was achieved using the acid catalysed reaction of 2-fluoroaniline, ammonium acetate, glyoxal and formaldehyde to give the N-substituted 1-(2-fluorobenzene)imidazole (Scheme 1).

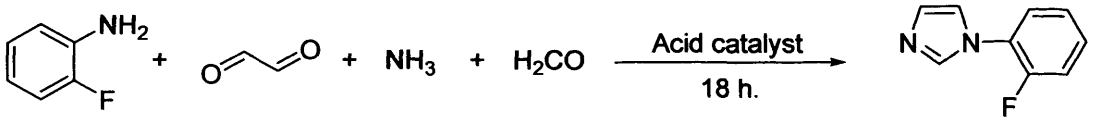

6.1

Scheme 1: N-substituted 1-(2-fluorobenzene)imidazole, **6.1**, synthesis.

The N-substituted 1-(2-fluorobenzene)imidazole, **6.1**, could then be reacted with alkyl halide, methyl iodide to give the corresponding imidazolium salts (1-fluorophenyl-3-methyl)imidazolium iodide, **6.2**, in quantitative yields (Scheme 2). It has been previously reported that the limiting factor of this synthesis is that only less bulky alkyl halides will react with imidazoles.[5] Alkylation with bulkier groups such as *iso*-propyl have however, been achieved when 1-(2-fluorobenzene)imidazole, **6.1**, was reacted with 2-bromopropane under refluxing conditions to give (1-fluorophenyl-3-*iso*-propyl)imidazolium bromide, **6.3** (Scheme 2).

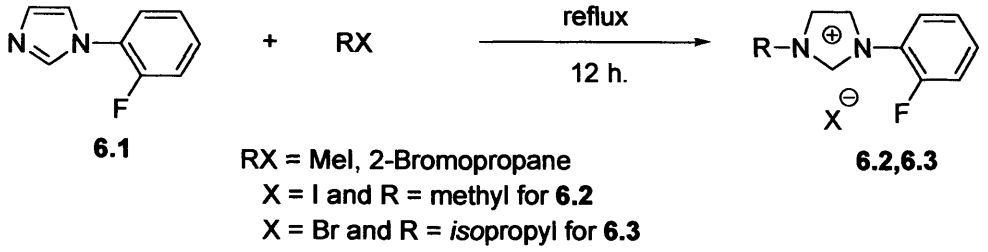

Scheme 2: Synthesis of compounds **6.2** and **6.3**.

6.2.2 Introduction of the primary phosphine

The strategy was then to add the fluorophenyl imidazolium salt **6.2** or **6.3** with $NaPH_2$ to lead to the desired phosphine-imidazolium salts **6.4** and **6.5** respectively (Scheme 3).

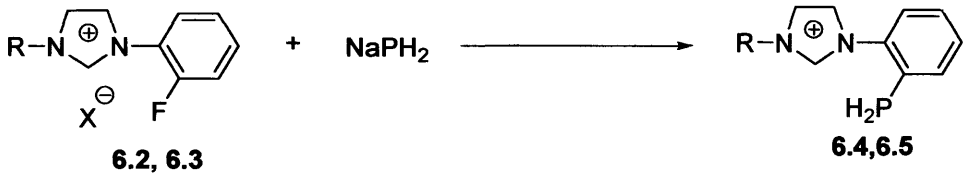

Scheme 3: synthesis of the phosphine-imidazolium salts **6.4** and **6.5**.

To date, we were unable to identify and prove that the primary phosphine had been formed. The following reaction schemes summarise the different approaches which have been explored in order to obtain the desired product.

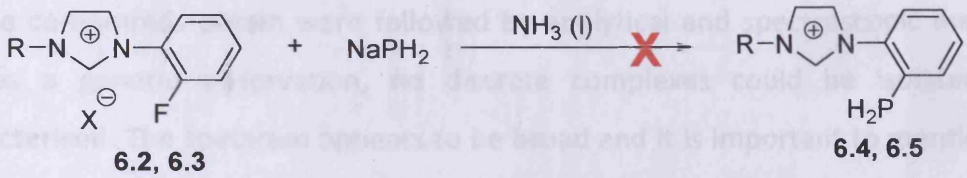

6.2, 6.3 **6.4, 6.5**

Scheme 4

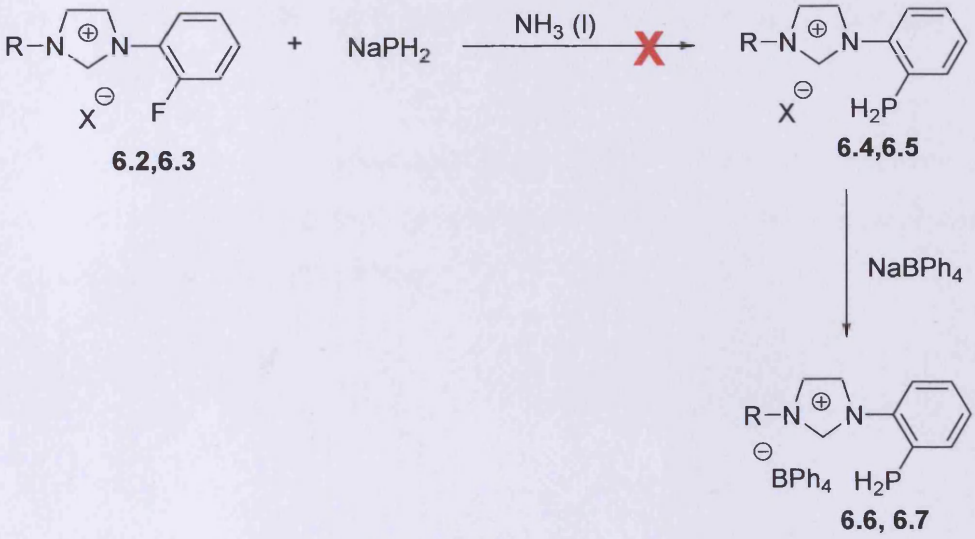

6.2,6.3 **6.4,6.5** **6.6, 6.7**

Scheme 5

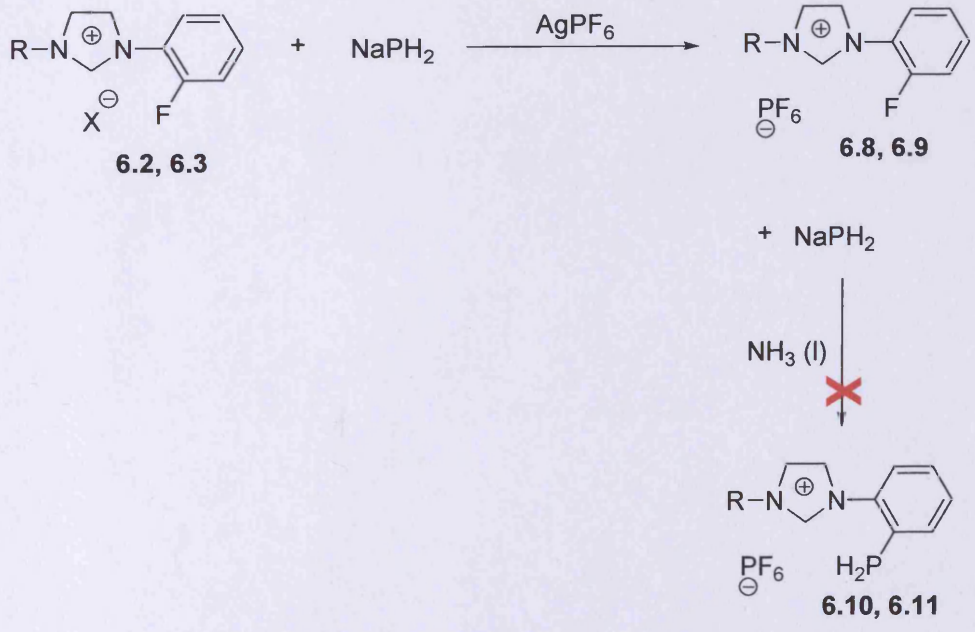

6.2, 6.3 **6.8, 6.9** **6.10, 6.11**

Scheme 6

All the compounds obtain were followed by analytical and spectroscopic methods but as a general observation, no discrete complexes could be isolated and characterised. The spectrum appears to be broad and it is important to mention the polymeric nature of the new compound formed, which amplified the difficulties to study them.

6.3 References

[1] S. Al Saadi, unpublished results, Cardiff University (Cardiff).

[2] R. J. Lane, Thesis, Cardiff University (Cardiff), **2005**.

[3] A. A. Gridnev, I. M. Mihaltseia, *Synth. Commun.*, **1994**, *24*, 1547.

[4] A. J. Arduengo . III, F. P. Gentry, P. K. Taverkene, H. E. Simmons, **2001**, 6177575, U. S.

[5] D. J. Nielsen, *Functionalised nucleophilic heterocyclic carbene (NHC) complexes of silver(I) and palladium(II): chemistry, structure, and catalysis*, University of Tasmania, **2004**.